

Ger de Bruyn's legacy work on the Perseus cluster

M.A. Brentjens

Radio Observatory and R&D divisions
ASTRON, Dwingeloo, The Netherlands

IAUS Perseus in Sicily

Prof. Ger de Bruyn 1948 – 2017



Current

- Interstellar scintillation and the local ISM: AGN, Pulsars, GRB's, (any) transients, ...
- Galactic synchrotron foreground polarimetry
- Active Galactic Nuclei: nuclear variability, double–double radio galaxies and recurrent activity
- Clusters of galaxies (diffuse emission)
- High redshift HI: damped Ly- α absorbers, Epoch of Reionization (LOFAR)

Past

- Radio emission from young (extragalactic) SNR
- Optical spectrophotometric monitoring of Seyfert galaxies
- Radio gravitational lensing
- Surveys of the sky, e.g. WENSS/WISH

Technical / radio interferometry

- synthesis array calibration (WSRT, LOFAR, SKA)
- extreme dynamic range issues ($> 10^6 : 1$)
- radio polarization methods (RM-synthesis)

Technical / radio interferometry

- synthesis array calibration (WSRT, LOFAR, SKA)
- extreme dynamic range issues ($> 10^6 : 1$)
- radio polarization methods (RM-synthesis)

Well-being of others

- **Ger de Bruyn**

- **Ger de Bruyn**
- Harry van der Laan (Former director ESO)

- **Ger de Bruyn**
- Harry van der Laan (Former director ESO)
- Martin Ryle (Nobel prize, aperture synthesis)

- **Ger de Bruyn**

- Harry van der Laan (Former director ESO)
- Martin Ryle (Nobel prize, aperture synthesis)
- Jack Ratcliffe (Ionospheric physics)

- **Ger de Bruyn**

- Harry van der Laan (Former director ESO)
- Martin Ryle (Nobel prize, aperture synthesis)
- Jack Ratcliffe (Ionospheric physics)
- Edward Victor Appleton (Nobel prize, ionospheric physics)

- **Ger de Bruyn**

- Harry van der Laan (Former director ESO)
- Martin Ryle (Nobel prize, aperture synthesis)
- Jack Ratcliffe (Ionospheric physics)
- Edward Victor Appleton (Nobel prize, ionospheric physics)
- J.J. Thomson (Nobel prize, plasma physics, scattering)

- **Ger de Bruyn**

- Harry van der Laan (Former director ESO)
- Martin Ryle (Nobel prize, aperture synthesis)
- Jack Ratcliffe (Ionospheric physics)
- Edward Victor Appleton (Nobel prize, ionospheric physics)
- J.J. Thomson (Nobel prize, plasma physics, scattering)
- John William Strutt, 3rd Baron Rayleigh (Nobel prize, also Rayleigh-Jeans law)

- **Ger de Bruyn**

- Harry van der Laan (Former director ESO)
- Martin Ryle (Nobel prize, aperture synthesis)
- Jack Ratcliffe (Ionospheric physics)
- Edward Victor Appleton (Nobel prize, ionospheric physics)
- J.J. Thomson (Nobel prize, plasma physics, scattering)
- John William Strutt, 3rd Baron Rayleigh (Nobel prize, also Rayleigh-Jeans law)
- George Stokes

- **Ger de Bruyn**

- Harry van der Laan (Former director ESO)
- Martin Ryle (Nobel prize, aperture synthesis)
- Jack Ratcliffe (Ionospheric physics)
- Edward Victor Appleton (Nobel prize, ionospheric physics)
- J.J. Thomson (Nobel prize, plasma physics, scattering)
- John William Strutt, 3rd Baron Rayleigh (Nobel prize, also Rayleigh-Jeans law)
- George Stokes
- a couple more...

- **Ger de Bruyn**

- Harry van der Laan (Former director ESO)
- Martin Ryle (Nobel prize, aperture synthesis)
- Jack Ratcliffe (Ionospheric physics)
- Edward Victor Appleton (Nobel prize, ionospheric physics)
- J.J. Thomson (Nobel prize, plasma physics, scattering)
- John William Strutt, 3rd Baron Rayleigh (Nobel prize, also Rayleigh-Jeans law)
- George Stokes
- a couple more...
- Isaac Newton



1/15/84 17:53:23

PERSEUS

RESTORED (CONTINUOUS)

3C84

210

1987

Database:

Note:

File:

Full contours:

Dotted contours:

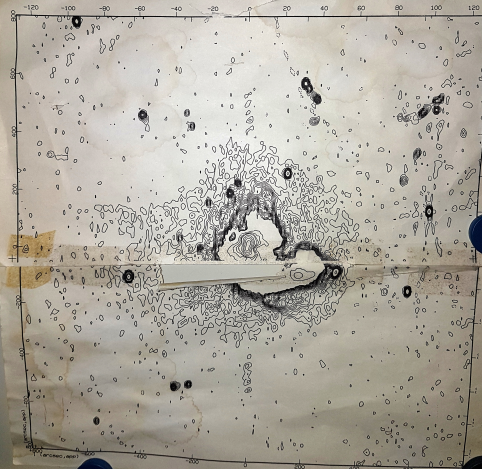
DR 200,000

12750bb
NGC1275.CDB.FOUR.GUB8304.RES
USER1:IDL,BER,DUMPRDATA10002110009,SP1

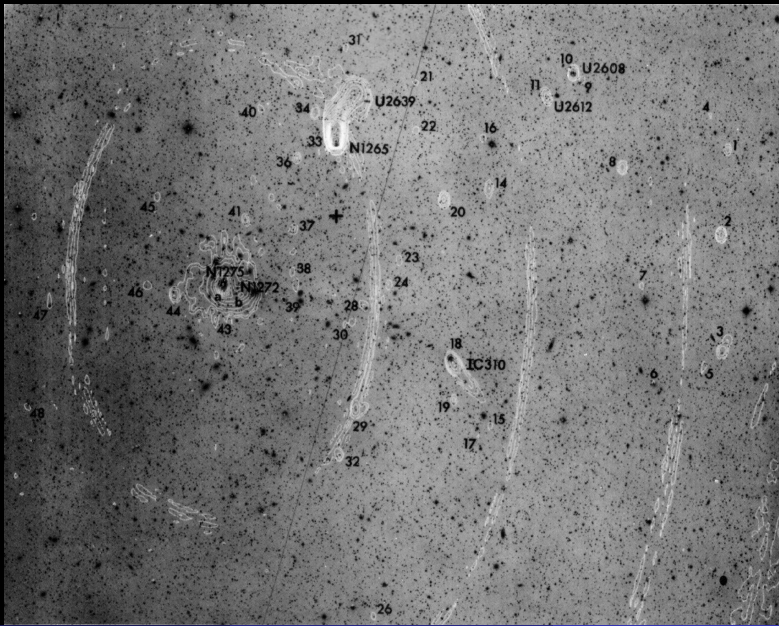
0.000, 0.1200, 0.1700, 0.2200, 0.2700, 0.3800, 0.3700, 0.4200, 0.4700, 0.5200, 0.5700, 0.6200, 0.6700, 0.5800, 0.9700, 0.9700, 2.0000, 3.0000, 4.0000, 5.0000, 10.000, 20.000, 40.000, 80.000

0.25 mJy contours (offset -0.03 mJy)

DR 200,000



103-a-E+Channel N, RA E, Dec D



ARTICLES

High dynamic range mapping of strong radio sources, with application to 3C84

J. E. Noordam & A. G. de Bruyn

Radiosterrenwacht, Postbus 2, 7990 AA Dwingeloo, The Netherlands

A new reduction procedure is described to correct data obtained by the Westerbork Synthesis Radio Telescope. The technique allows very high dynamic range mapping of strong radio sources by also using redundant interferometers. The performance is illustrated with 6-cm and 21-cm continuum maps of 3C84, which have a dynamic range of about 10,000:1.

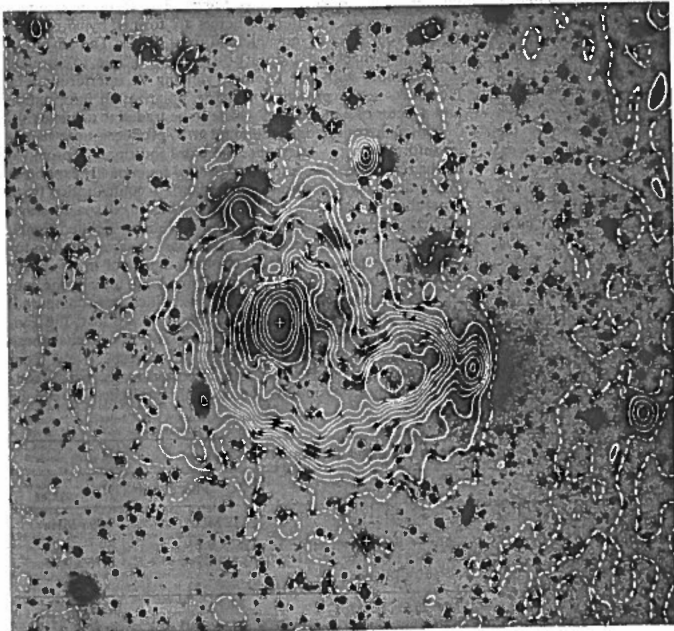


Fig. 2 The convolved 21-cm map of August 1980 superimposed on a deep optical photograph¹⁶. North is up and east to the left; the area shown measures 16.5×18 arc min. The resolution (30×45 arc s FWHM) can be judged from the appearance of the point source in the upper-right quadrant. A point source of flux density 13.2 Jy has been subtracted at the position of the cross centred on NGC1275. The displayed contour levels are -5, 0 (2.5) 10 (5) 40, 60, 80, 160, 320 and .640 mJy per beam; the peak brightness is at 2,060 mJy per beam. The true zero level varies slightly across the map but lies at about -2.5 mJy in the inner 10 arc min of the map.



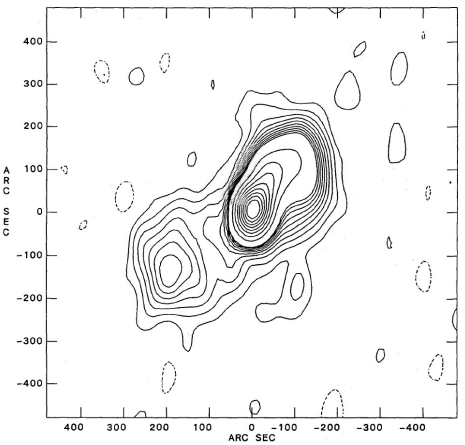


Figure 2: Contour map of the radio source 0309+411 obtained with the WSRT at 327 MHz. The contour levels are $1.6 \times (-6, -3, 3, 6, 9, 12, 15, 18, 21, 24, 27, 30)$ and $1.6 \times (60, 90, 120, 150, 180, 210, 240, 270)$ mJy/beam. The factor 1.6 corrects for the primary beam attenuation. The peak flux density of the source is 480 mJy. The coordinates are in arc seconds relative to the core of 0309+411. North is up, east to the left.

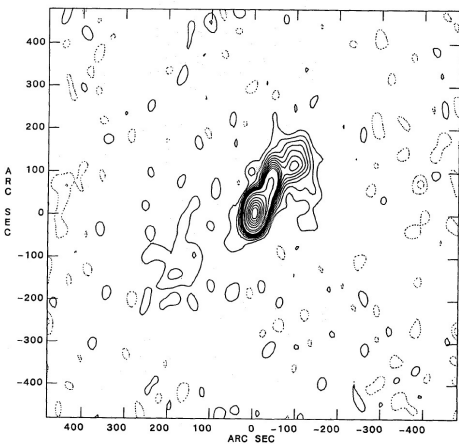


Figure 3: Contour map of the radio source 0309+411 obtained with the WSRT at 608 MHz. Contour levels are $5.9 \times (-1.2, -0.6, 0.6, 1.2, 1.8, 2.4, 3, 3.6, 4, 4.2, 4.8, 5, 4, 6, 0)$ and $5.9 \times (9, 12, 18, 24, 30, 36, 42, 48)$ mJy/beam. The factor 5.9 corrects for the primary beam attenuation. The peak flux density of the source is 380 mJy. The coordinates are relative to the core.

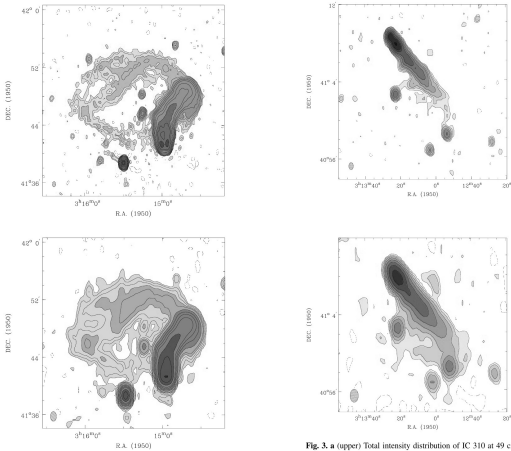


Fig. 3. **a** (upper) Total intensity distribution of IC 310 at 49 cm uncorrected for primary beam response. The contour levels are -0.8 (dashed), 0.8 , 1.5 , 2.5 , 5 , 8 , 15 , 25 , 50 , 80 , 150 , 250 , 500 and 800 mJy/beam. The greyscales represent values of 0.8 , 2.5 , 8 , 150 and 500 mJy/beam. The maps are not primary beam corrected. The primary beam response is 0.80 . The small filaments connecting to the strong point source (3C 83.1A) south-east of NGC 1265 are instrumental artifacts. **b** (lower) Same as **a** at 92 cm. The contour levels are -4 (dashed), 4 , 8 , 15 , 25 , 40 , 80 , 150 , 250 , 400 , 800 , 1500 and 2500 mJy/beam. The greyscales represent values of 4 , 25 , 80 , 800

3. Short title (10 words maximum) of proposed programme

Nature of the polarized diffuse emission in the Perseus cluster

4. Abstract (Concise summary of the proposal)

We propose a new deep radio continuum study of the Perseus cluster at 21cm. The main science driver is the nature of the diffuse polarized emission, first discovered in 1995. If, as we suspect, the emission is due to Thomson scattering of the central radio source by the hot diffuse gas in the cluster we can study the latter distribution, providing an X-ray independent handle on the baryonic mass in the cluster. Using the Rotation Measure of the polarized emission we can also derive the strength and topology of the large scale cluster magnetic field. The observations will complement ~~new high quality 80-100 cm observations obtained in Dec 2002.~~

3. Short title (10 words maximum) of proposed programme

Nature of the polarized diffuse emission in the Perseus cluster

4. Abstract (Concise summary of the proposal)

We propose a new deep radio continuum study of the Perseus cluster at 21cm. The main science driver is the nature of the diffuse polarized emission, first discovered in 1995. If, as we suspect, the emission is due to Thomson scattering of the central radio source by the hot diffuse gas in the cluster we can study the latter distribution, providing an X-ray independent handle on the baryonic mass in the cluster. Using the Rotation Measure of the polarized emission we can also derive the strength and topology of the large scale cluster magnetic field. The observations will complement ~~new high quality 80-100 cm observations obtained in Dec 2002.~~

In 1995 the cluster was re-observed in 21cm continuum radiation by de Bruyn in an attempt to image the polarized emission in the cluster. The results of this 6x12h 21cm continuum observation using the 8x5 Mhz DCB in 1995 are shown in Figure 1abcd. The peak flux divided by the rms noise in clean areas is more than 1 million to 1 (de Bruyn, 1996, High Sensitivity Radio Astronomy Workshop, Jodrell Bank, Ed. N. Jackson, CUP). The noise level in these images is about 25 microJy/beam and revealed in the Stokes V image. This is not the place to discuss the origin of the various artefacts in the Stokes Q and U images. Suffice it to say that there is no doubt that there is wide-spread diffuse polarized emission approximately centered on 3C84 and extending over at least 30', predominantly in the SW-NE direction.

Stokes IQUV 21 cm (1995 unpublished)

ASTRON

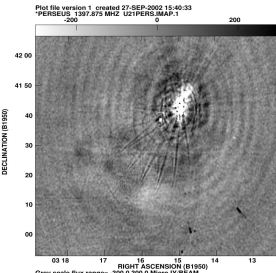
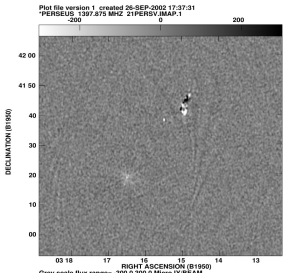
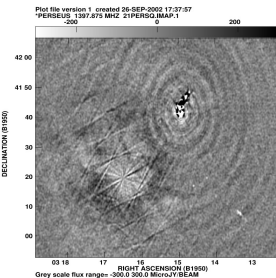
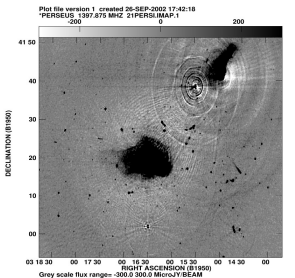
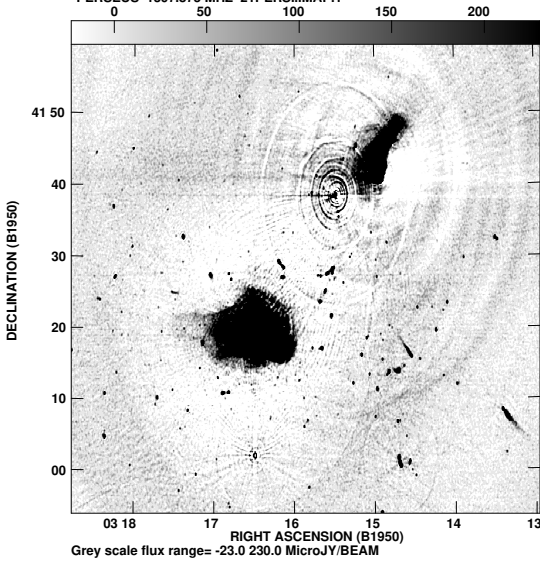


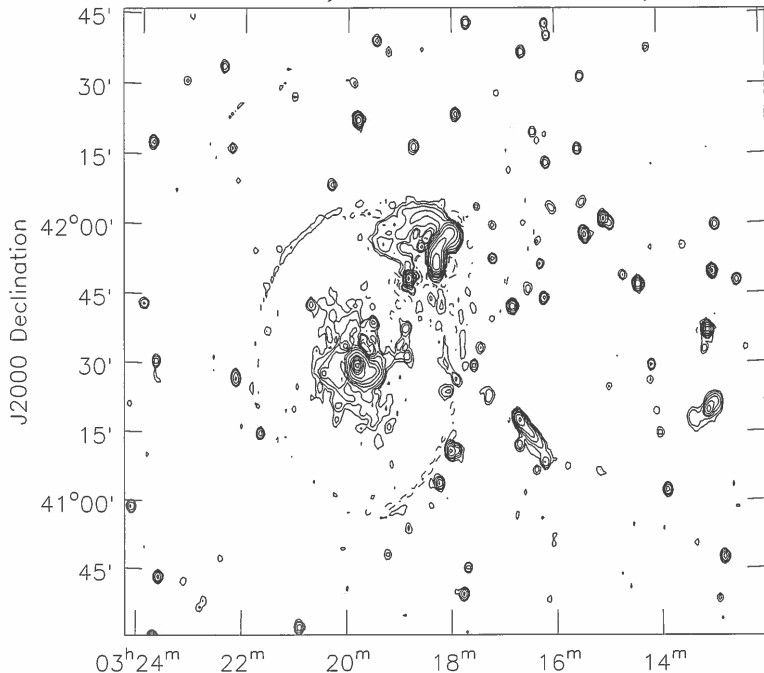
FIG. 3.— From top left clockwise: Stokes I , Q , U and V . These are 21 cm WSRT observations of Perseus by de Bruyn (unpublished, see also: de Bruyn (1996a)). The scale of the I images differs slightly from that of the polarized images. The Q and U images show diffuse linearly polarized emission in the central parts of the cluster. An RM study of this emission may reveal its origin.

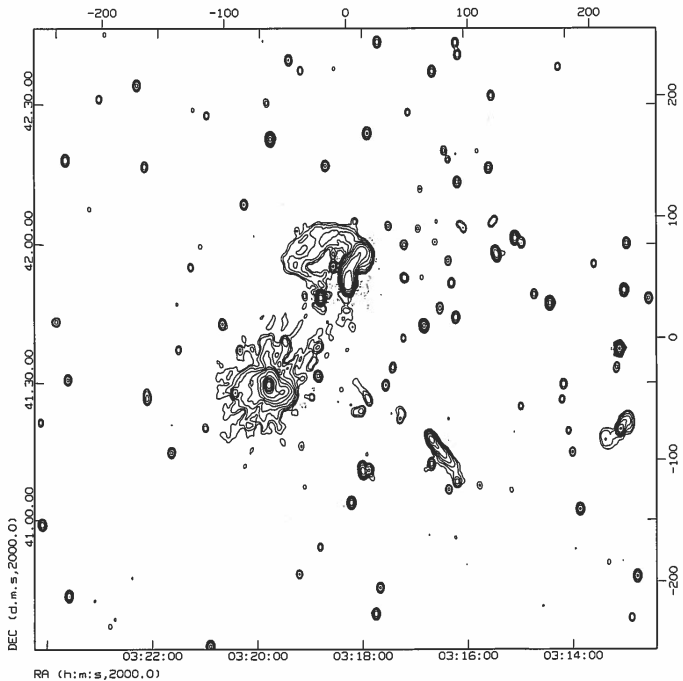
Plot file version 2 created 27-SEP-2002 17:53:30
*PERSEUS 1397.875 MHZ 21PERSIMAP.1



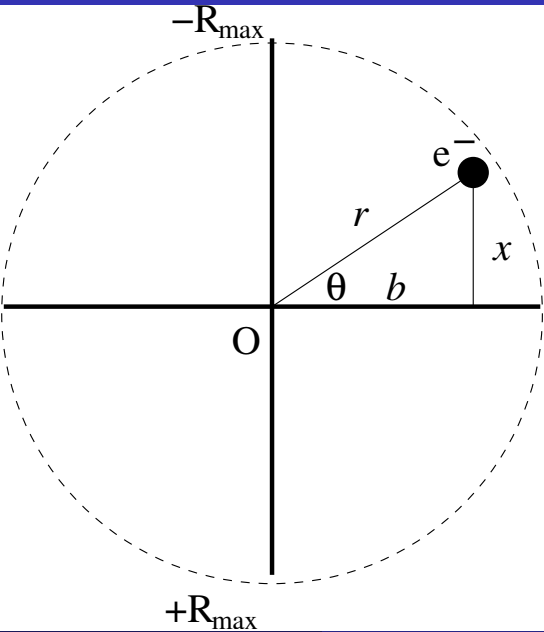
*"The description of the analysis plan
"de Bruyn will reduce the data in
Newstar" is unsatisfactory for such a
significant request of 156 hrs."*

-20 mJy,-10,10,20,40,... Max 30Jy



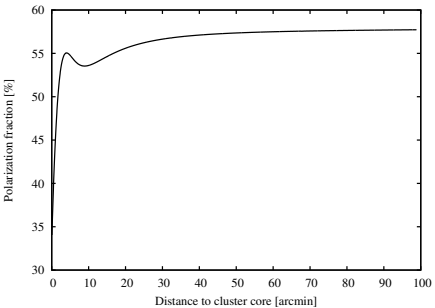
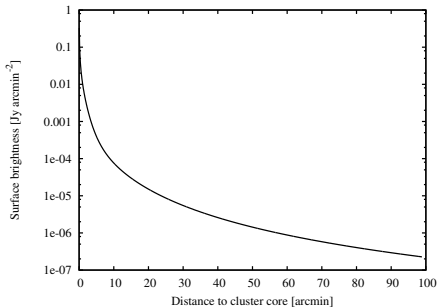


Thomson scattering



Towards observer

Thomson scattering



NETHERLANDS FOUNDATION FOR
RESEARCH IN ASTRONOMY

NOTE 655

RM-synthesis via wide-band low-frequency polarimetry

MAART 1996

BY A.G. de Bruyn

Future applications

We expect the new tool to be particularly powerful in the study of weakly polarized extended sources, such as giant radio galaxies where the *RM*'s are known to be small. Small changes in the *RM* across the surface of extended sources should be easily traceable, especially if these *RMs* are showing some spatial coherence.

The wideband spectrometer (the DZB) currently being built for the WSRT makes it possible to search for and study weakly polarized structure over a much wider range of *RM*. The side-lobe levels in the RMTF that occur with an 8-channel system will be much reduced when 128 frequency channels can be used to cover a wide (80 MHz) low frequency band.

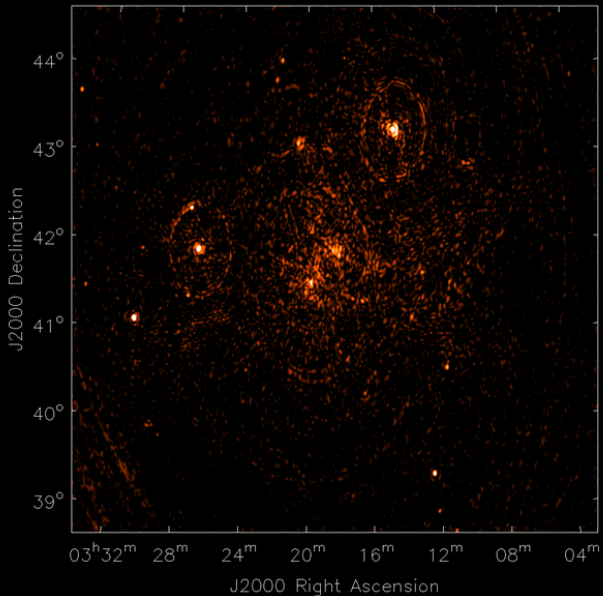
Very small variations in *RM* can be expected to occur close to the core of AGN when polarized structure moves relative to a foreground Faraday screen. With a sensitivity of 0.1 rad/m² extremely sensitive measurements of the ionized gas around polarized radio sources can be made. If several sources with a well-determined *RM* are found within the synthesized field of view the fundamental limit imposed by the uncertainty of the ionospheric *RM* can be avoided by the study of *differential RM* variations. The diffuse galactic background emission, which is highly polarized at low frequencies, and has a typical *RM* of $\approx 5\text{--}10 \text{ rad/m}^2$, may well be useful as a non-variable *RM* reference.

The range in *RM* where the RM-synthesis technique will be a useful tool depends on frequency. At 1400 MHz, and a bandwidth of 160 MHz, this range begins at a few hundred rad/m². A practical limit, in real radio sources, will occur when depolarization due to fine-scale structure in *RM* within the beam, i.e. beam-depolarization, begins to dominate over bandwidth-depolarization.

A final intriguing possibility opened up by low frequency wide-band polarimetry is the study of the Faraday rotating material *within* radio sources. The Fourier-relationship between the complex polarization and the 'Faraday depth' suggests that observations over a large range in frequency may be used to derive information about the spatial disposition of the emitting and depolarizing material.

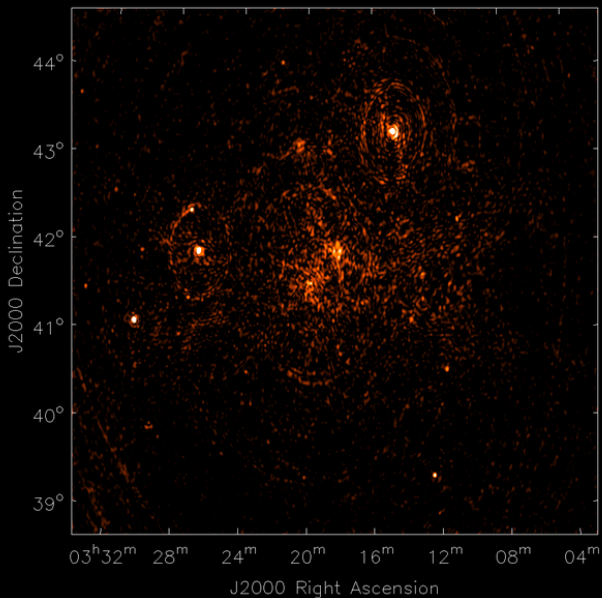
RM = -30 rad/m²

ASTRON



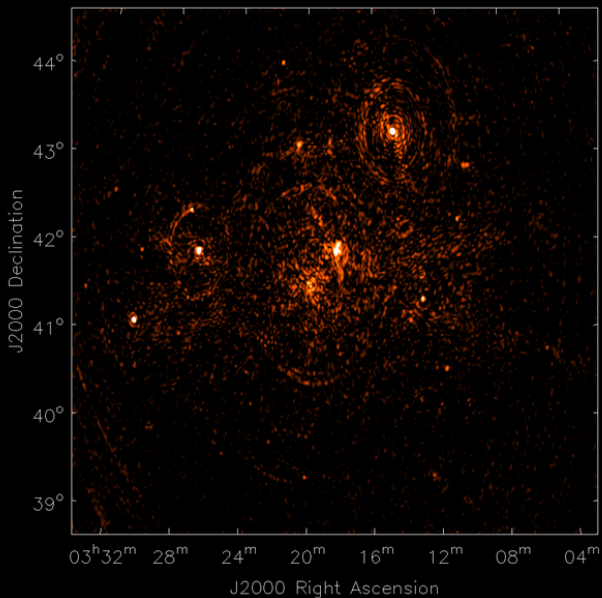
$\text{RM} = -27 \text{ rad/m}^2$

ASTRON



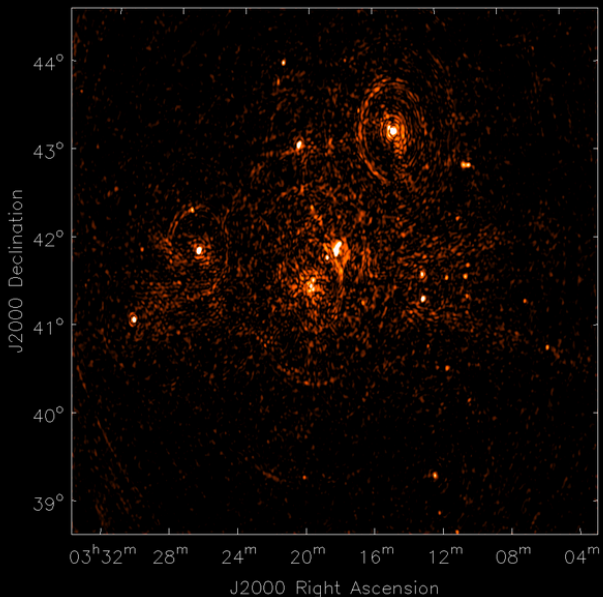
RM = -24 rad/m²

ASTRON



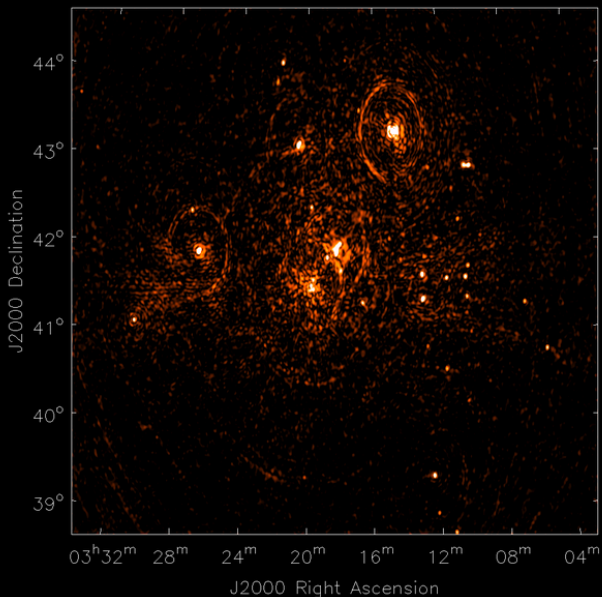
RM = -21 rad/m²

ASTRON



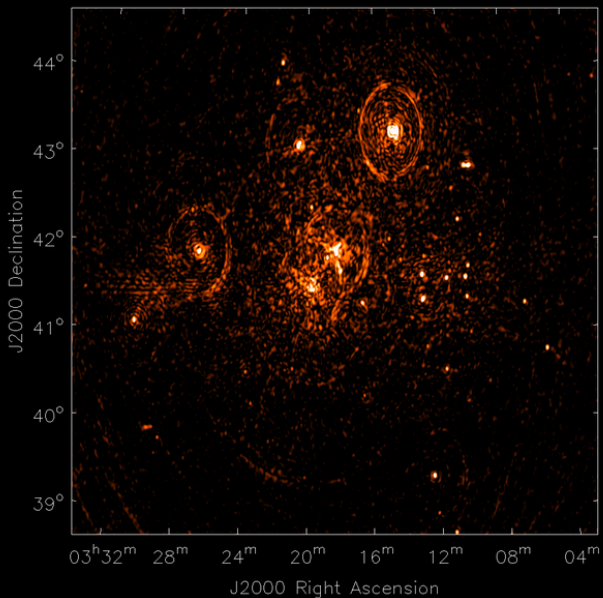
RM = -18 rad/m²

ASTRON



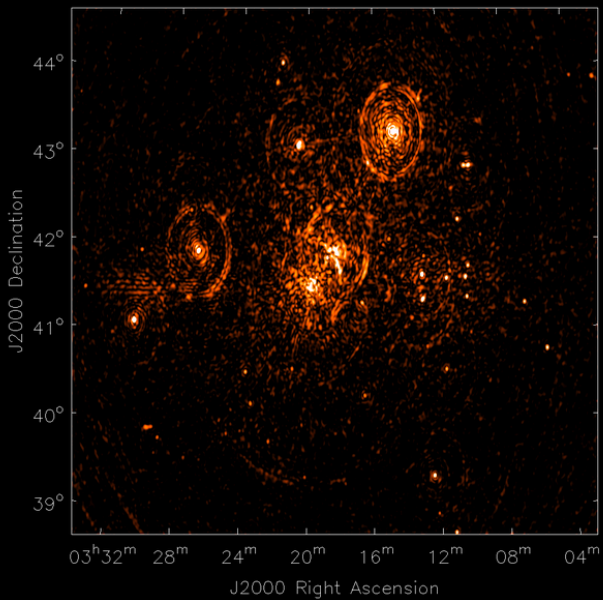
RM = -15 rad/m²

ASTRON



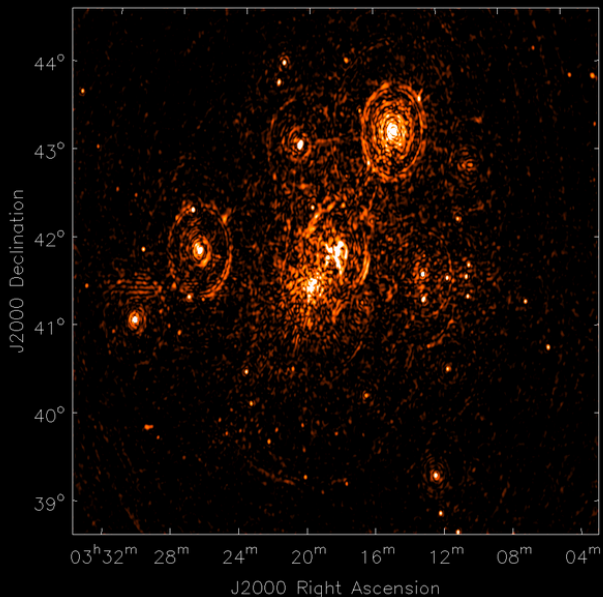
RM = -12 rad/m²

ASTRON



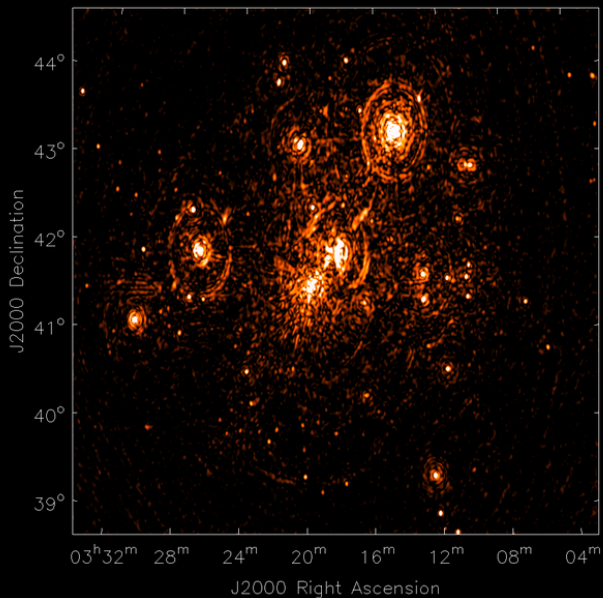
RM = -9 rad/m²

ASTRON



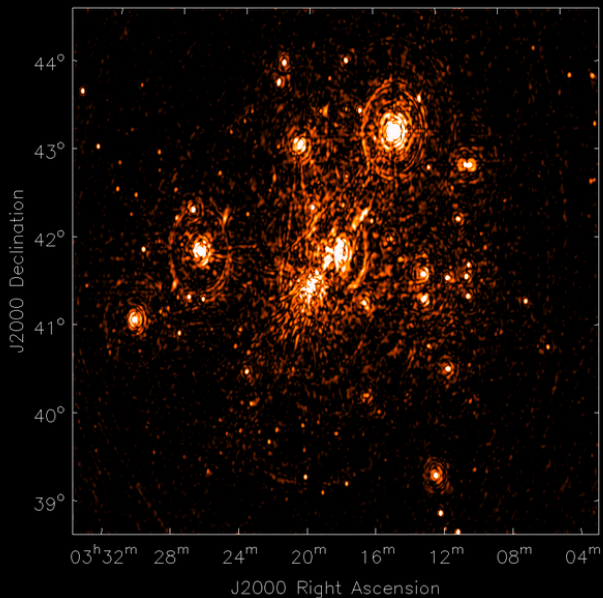
RM = -6 rad/m²

ASTRON



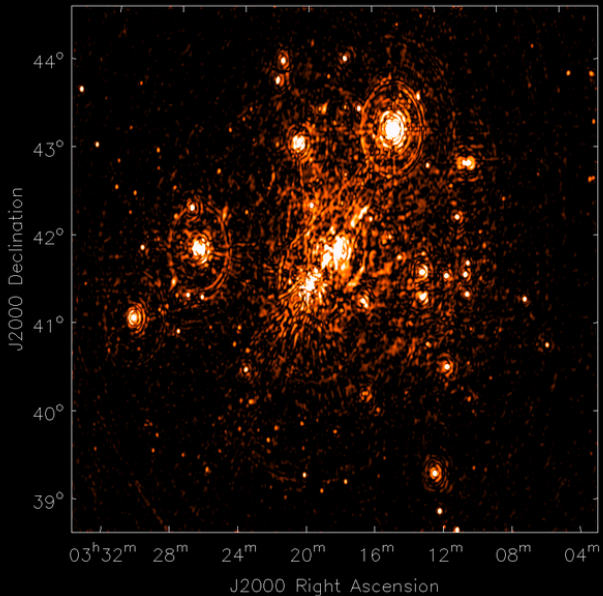
RM = -3 rad/m²

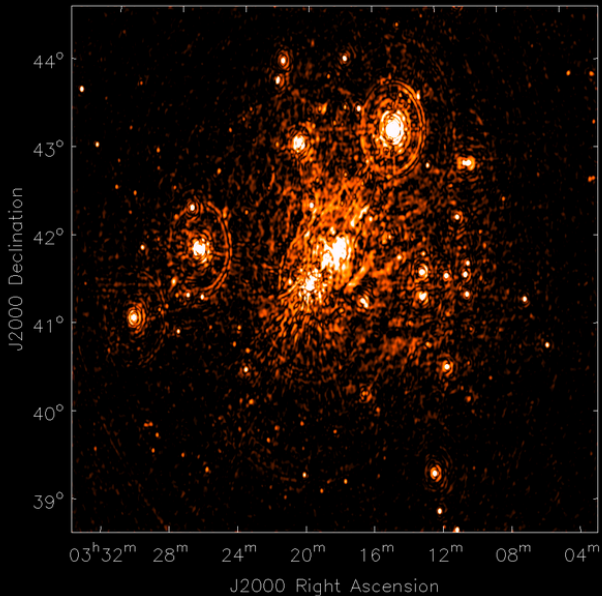
ASTRON

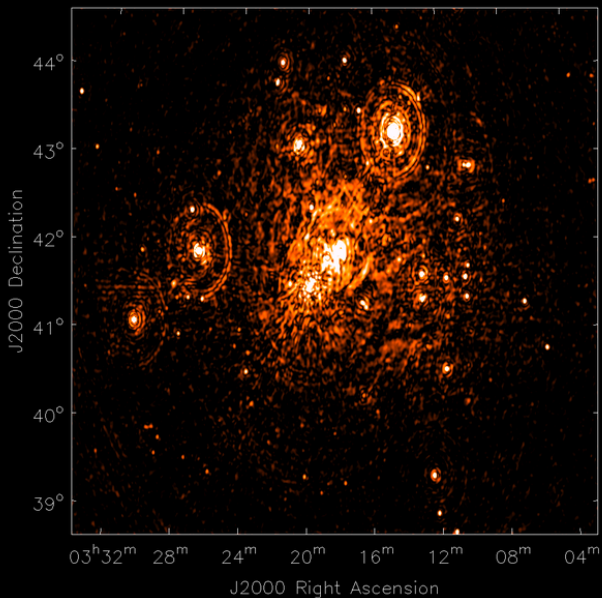


RM = 0 rad/m²

ASTRON

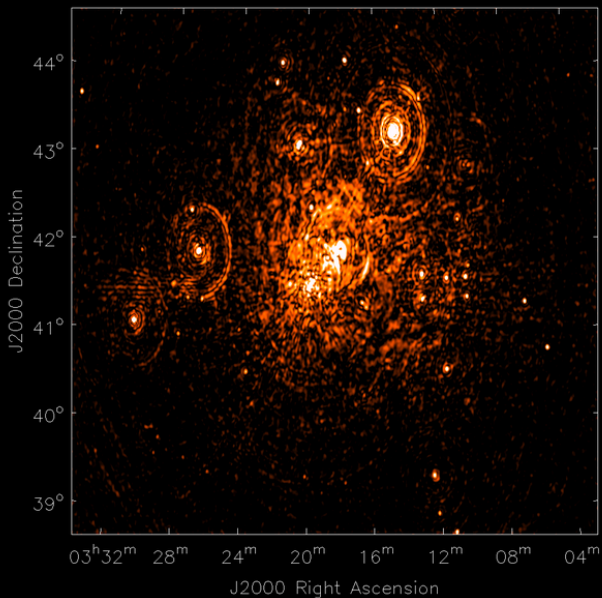






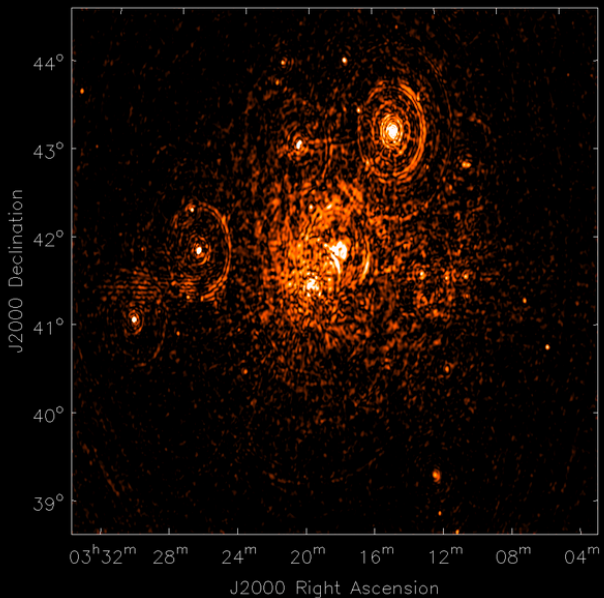
RM = 9 rad/m²

ASTRON



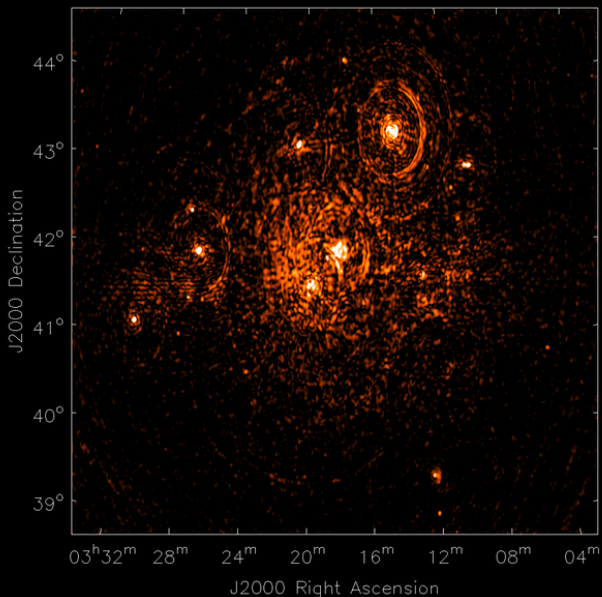
RM = 12 rad/m²

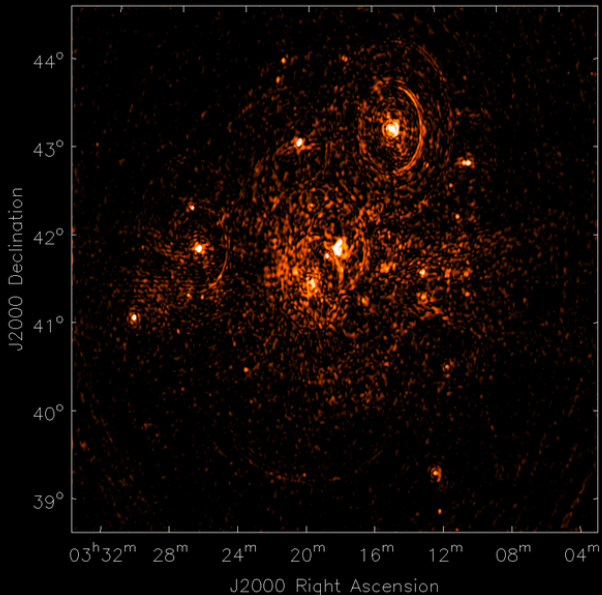
ASTRON



RM = 15 rad/m²

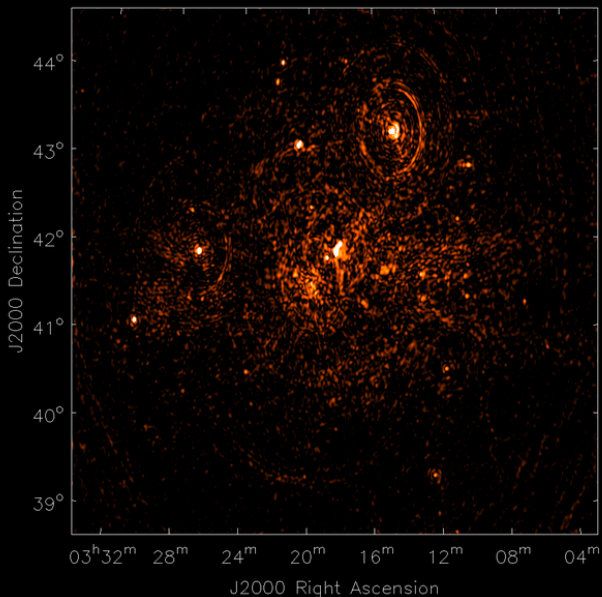
ASTRON





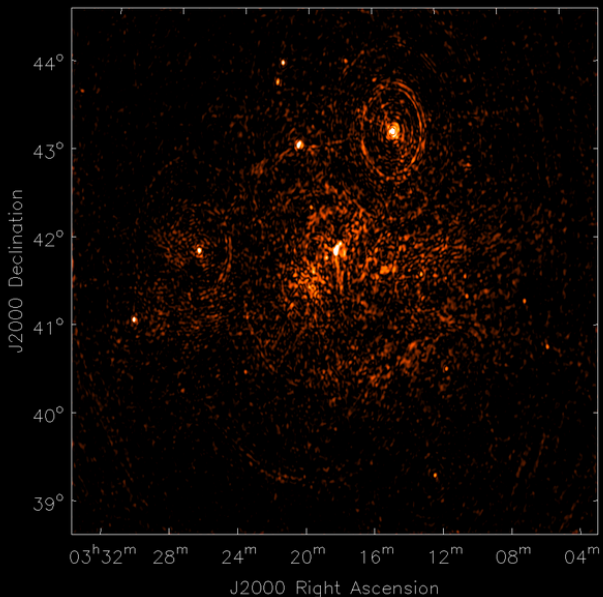
RM = 21 rad/m²

ASTRON



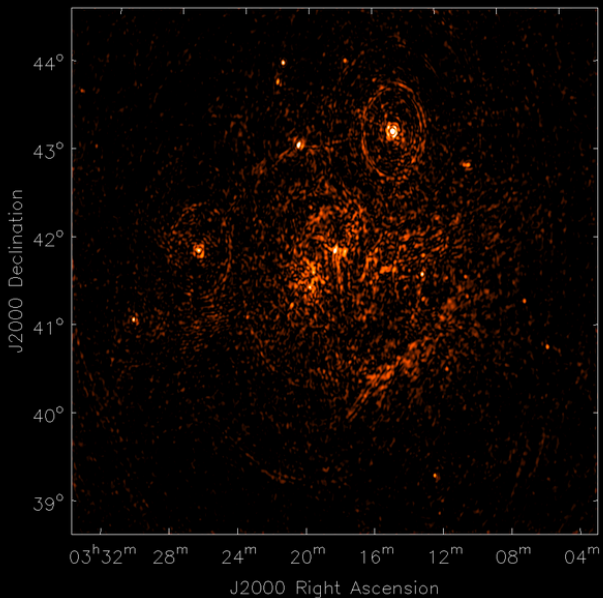
RM = 24 rad/m²

ASTRON



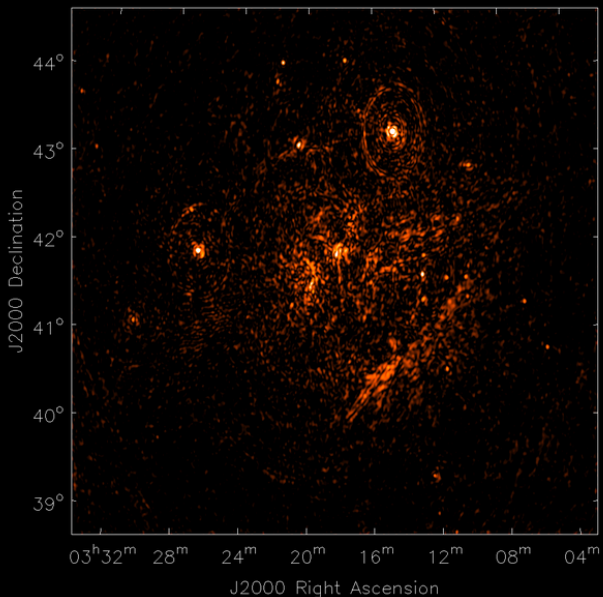
RM = 27 rad/m²

ASTRON



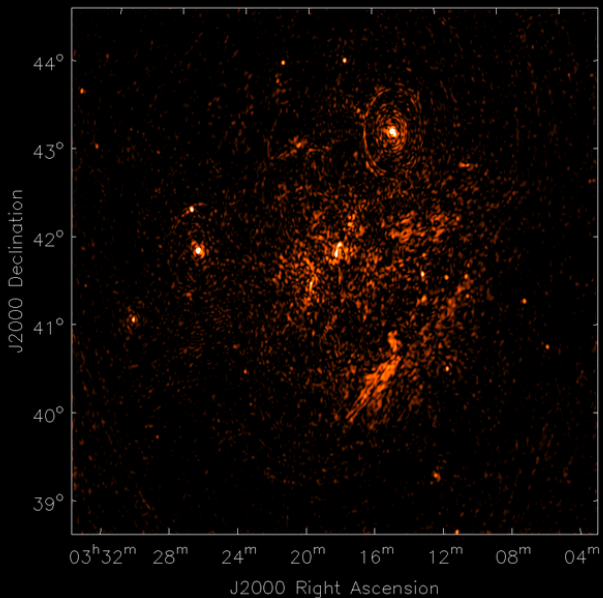
RM = 30 rad/m²

ASTRON



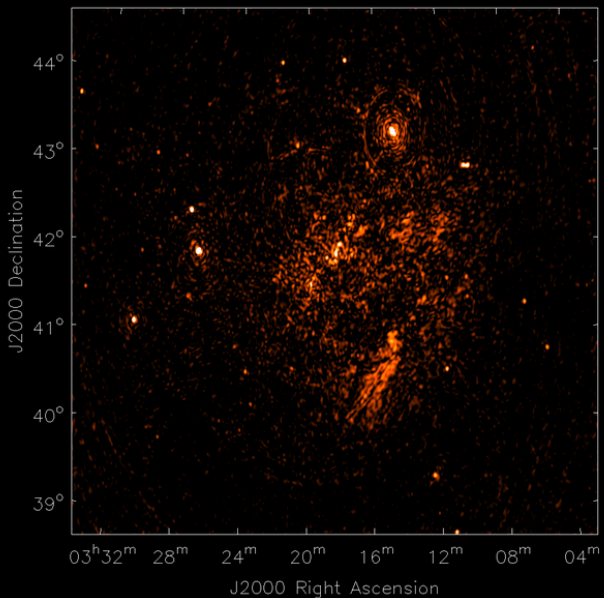
RM = 33 rad/m²

ASTRON



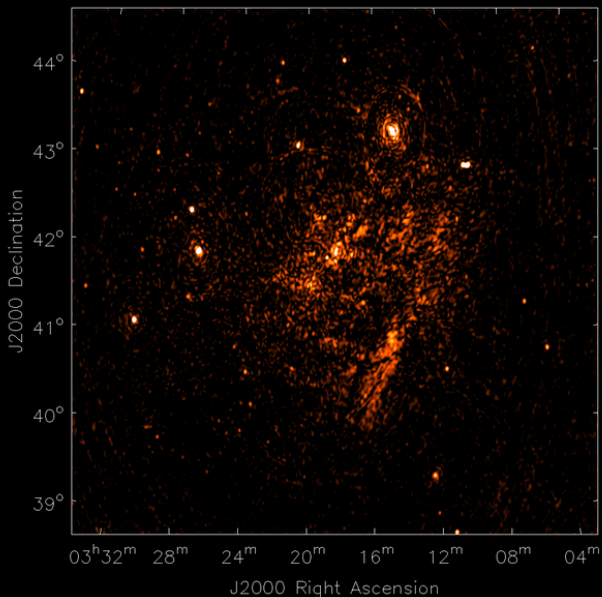
RM = 36 rad/m²

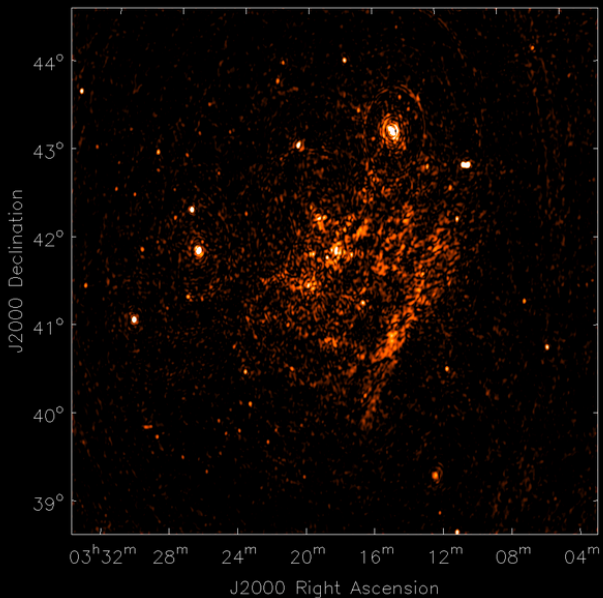
ASTRON



RM = 39 rad/m²

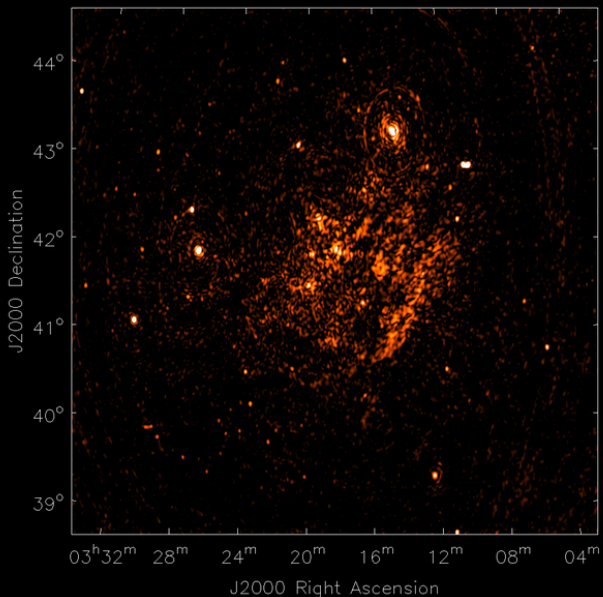
ASTRON





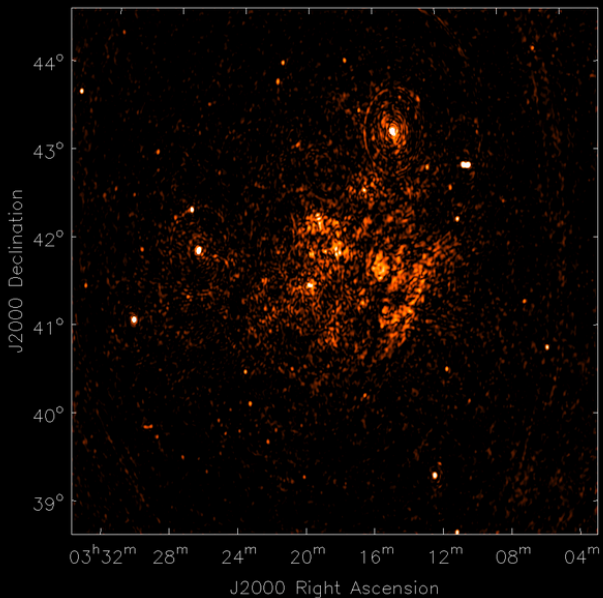
RM = 45 rad/m²

ASTRON



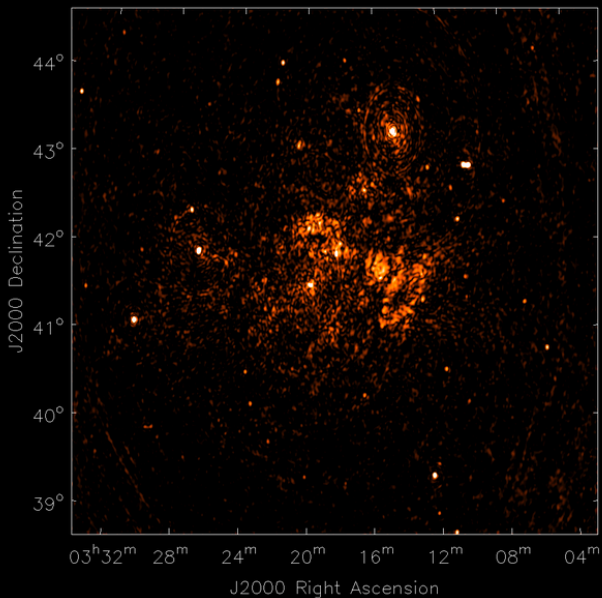
RM = 48 rad/m²

ASTRON



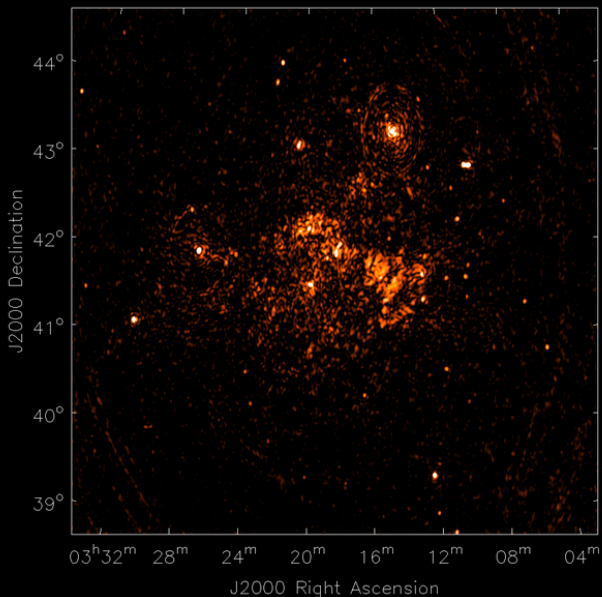
RM = 51 rad/m²

ASTRON



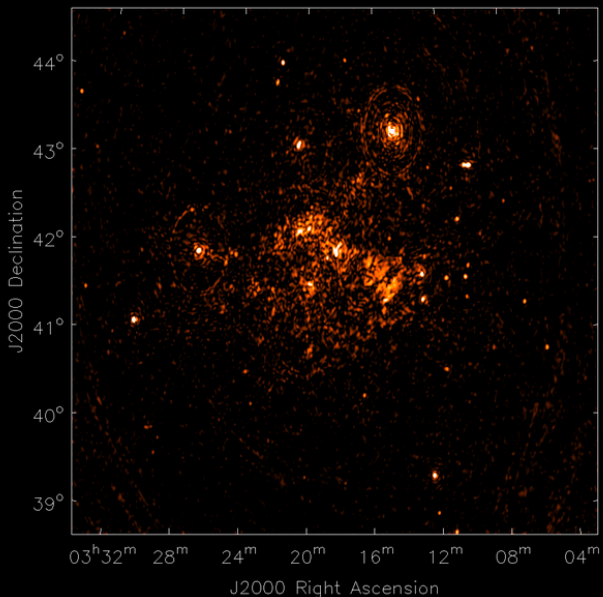
RM = 54 rad/m²

ASTRON



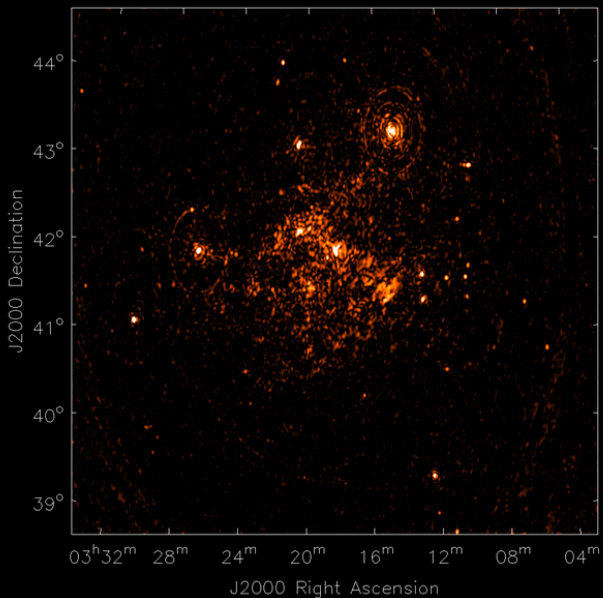
RM = 57 rad/m²

ASTRON



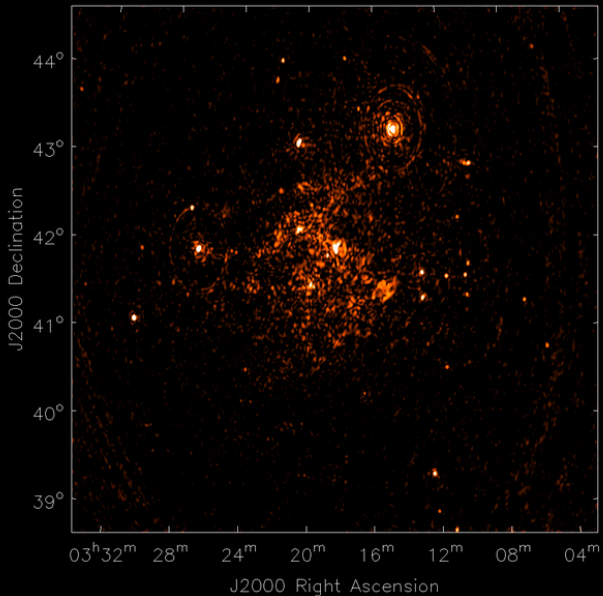
RM = 60 rad/m²

ASTRON



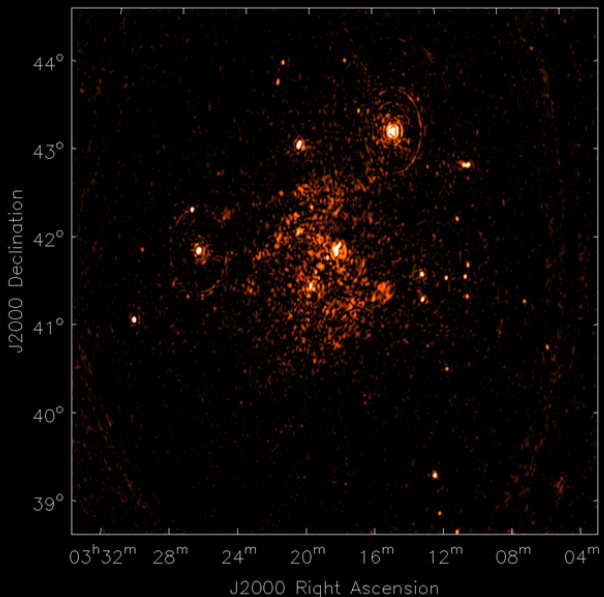
RM = 63 rad/m²

ASTRON



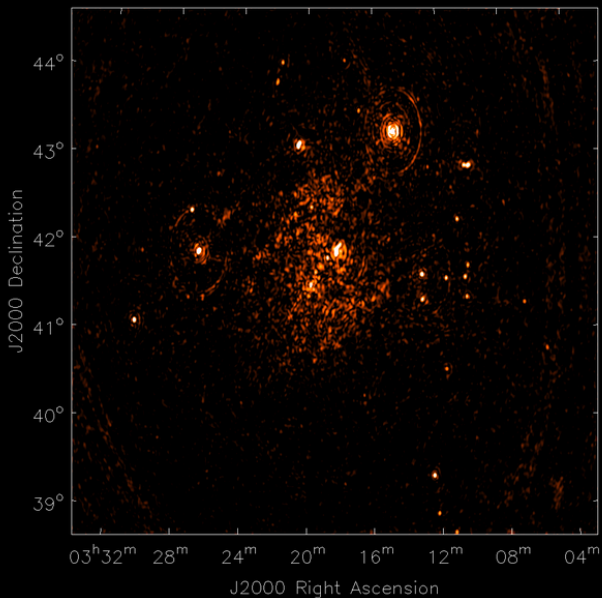
RM = 66 rad/m²

ASTRON



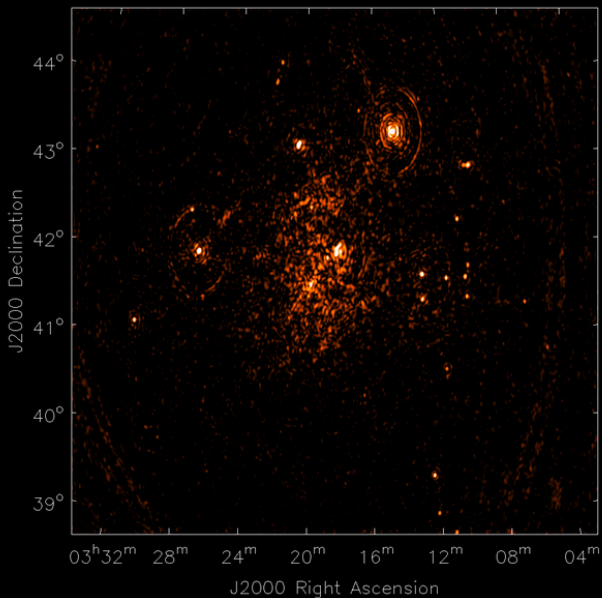
RM = 69 rad/m²

ASTRON



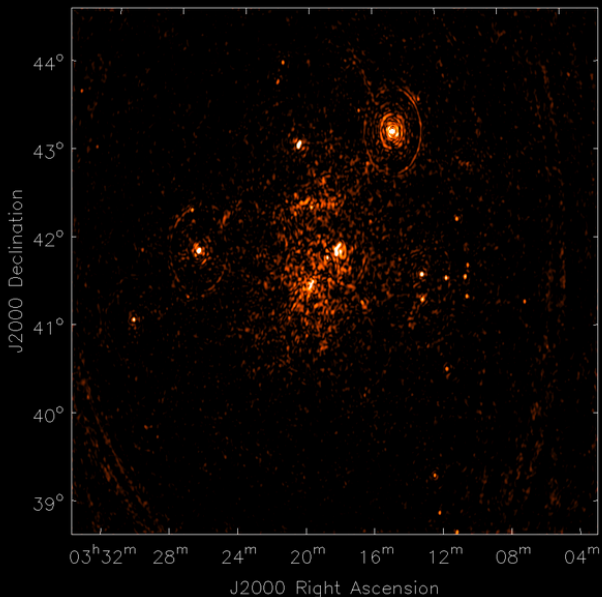
RM = 72 rad/m²

ASTRON



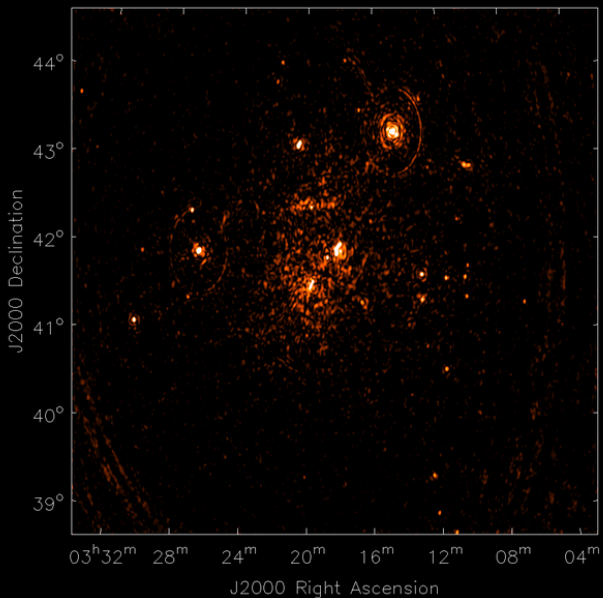
RM = 75 rad/m²

ASTRON



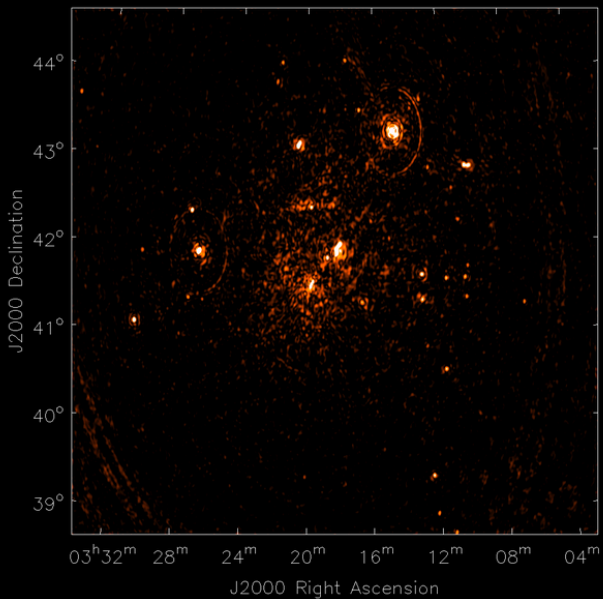
RM = 78 rad/m²

ASTRON



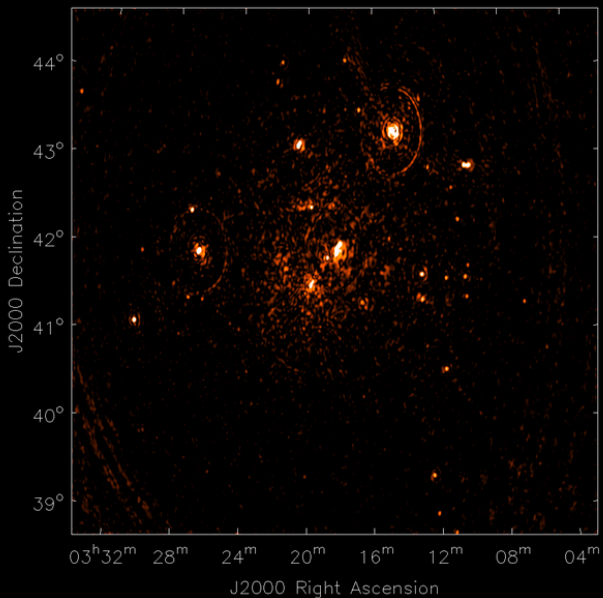
RM = 81 rad/m²

ASTRON



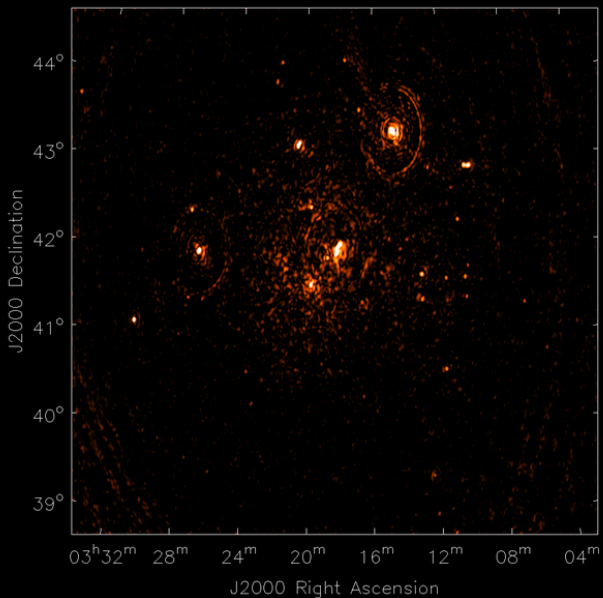
RM = 84 rad/m²

ASTRON



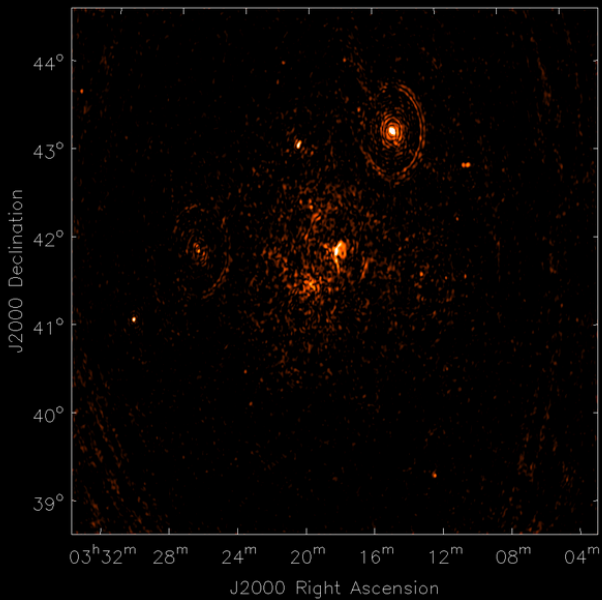
RM = 87 rad/m²

ASTRON



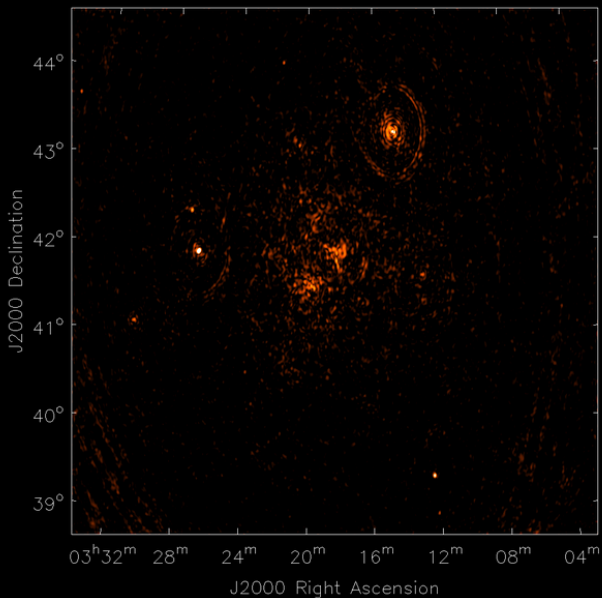
RM = 90 rad/m²

ASTRON



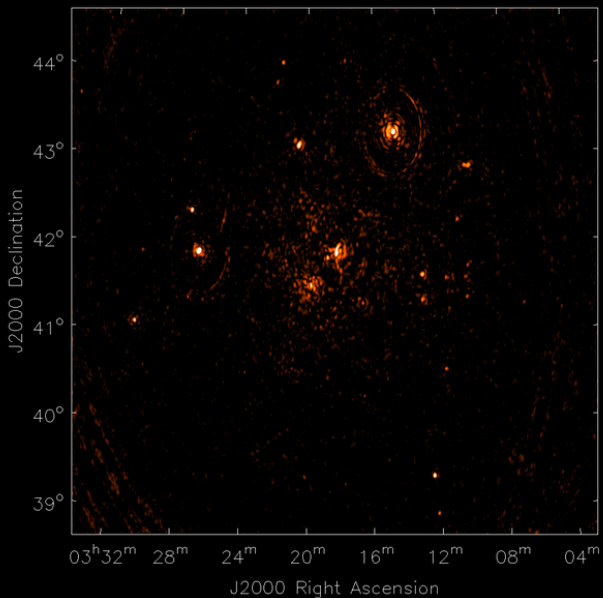
RM = 93 rad/m²

ASTRON



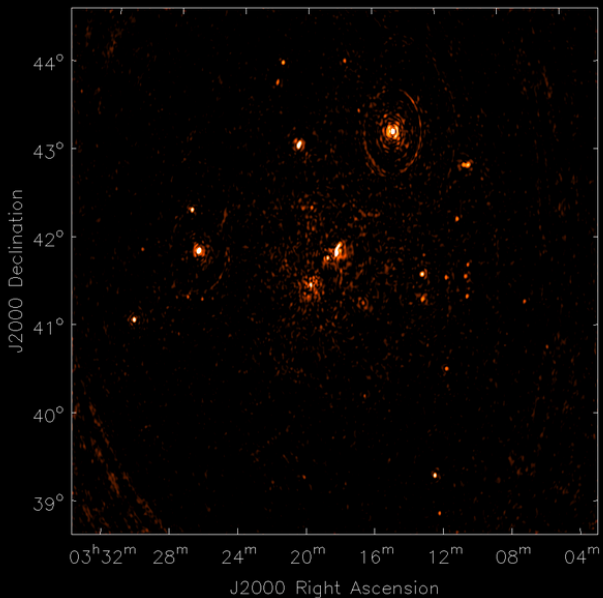
RM = 96 rad/m²

ASTRON



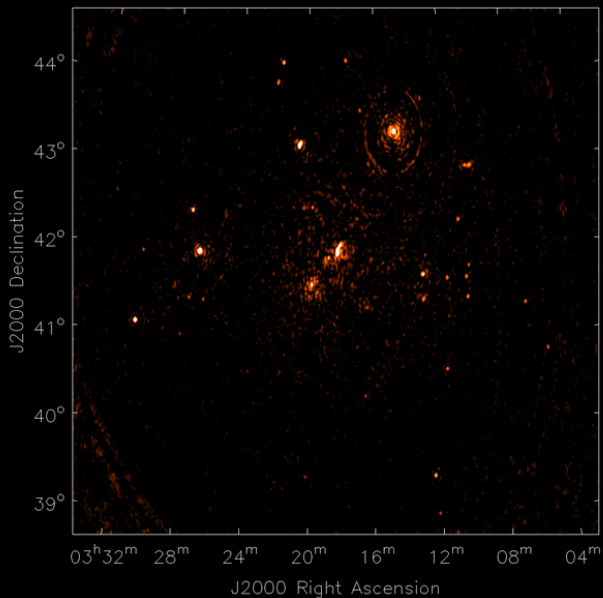
RM = 99 rad/m²

ASTRON



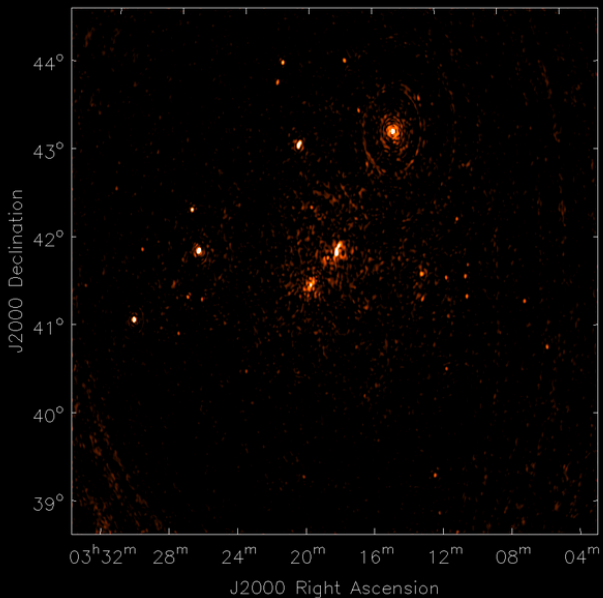
RM = 102 rad/m²

ASTRON



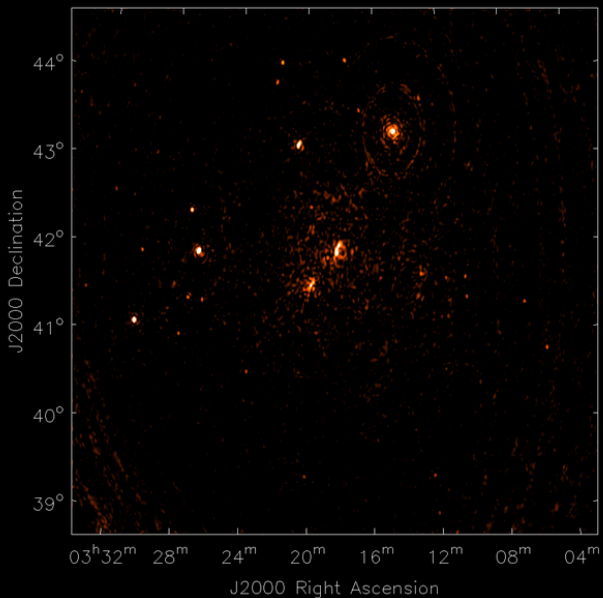
RM = 105 rad/m²

ASTRON



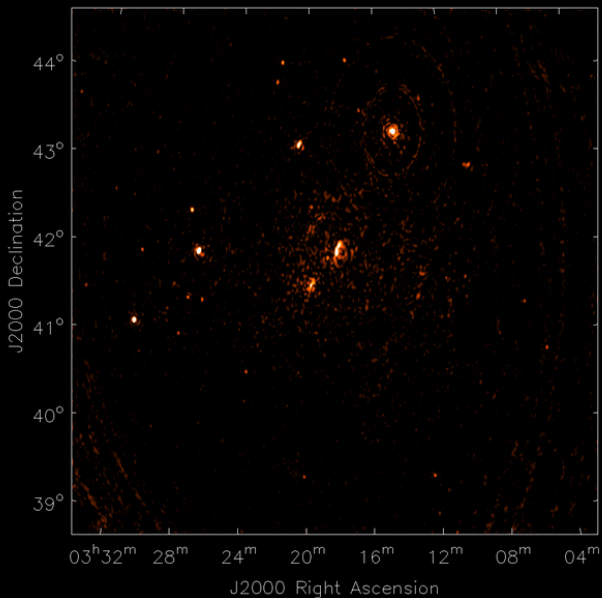
RM = 108 rad/m²

ASTRON



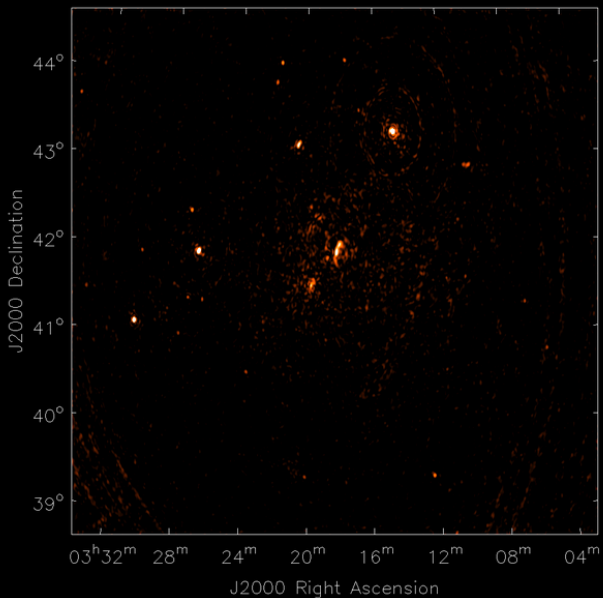
RM = 111 rad/m²

ASTRON



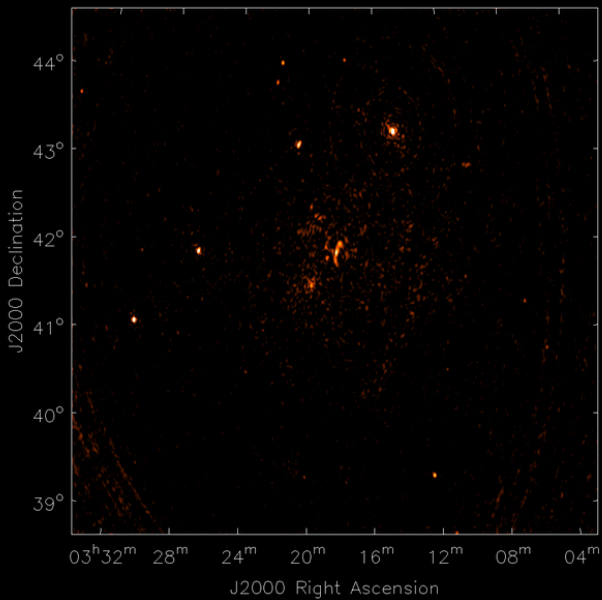
RM = 114 rad/m²

ASTRON



RM = 117 rad/m²

ASTRON

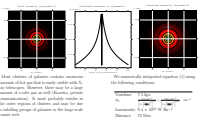


Diffuse Radio Emission From the Perseus Cluster

M.A. Brentjens and A.G. de Bruyn

ASTRON, Dwingeloo and Kapteyn Institute, Groningen

Introduction and simulations



Most clusters of galaxies contain numerous compact sources of hot gas that are mostly radio-quiet, but can also contain diffuse radio emission. This emission consists of radio noise as well (radio-loud galaxies). It emits probably much more radio noise than radio-loud galaxies, but it is difficult to deduce the global properties of the large-scale emission.

It is difficult to detect this radio noise using X-ray. Therefore we attempt to detect it using the radio. We have developed a new technique: Thomson softening of synthesis. With our own computer software like the Faraday tomography algorithm, we can now detect the radio noise. We find the polarized spectrum of the cluster emission, and the total intensity spectrum in three cluster environments.

The total intensity ($\text{W} \cdot (\text{Hz})^{-1} \cdot \text{deg}^{-2}$) of the simulated environment grows by

$$I_{\text{tot}} = \int_{-\infty}^{\infty} F_{\text{tot}}(\nu) d\nu \frac{d\nu}{\nu} \quad (1)$$

where $F_{\text{tot}}(\nu)$ is the flux of a location due to the source and $d\nu/d\nu$ is the differential Thomson noise spectrum. ν is the differential Thomson noise spectrum.

Concerning the simulation output we find at 1, 0.3, 0.1, 0.03, ... MHz, only one square arcminute. At 100 MHz, the size of the radio source is the length of the polarized spectrum in spectrum space. At 1000 MHz, the size of the radio source is the length of the polarized spectrum in RM space. We detect this with the WSRT at our computer. In Fourier analysis and calculate suitable mean average.

WSRT Polarization imaging and RM synthesis

The highly polarized signal resulting from these simulated sources will be added to, and subtracted from, the real data of the Perseus cluster. The same parts of clusters of galaxies are removed from the real data as the parts of the very high RM field outside the cluster and lenses and depth deprojection effects. The remaining signal is then compared to the signal in the region bounded by NED 1275, NED 1280, and region 1000. The results are shown to be significantly stronger.

Our Galaxy introduces extra radio polarization noise due to the Faraday screen. We remove this noise by subtracting the radio signal from the Perseus cluster and the lensing cluster.

Figure 21 can observations of the Perseus cluster show late faint (about $10 \mu\text{Jy}/\text{MHz}$) low-frequency emission. The emission has a spectral spread over about 30 MHz and appears mostly radio-quiet. The emission is radio-loud. The required sensitivity and zero-wide bandwidth constraints are relaxed. The emission is detected after the rotation and through the RM deprojection analysis in single.

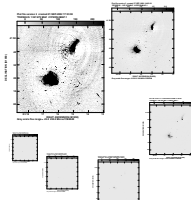
In order to characterize the Faraday screen and Faraday noise, we have acquired new low-frequency observations with the WSRT. The observations were made at 100 MHz, using 30 MHz total bandwidth, in 321 channels, ranging from 233 to 361 MHz.

Powers of ten



The figure on the left shows the visibility amplitude as a function of frequency for the epoch frequency on the right. From top to bottom, the visibility amplitude is for Epoch 1997 at 100, 200, 400, 800, 1600, and 3200 MHz. The figure on the right shows three components: the 100 MHz component (radio-loud), the 200 MHz component (radio-quiet), and the 3200 MHz component (radio-quiet).

The figure on the right shows the map on distances in the cluster. The left and right panels are for Epoch 1997 and the right panel is for Epoch 2002. The brightness scale of the peak to the surrounding extended emission is a scaling of 10⁻¹. The distance between the peaks is 100 kpc. The radio source is located at the center of the cluster.



The figure on the left shows the radio source at epoch 1997. The figure on the right shows the radio source at epoch 2002. The radio source is located at the center of the cluster. The distance between the peaks is 100 kpc.

References

- [1] A.G. de Bruyn, R.H. Lovell via email, low-frequency polarimetry, Thesis, University of Groningen, Groningen, 1998.
- [2] M.H. Wijnholds, Radio Polarization in the core of the Perseus PkD, Thesis, Leiden University, 2002.
- [3] G.J. de Bruyn, A. de Jong, T.J. Jolani, The 200 MHz spectral evolution of the radio source of NED 1275, *ApJ* 529:65-65, 2000.
- [4] G. Sijpkes, A radio continuum and polarization study of the radio source NED 1275, Thesis, Groningen University, 2002.
- [5] B.A. Synder, Interferometric polarization studies: Imaging and polarization of the radio source NED 1275, Thesis, Groningen University, 2002.
- [6] M.H. Wijnholds, A.G. de Bruyn, D. Jansen, H.W. Bremmer, and P. Kalberla, Small-scale polarization fluctuations in the radio source NED 1275, *A & A* 362:223-229, 2000.
- [7] M.H. Wijnholds, C.L. Rossetti, Electron scattering and polarization in radio clusters and radio galaxies, *ApJ* 534:145-155, November 2000.

The Westerbork Synthesis Radio Telescope is operated by the ASTRON (Netherlands Foundation for Research in Astronomical) with support from the Netherlands Foundation for Scientific Research (NWO).

WSRT Polarization imaging and RM synthesis

The highly polarized signal resulting from Thomson scattered emission will be added to, and confused by, any polarized diffuse emission from the cluster itself. The inner parts of clusters ($\theta < 10'$) are depolarized by the combined effects of the very high RM, its small scale structure and beam and depth depolarization effects. There is, however, also weak 92 cm diffuse emission in the region bounded by NGC 1275, NGC 1265 and IC 310, where depolarization effects are expected to be significantly smaller.

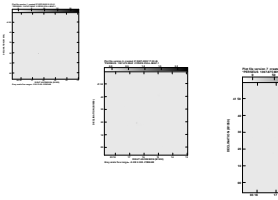
Our Galaxy interferes with this polarized emission in two ways. First, it Faraday-rotates any extragalactic polarized signal from the Perseus cluster, and second, it adds its own often strongly polarized emission.

Previous 21 cm observations of the Perseus cluster have shown faint (about $30 \mu\text{Jy}/30''$ beam) but highly structured polarized emission spread over about $30'$ diameter and approximately centered at 3C 84 / NGC 1275. The improved sensitivity and new wide bandwidth correlator at the WSRT should allow us to characterize this emission and through its RM distribution ascertain its origin.

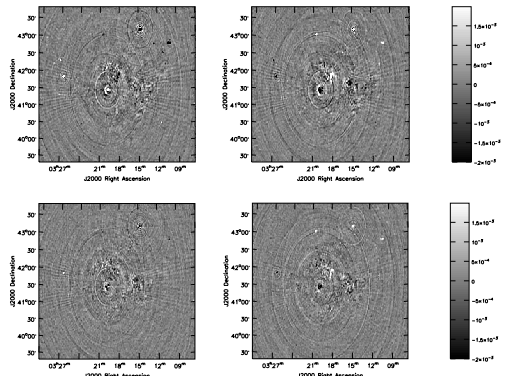
In order to disentangle the Faraday rotation and foreground emission effects we have acquired new low frequency observations with the WSRT in December 2002. We obtained a total of 6×12 hours spanning 70 MHz total bandwidth divided in 512 channels, ranging from 315 to 385 MHz.

The new wideband data allows a sensitive search in 'RM-space' across a field of view (about 3 degrees), hence extending well beyond the Perseus cluster. It should therefore allow us to separate cluster and foreground contributions. Images in RM space are coherently summed Q and U images for a range of acceptable RM values. We expect the polarization sensitivity to be better than $100 \mu\text{Jy}/1''$ beam. We hope to acquire new 21 cm observations next winter.

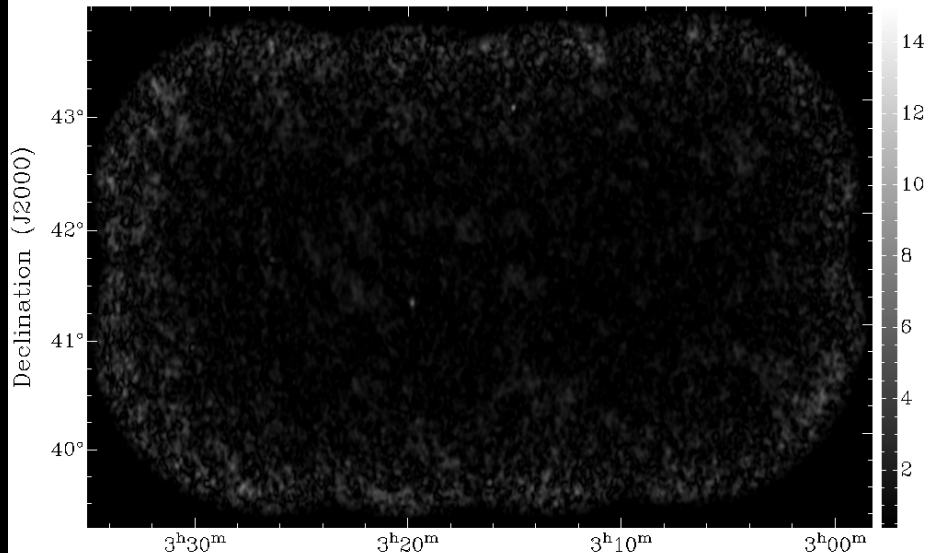
Shown below are pairs of Q and U images (hor.) for RMs of 50 and 60 rad m $^{-2}$ (vert.).



First results suggest that we have detected polarized emission from both the Perseus cluster and the Galactic foreground. The detected polarized emission is at a level of 0.5 to $1 \text{ mJy}/2''$ beam.



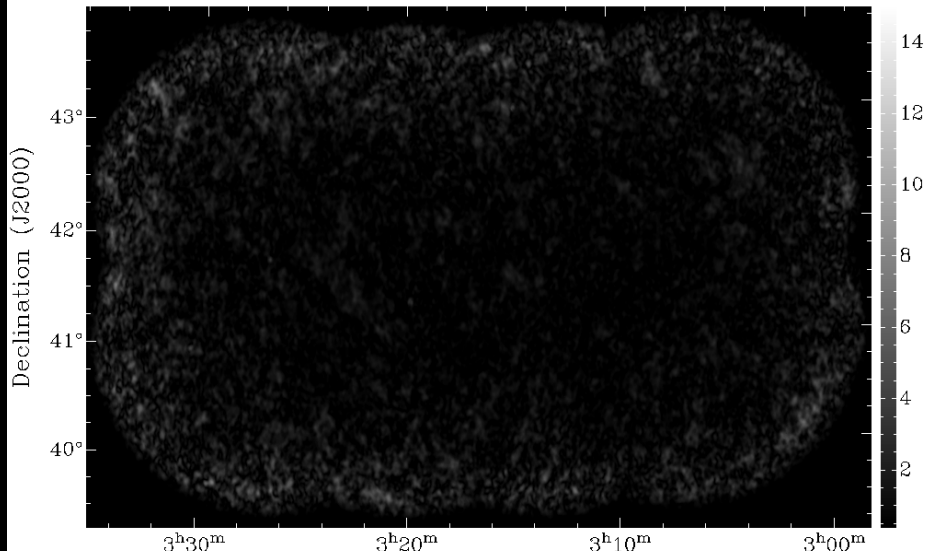
RM: -1.920000e+02



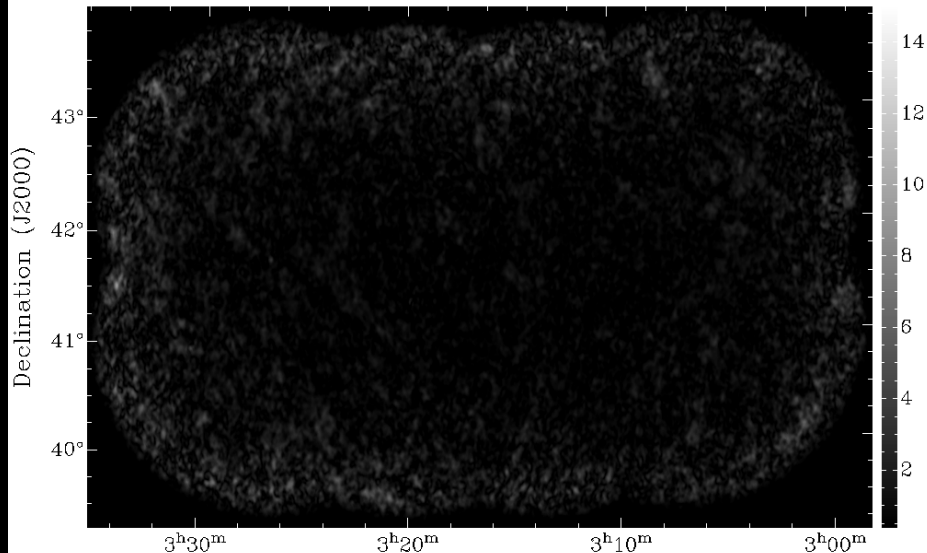
RM: -1.890000e+02



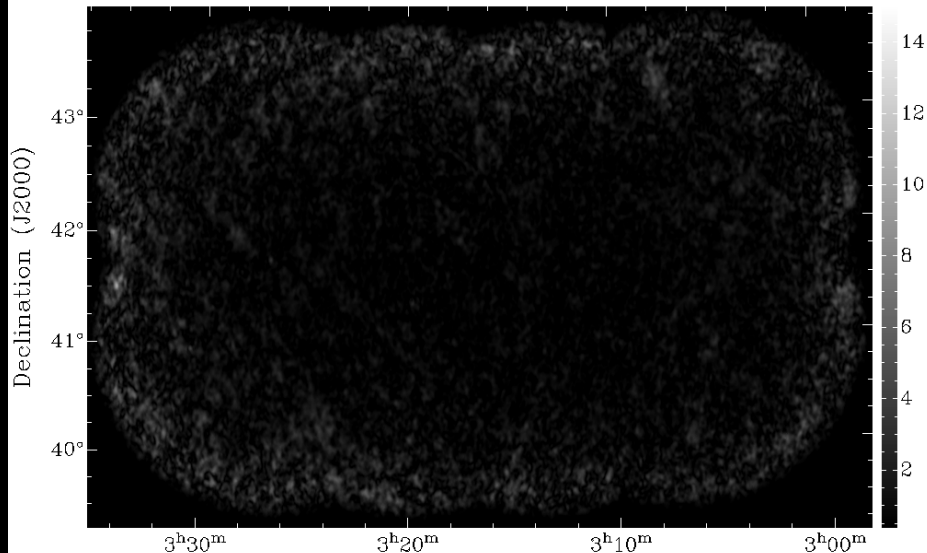
RM: -1.860000e+02



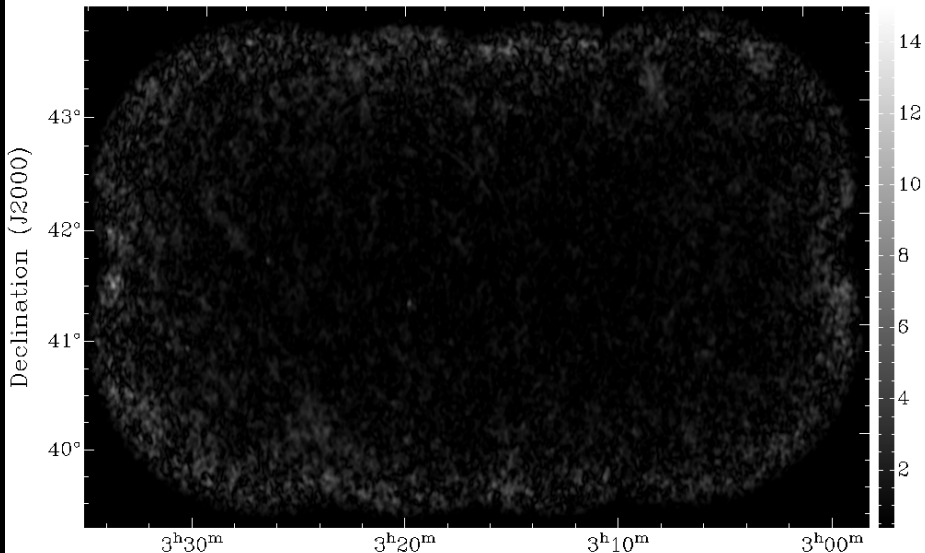
RM: -1.830000e+02



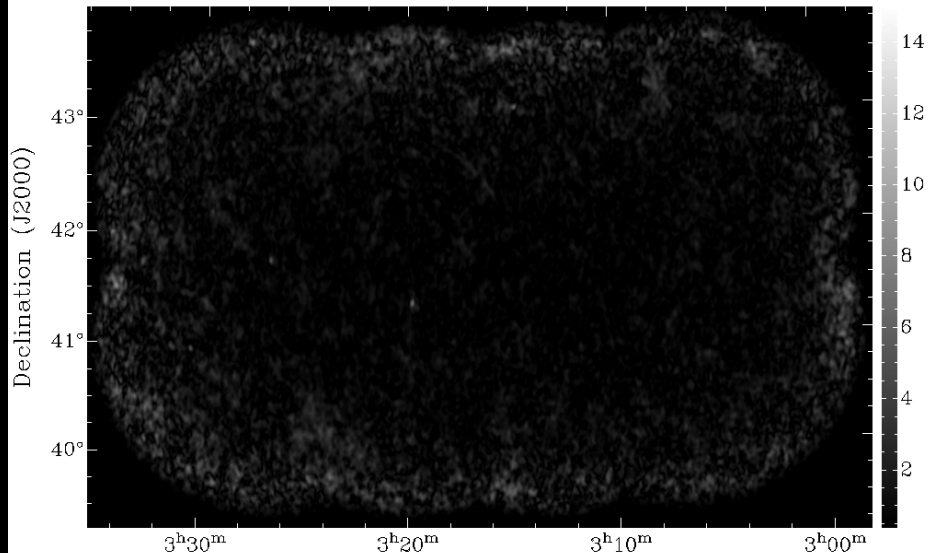
RM: -1.800000e+02



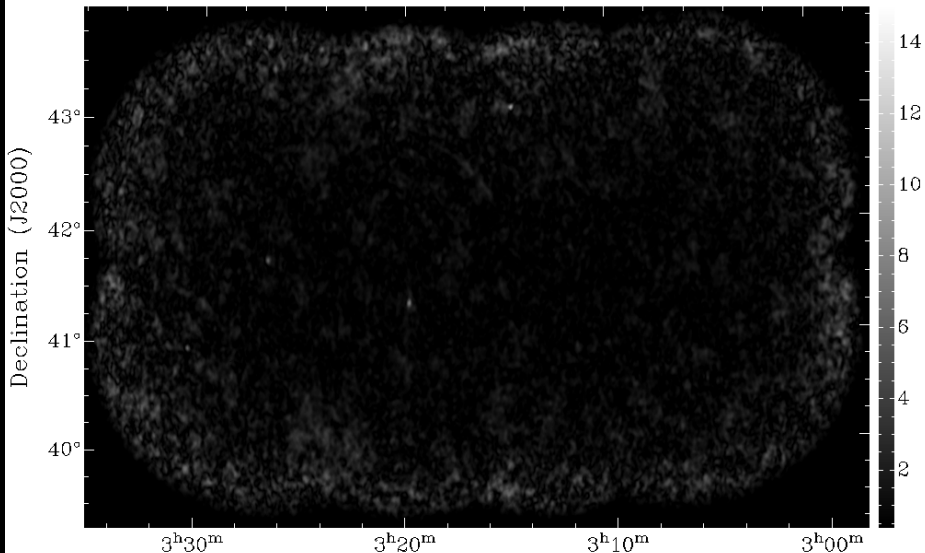
RM: -1.770000e+02



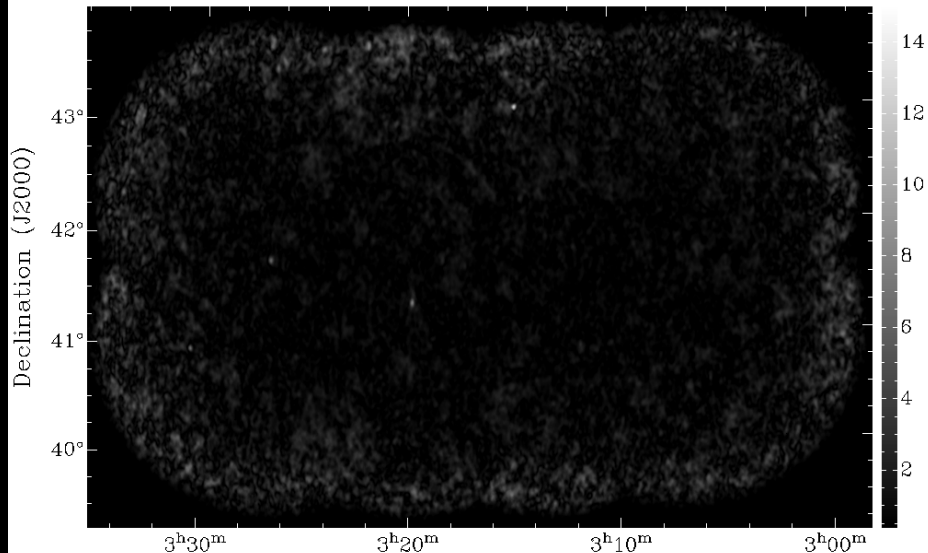
RM: -1.740000e+02



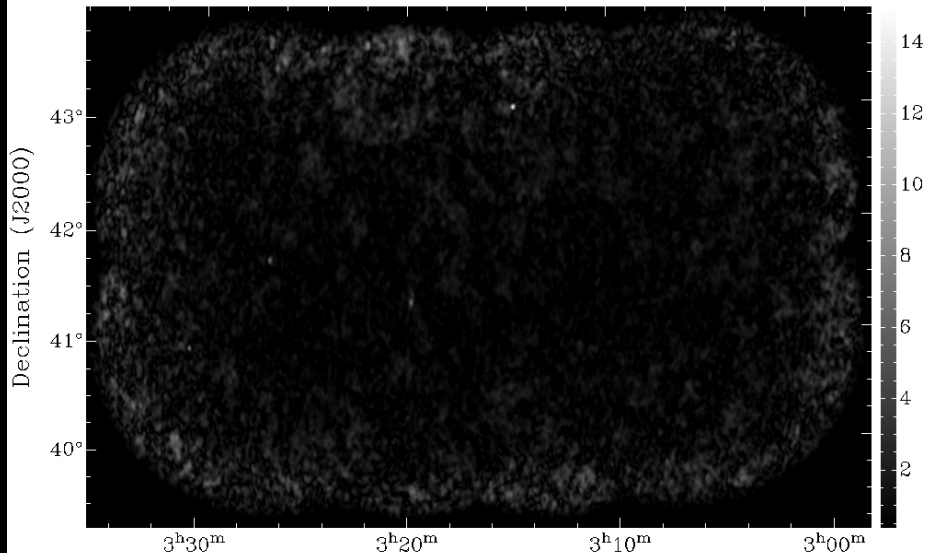
RM: -1.710000e+02



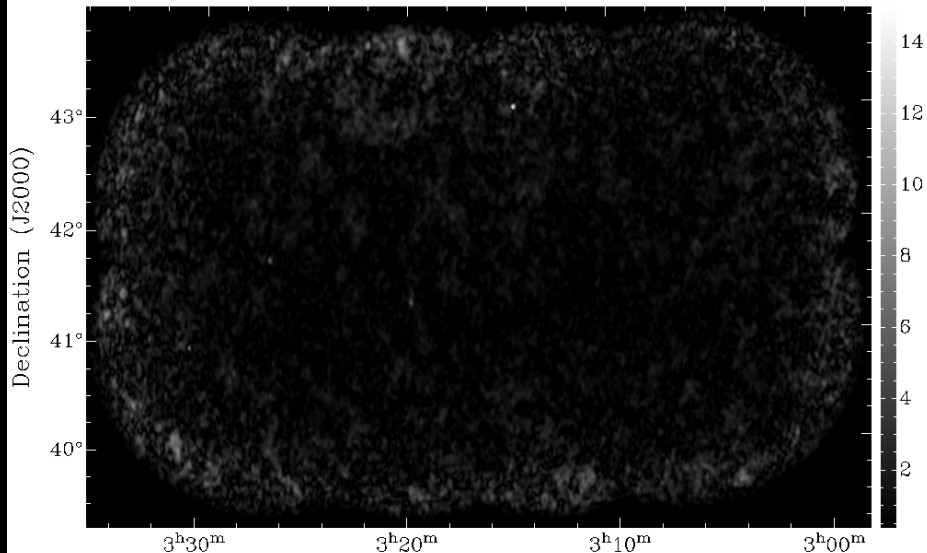
RM: -1.680000e+02



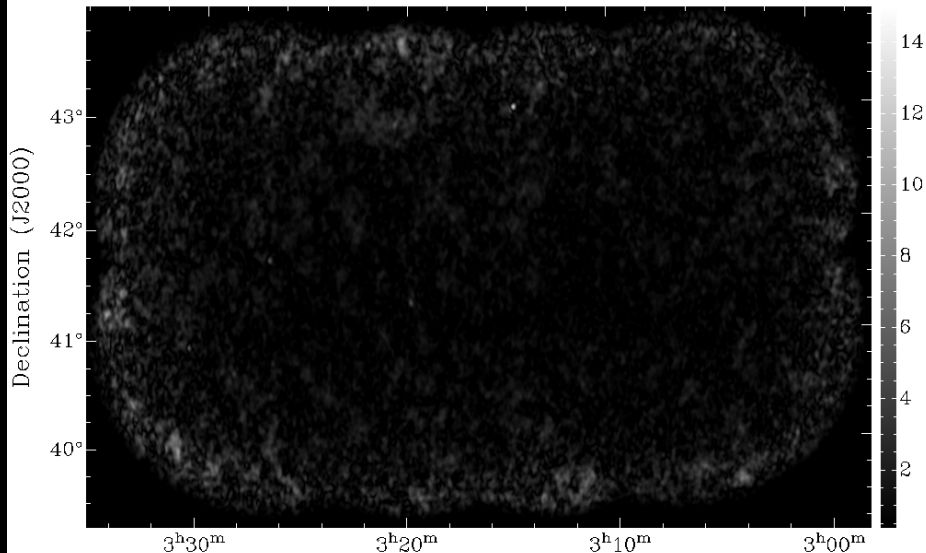
RM: -1.650000e+02



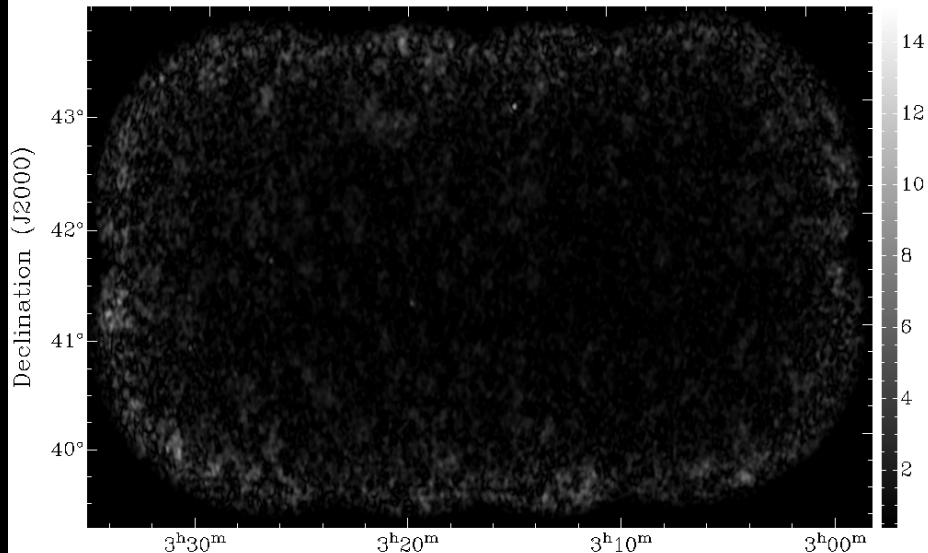
RM: -1.620000e+02



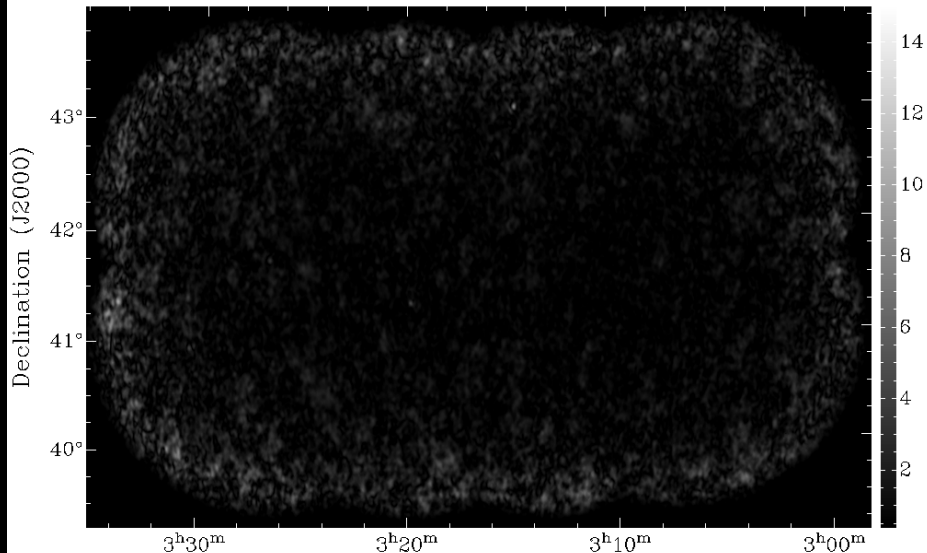
RM: -1.590000e+02



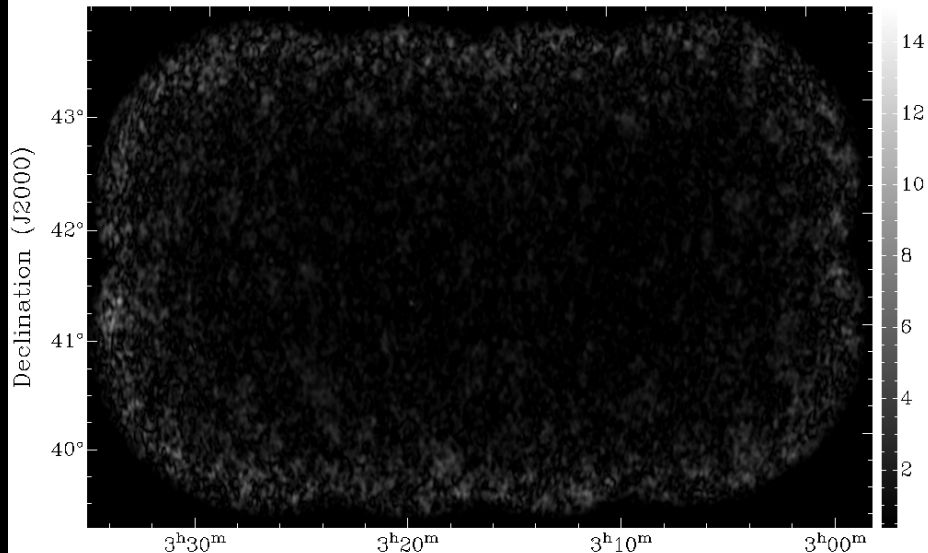
RM: -1.560000e+02



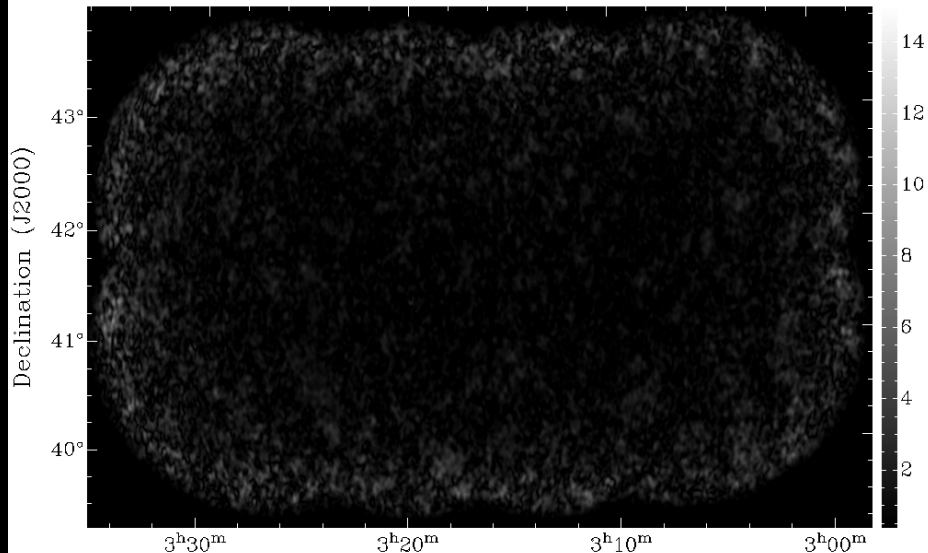
RM: -1.530000e+02



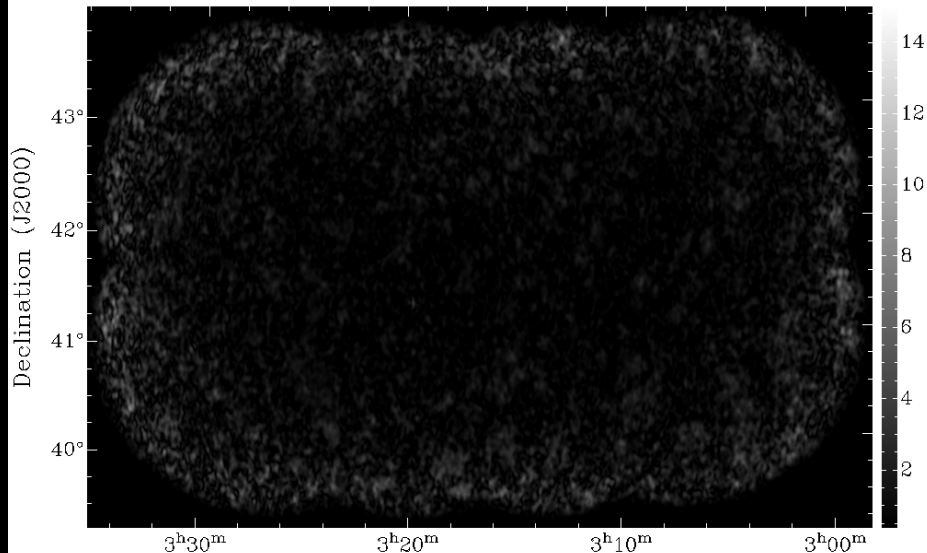
RM: -1.500000e+02



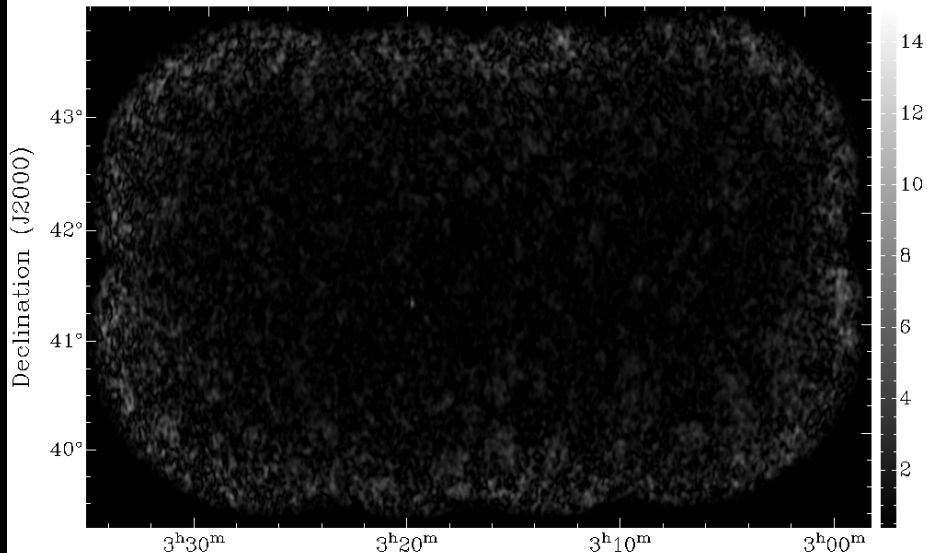
RM: -1.470000e+02



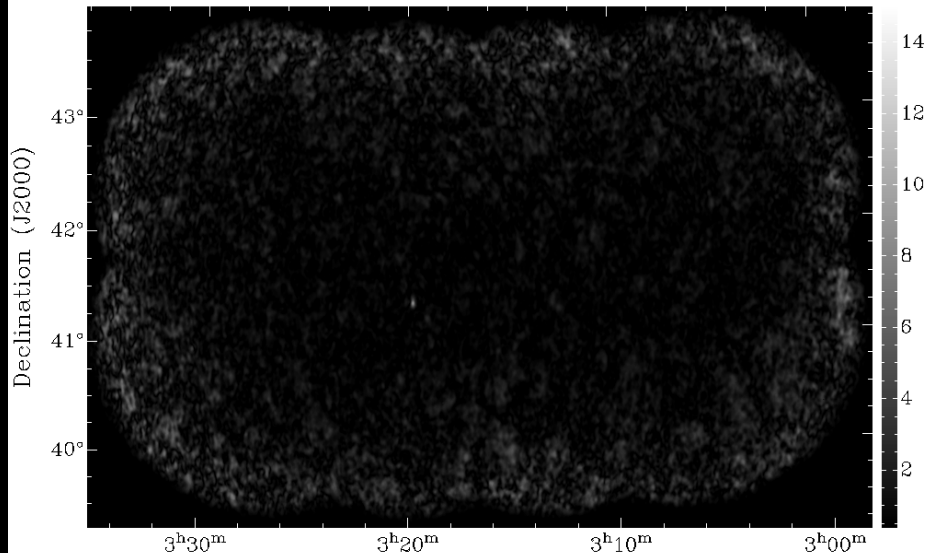
RM: -1.440000e+02



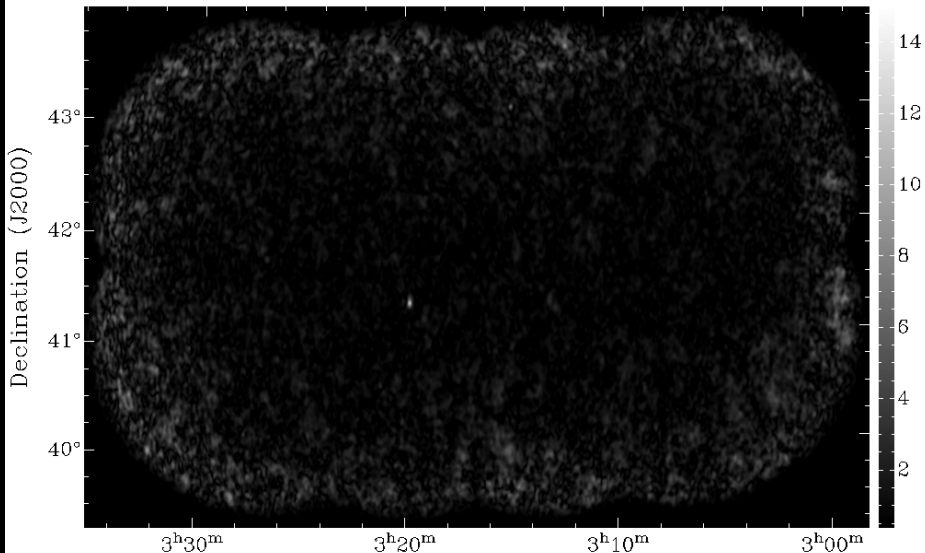
RM: -1.410000e+02



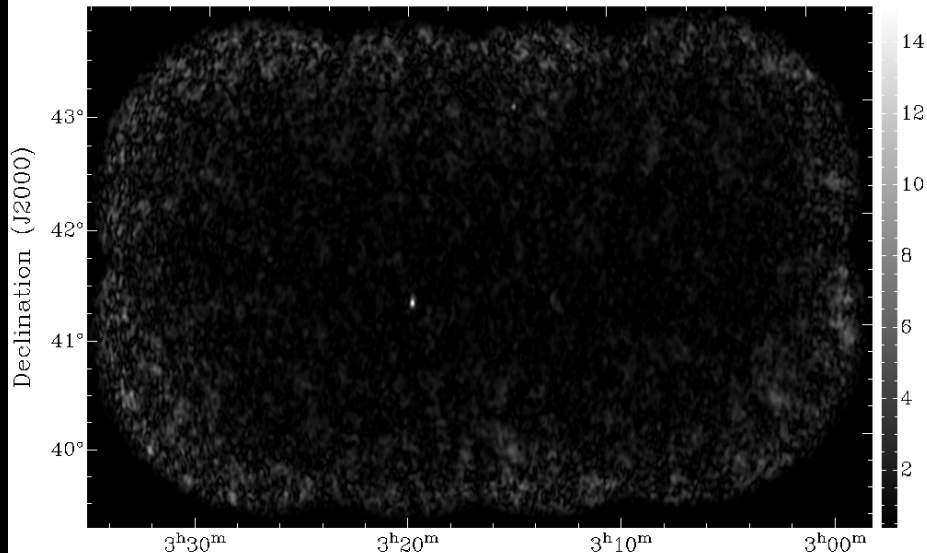
RM: -1.380000e+02



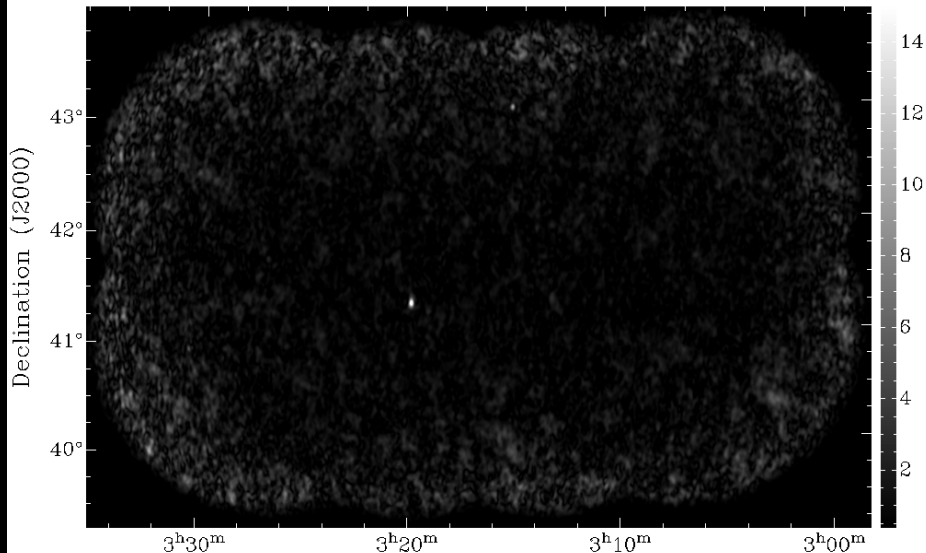
RM: -1.350000e+02



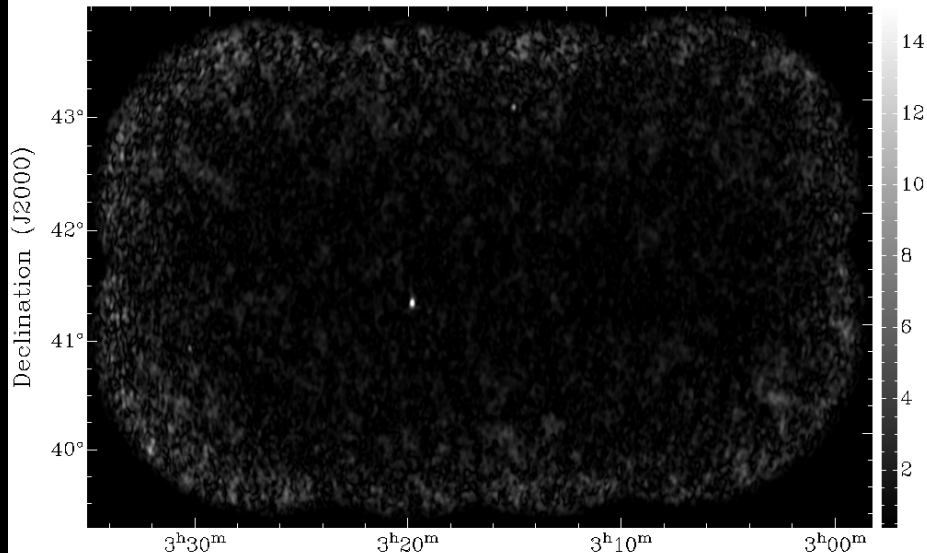
RM: -1.320000e+02



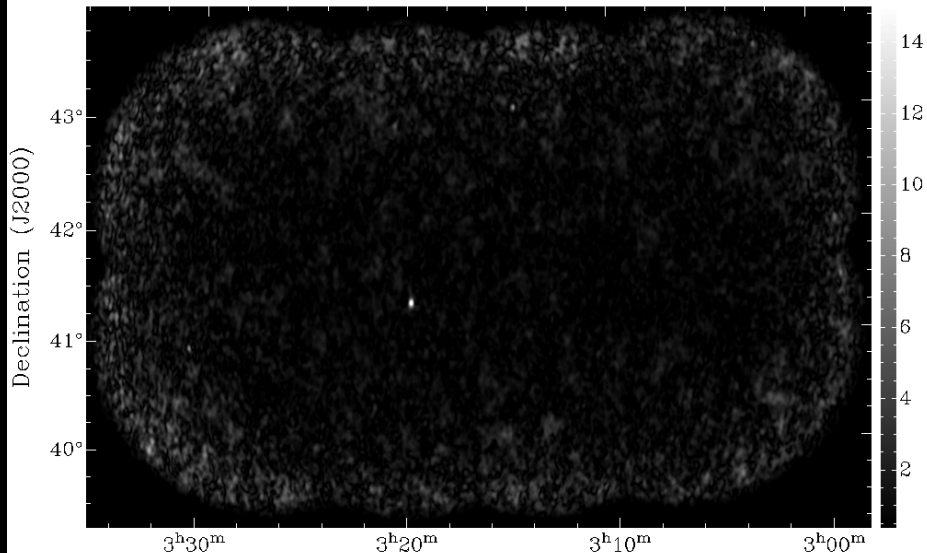
RM: -1.290000e+02



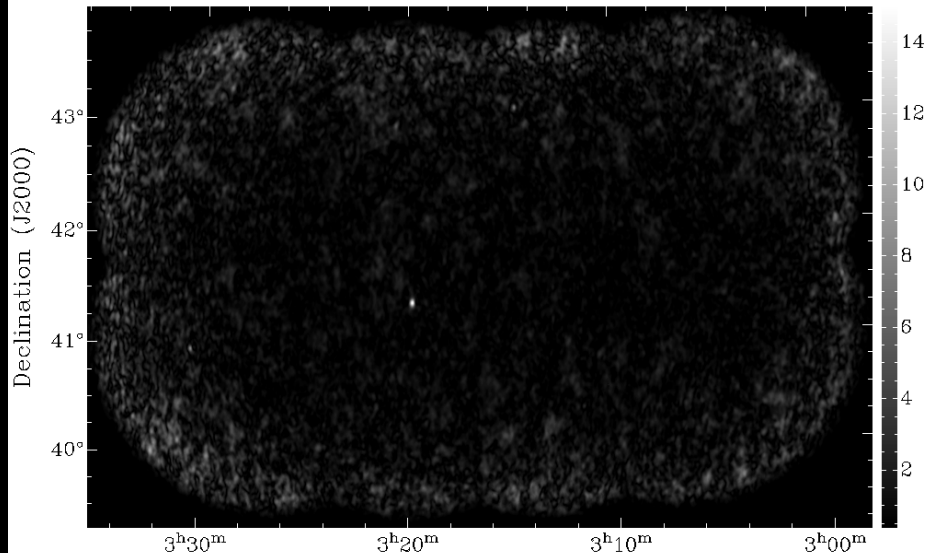
RM: -1.260000e+02



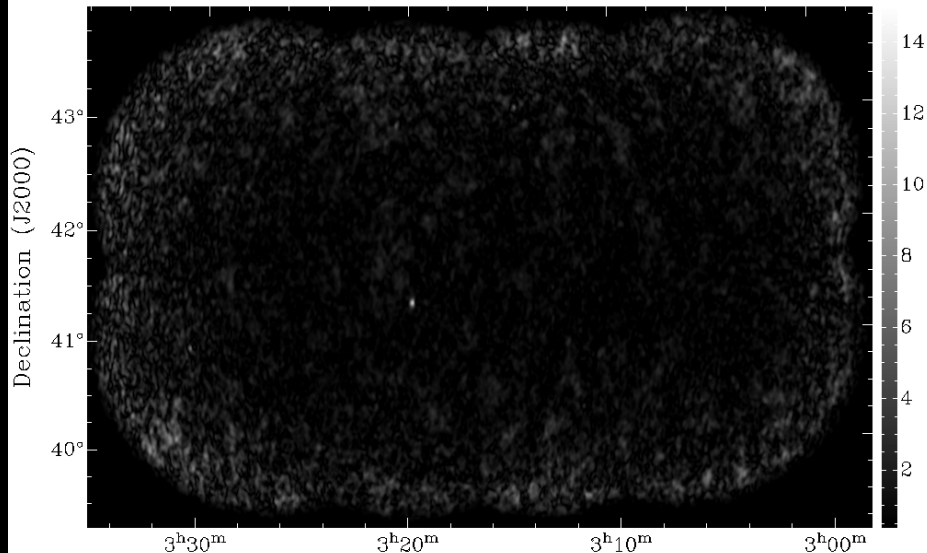
RM: -1.230000e+02



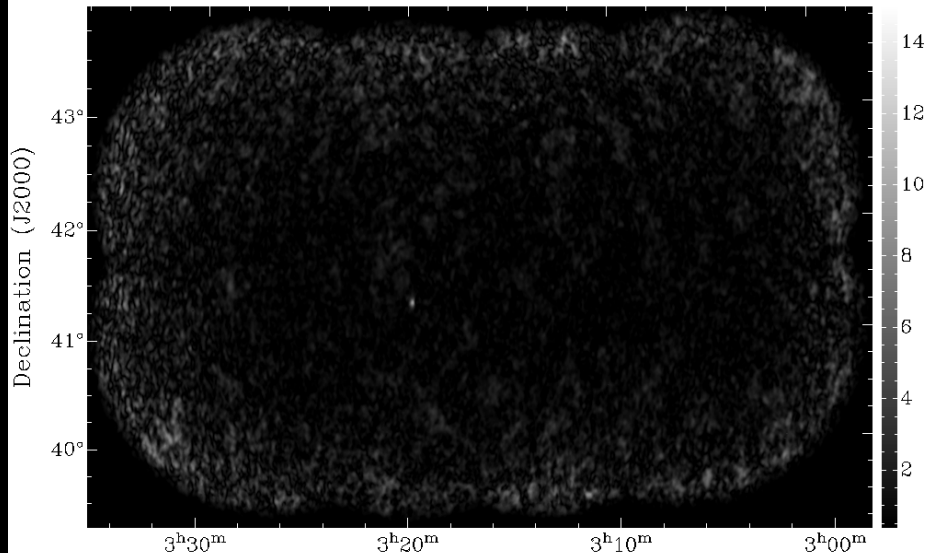
RM: -1.200000e+02



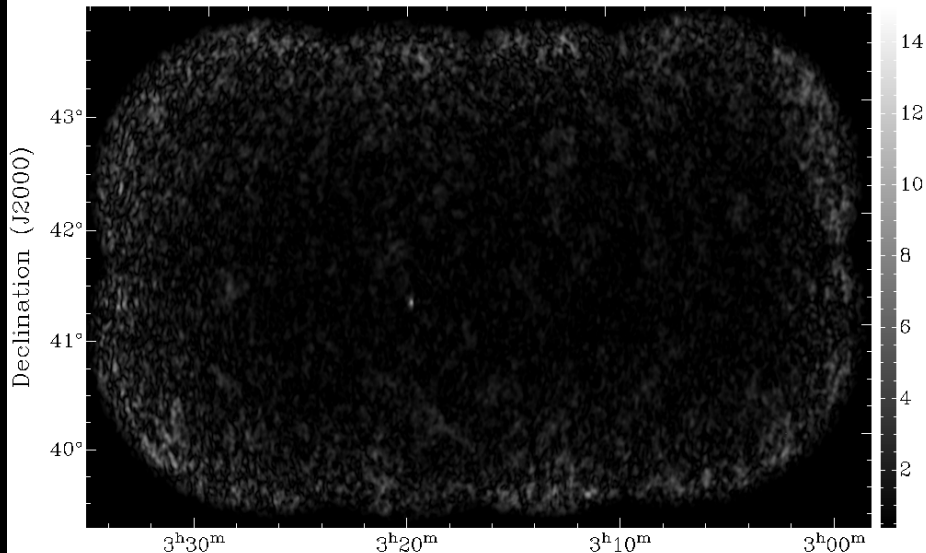
RM: -1.170000e+02



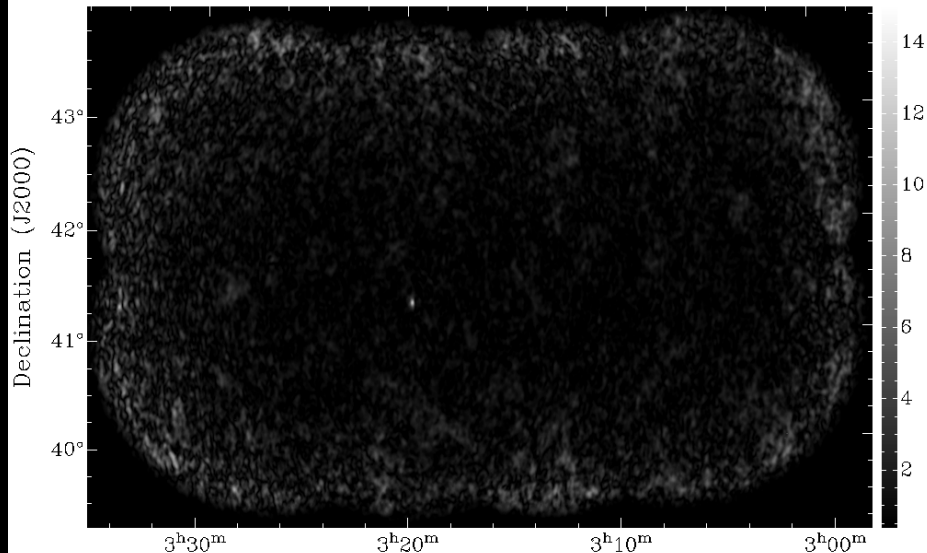
RM: -1.140000e+02



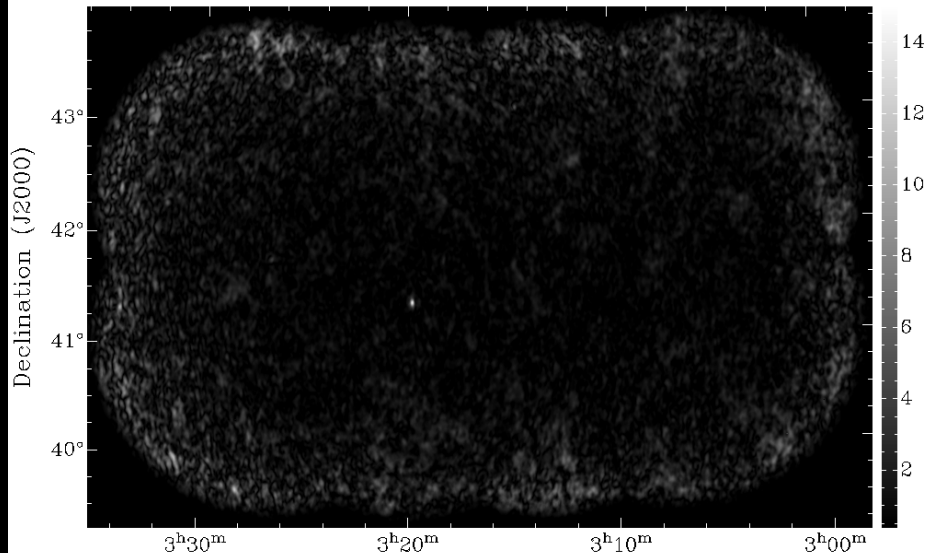
RM: -1.110000e+02



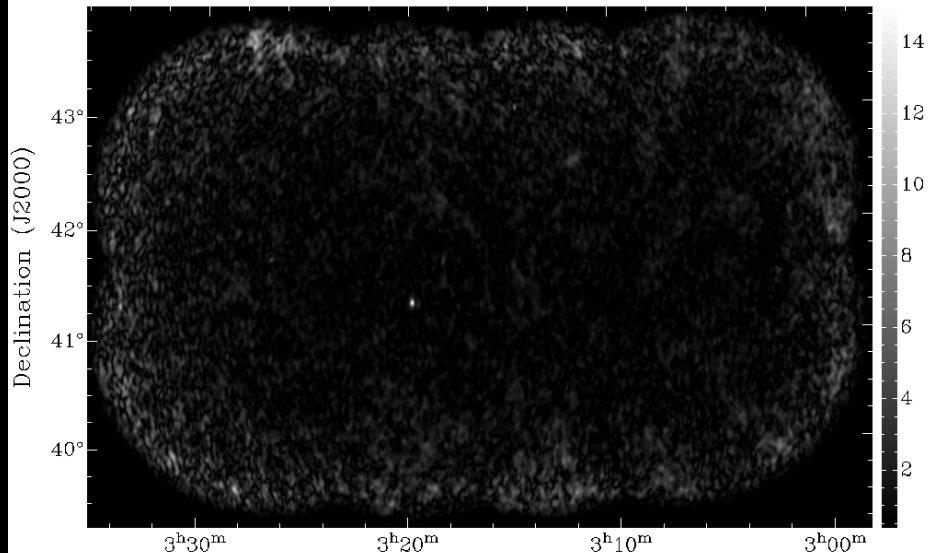
RM: -1.080000e+02



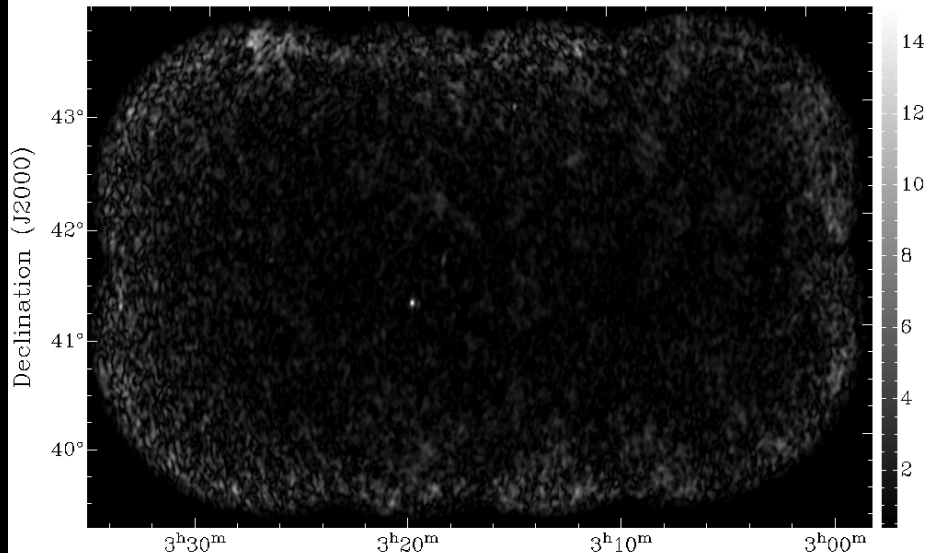
RM: -1.050000e+02



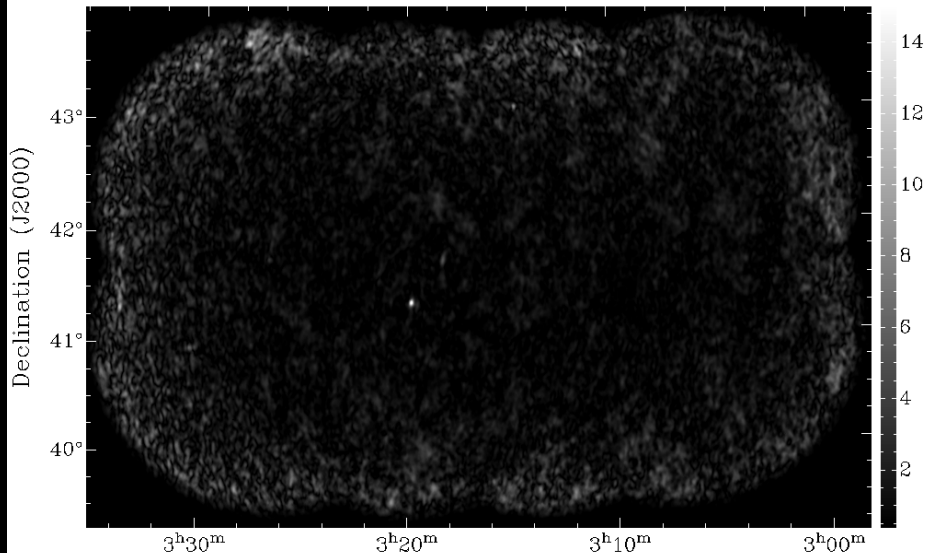
RM: -1.020000e+02



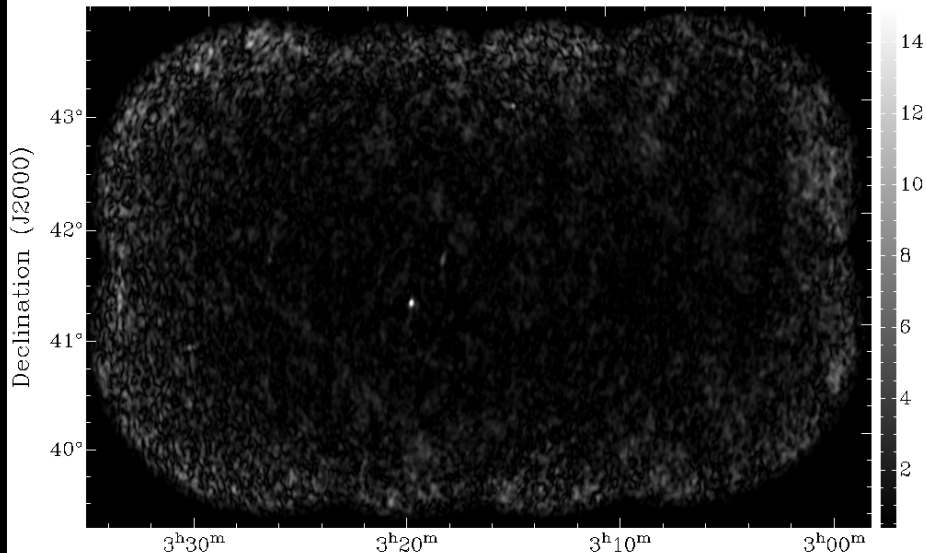
RM: -9.900000e+01



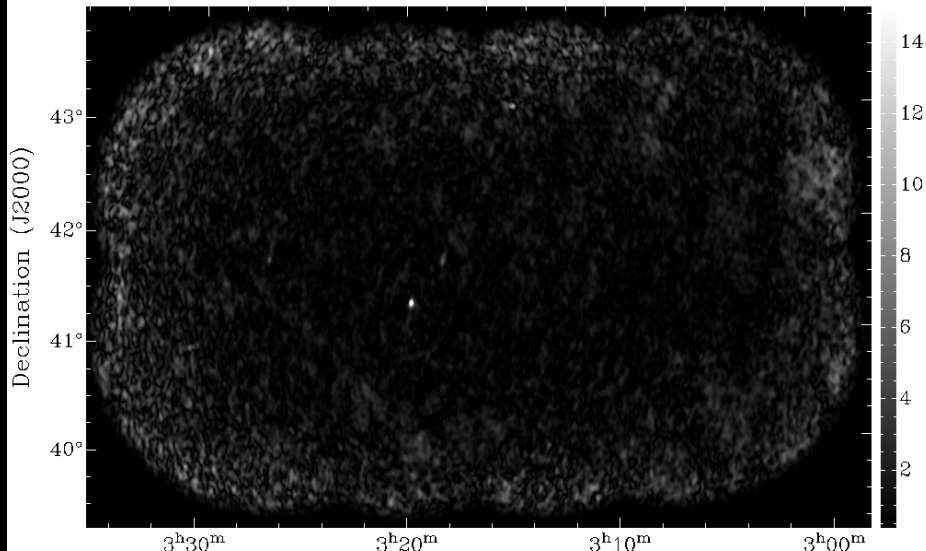
RM: -9.600000e+01



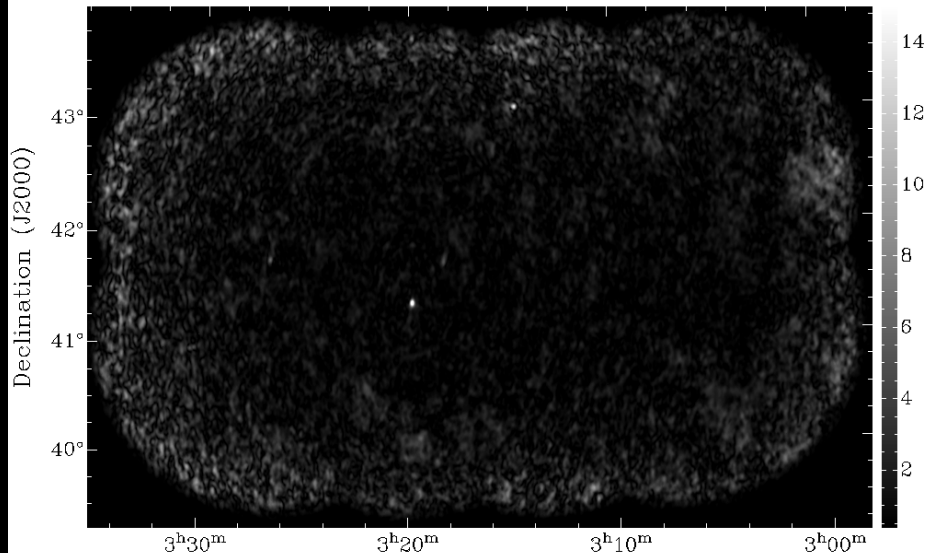
RM: -9.300000e+01



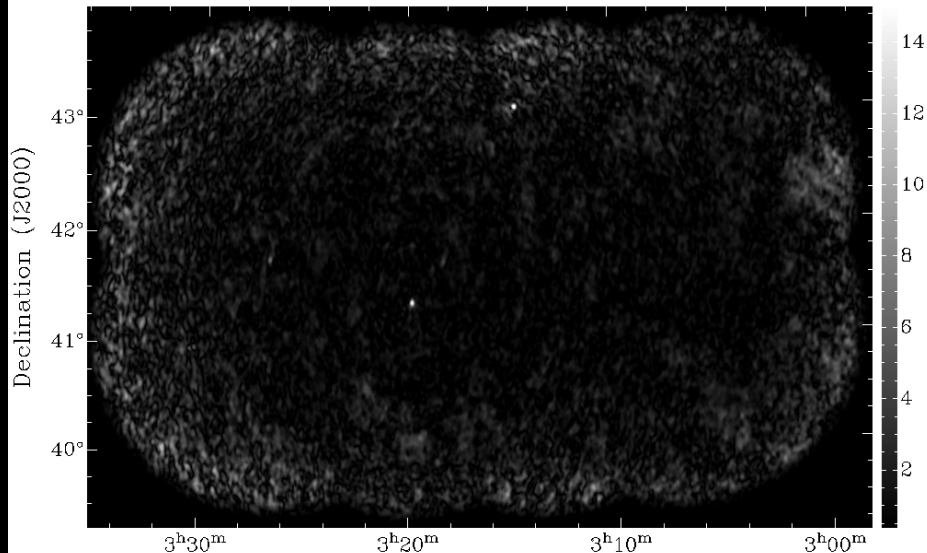
RM: -9.000000e+01



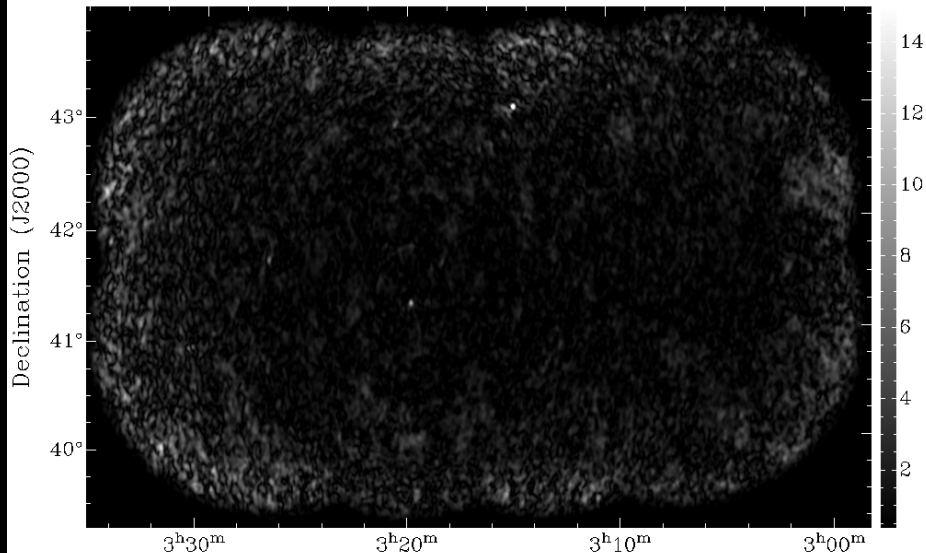
RM: -8.700000e+01



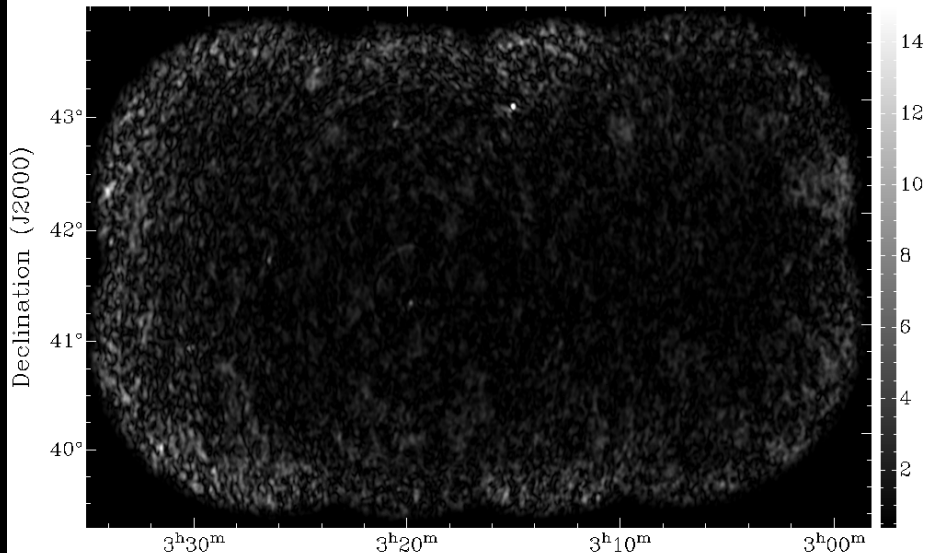
RM: -8.400000e+01



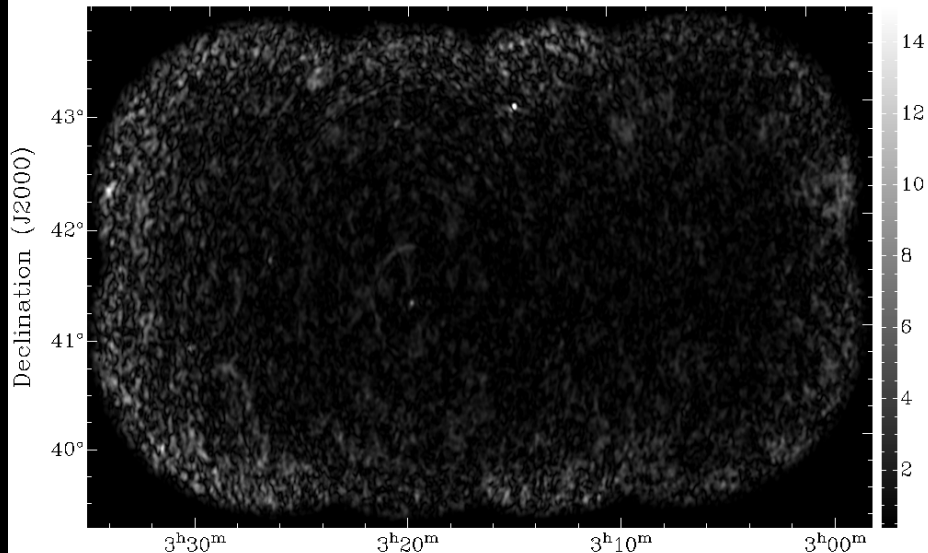
RM: -8.100000e+01



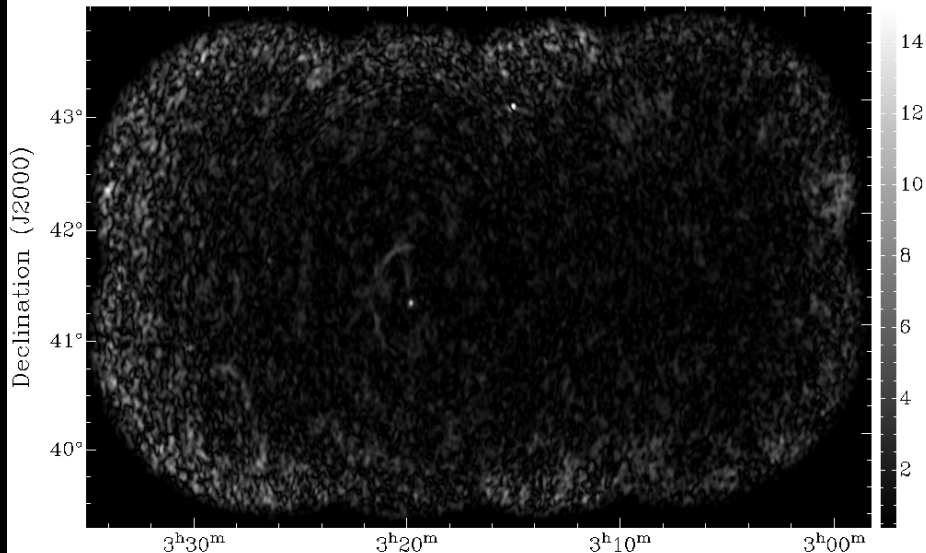
RM: -7.800000e+01



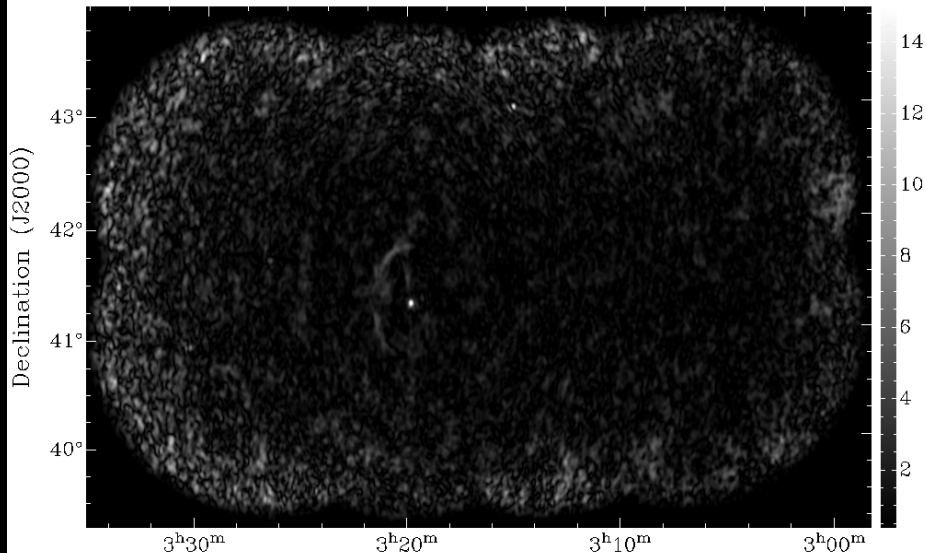
RM: -7.500000e+01



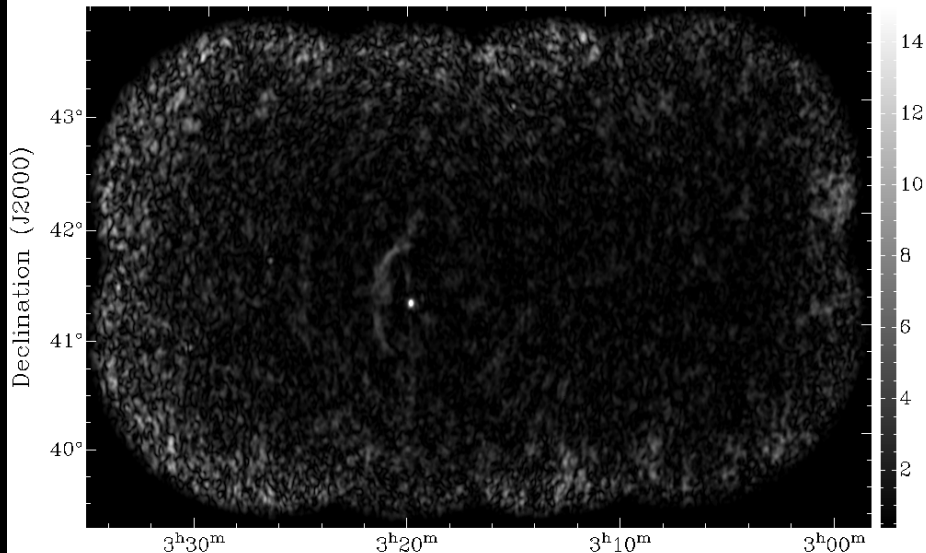
RM: -7.200000e+01



RM: -6.900000e+01



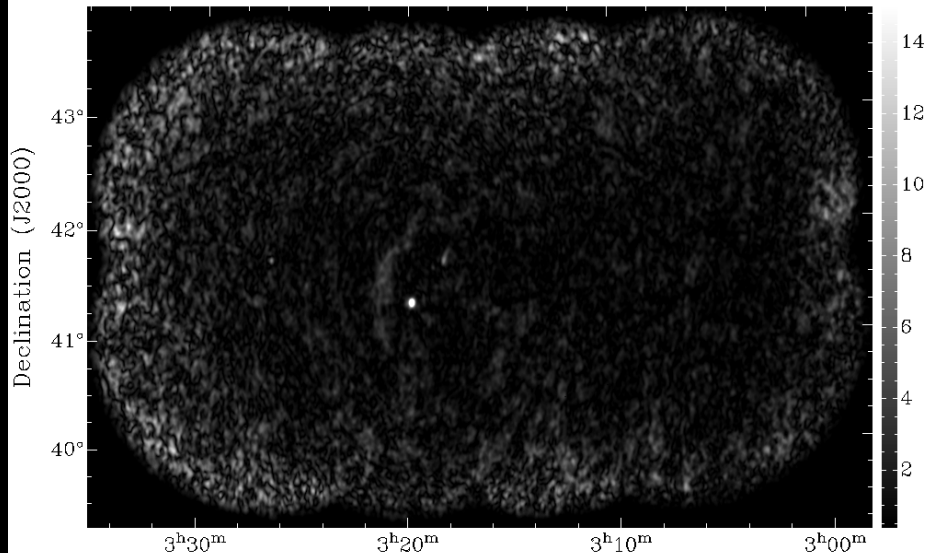
RM: -6.600000e+01



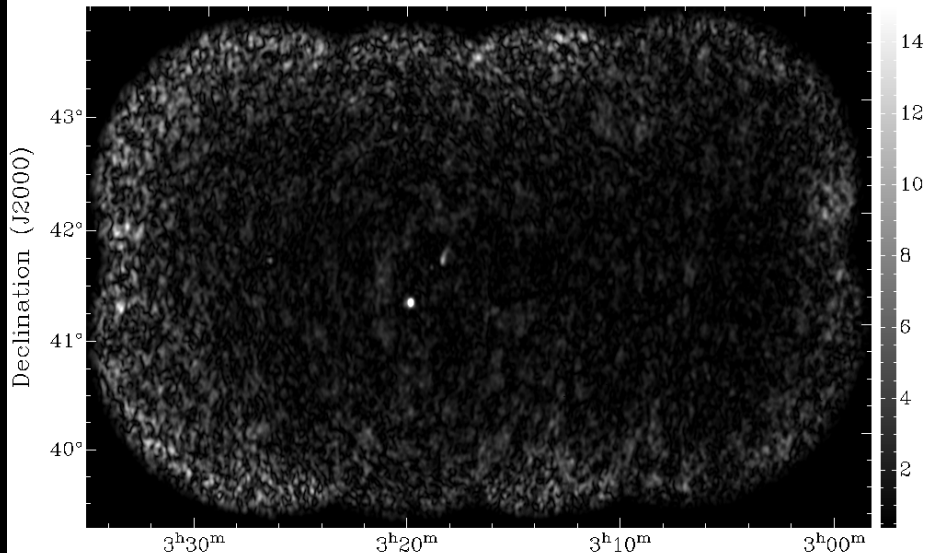
RM: -6.300000e+01



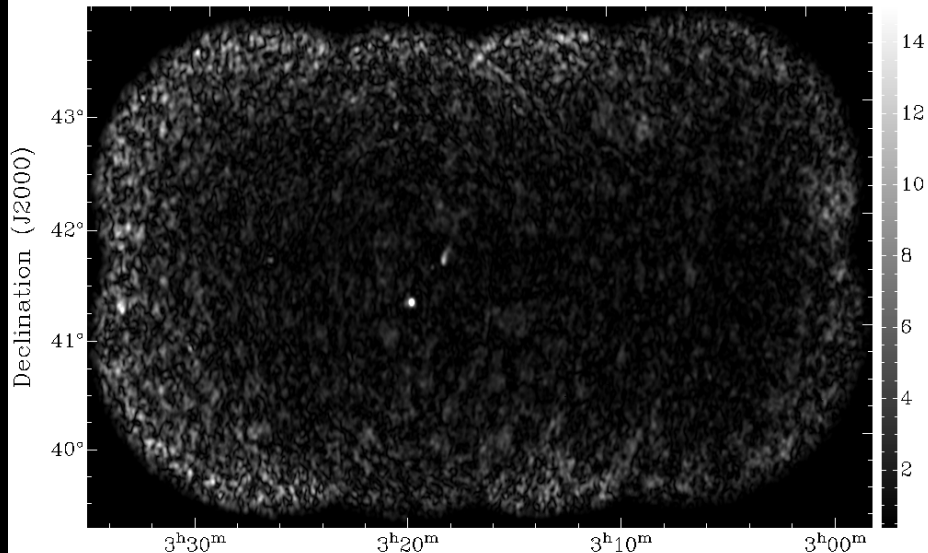
RM: -6.000000e+01



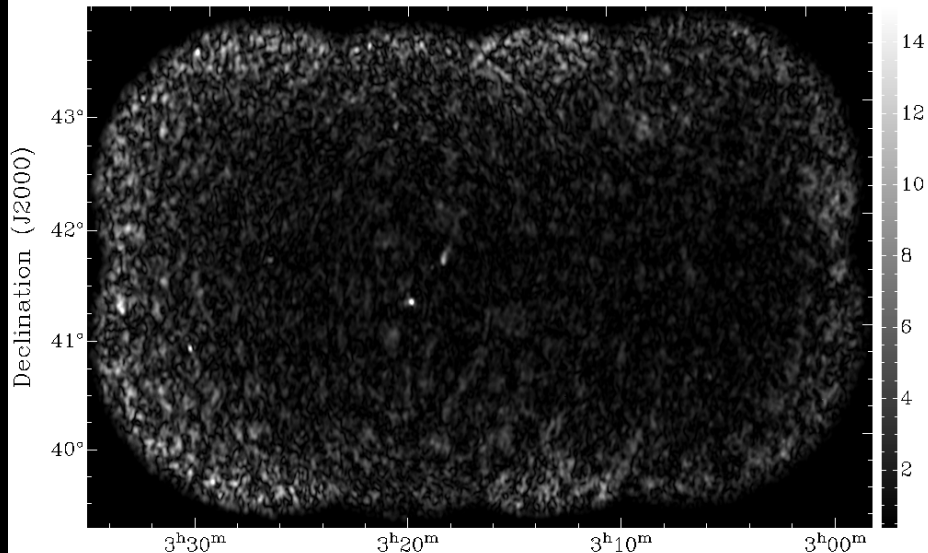
RM: -5.700000e+01



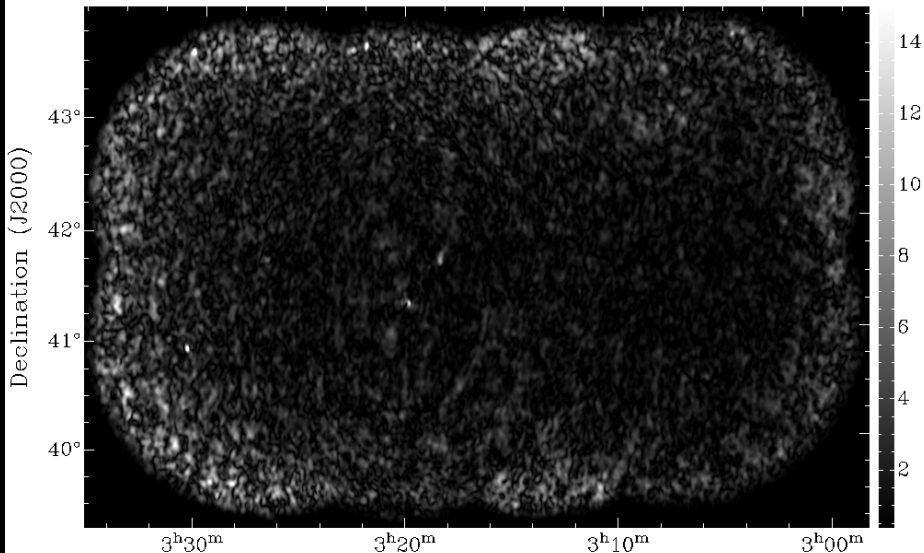
RM: -5.400000e+01



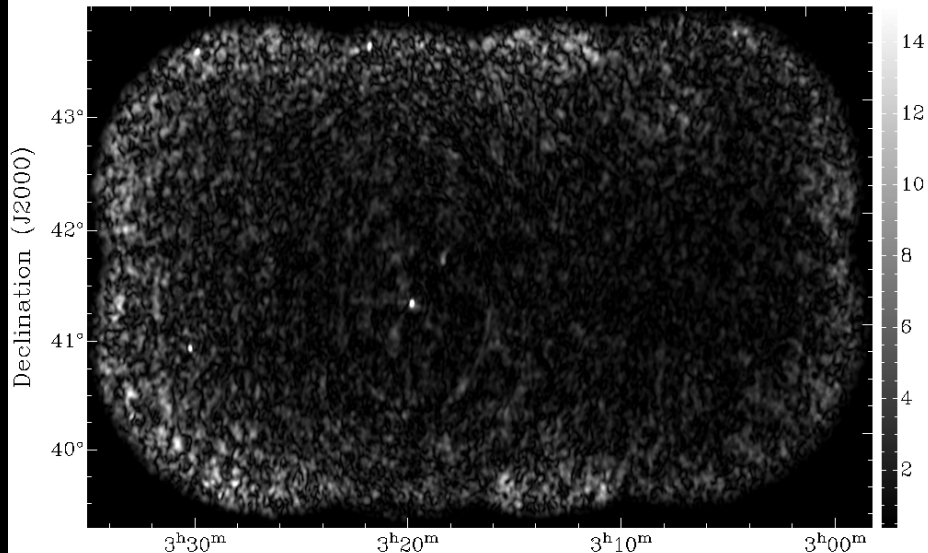
RM: -5.100000e+01



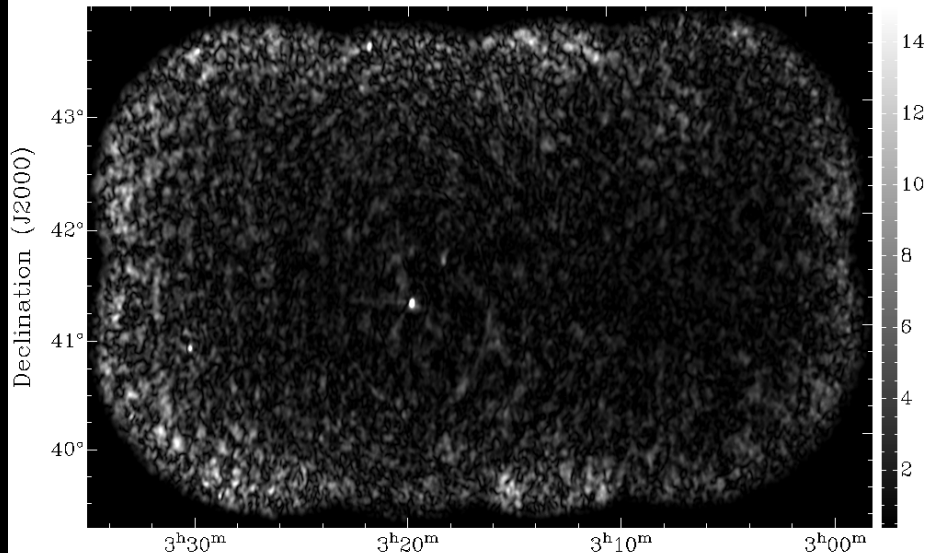
RM: -4.800000e+01



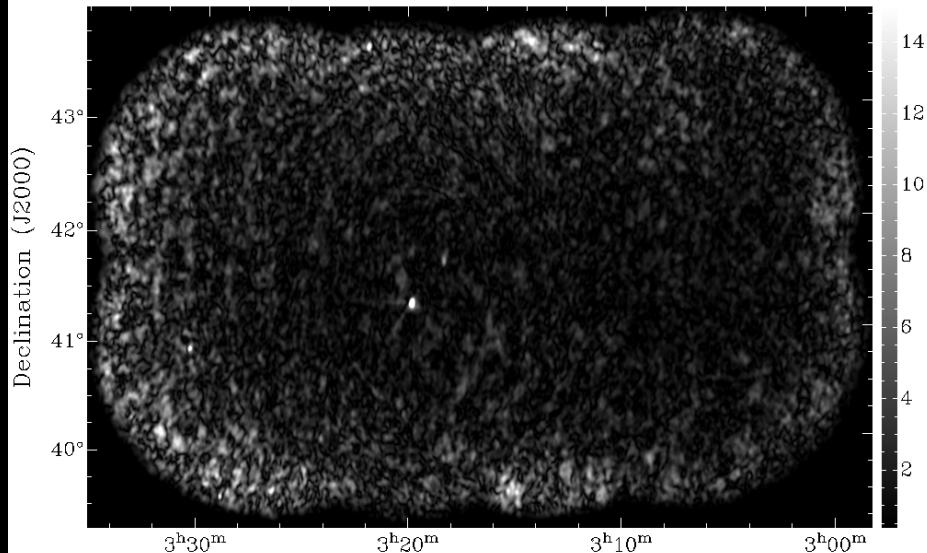
RM: -4.500000e+01



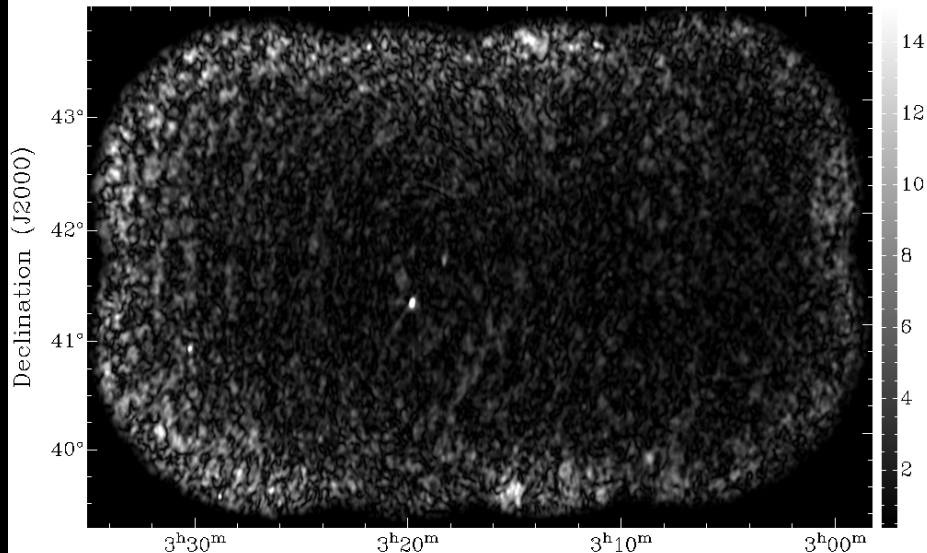
RM: -4.200000e+01



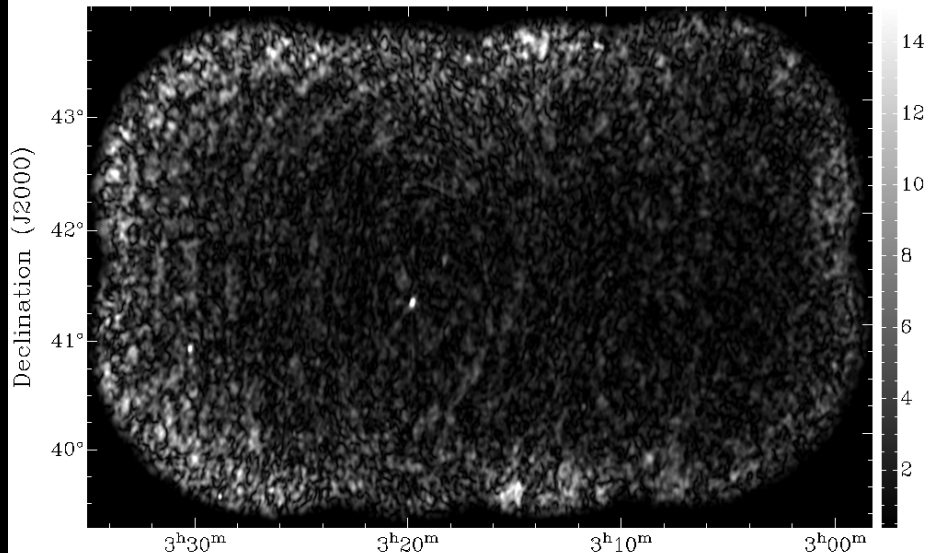
RM: -3.900000e+01



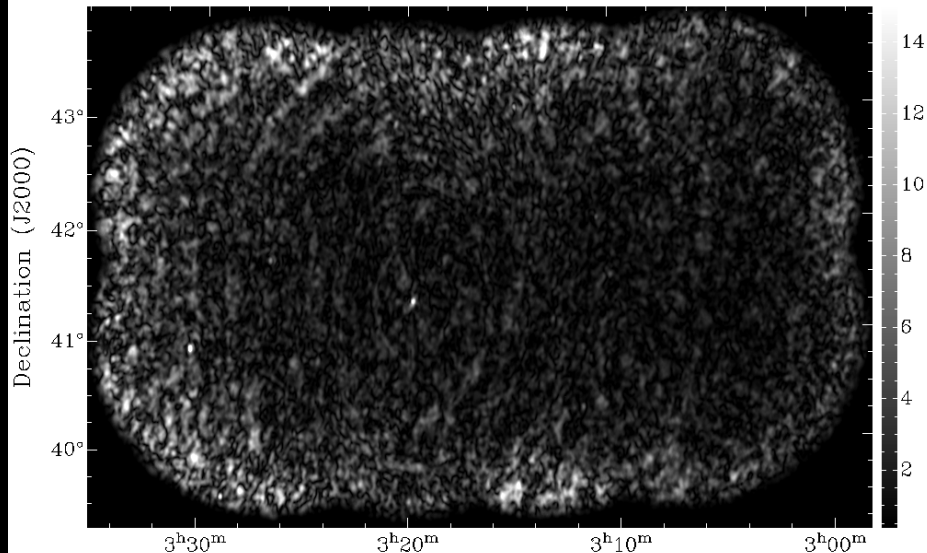
RM: -3.600000e+01



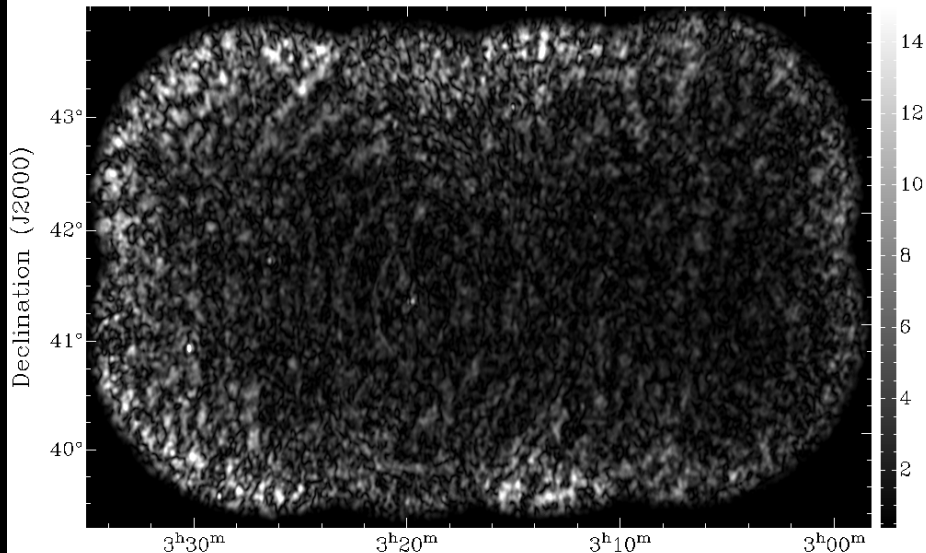
RM: -3.300000e+01



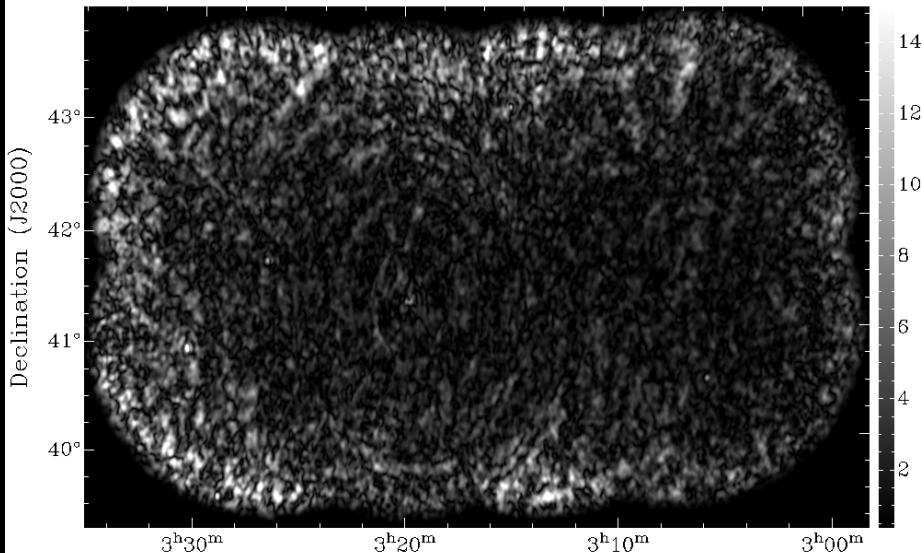
RM: -3.000000e+01



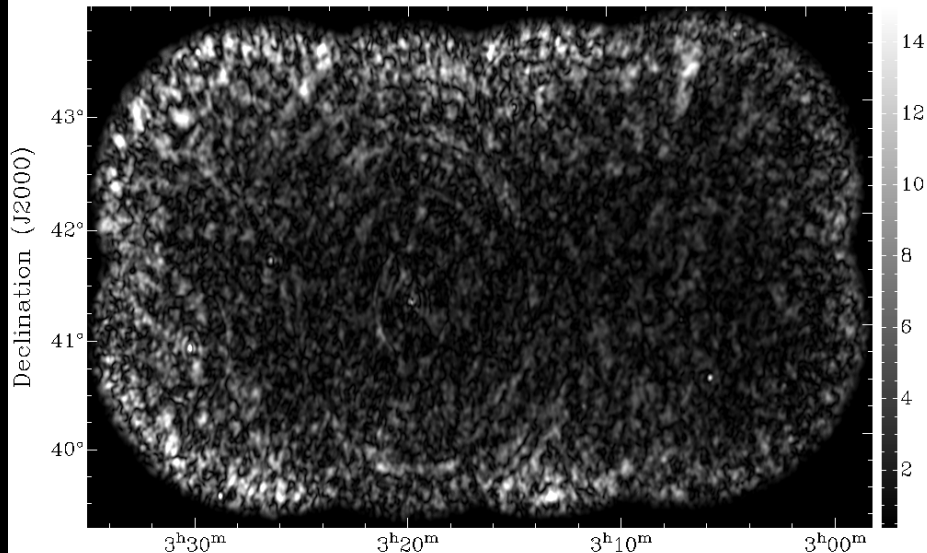
RM: -2.700000e+01



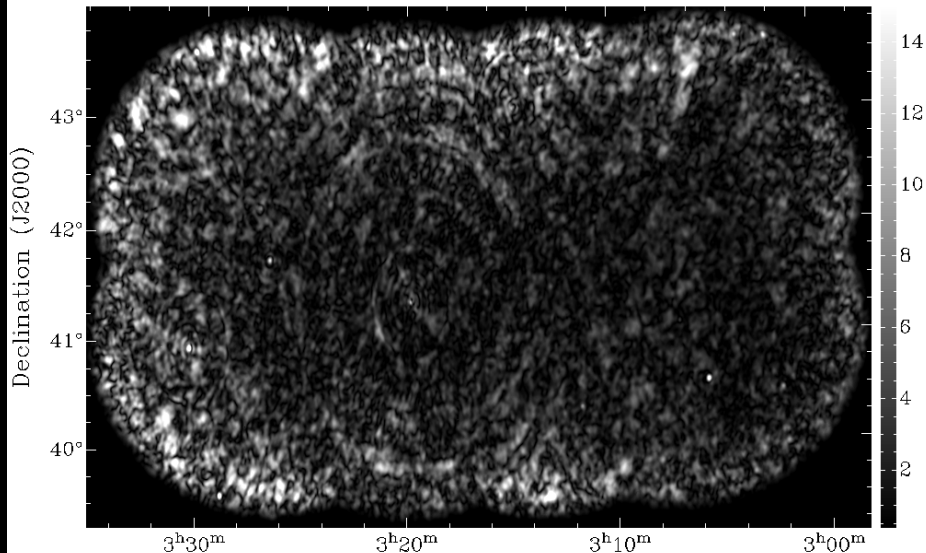
RM: -2.400000e+01



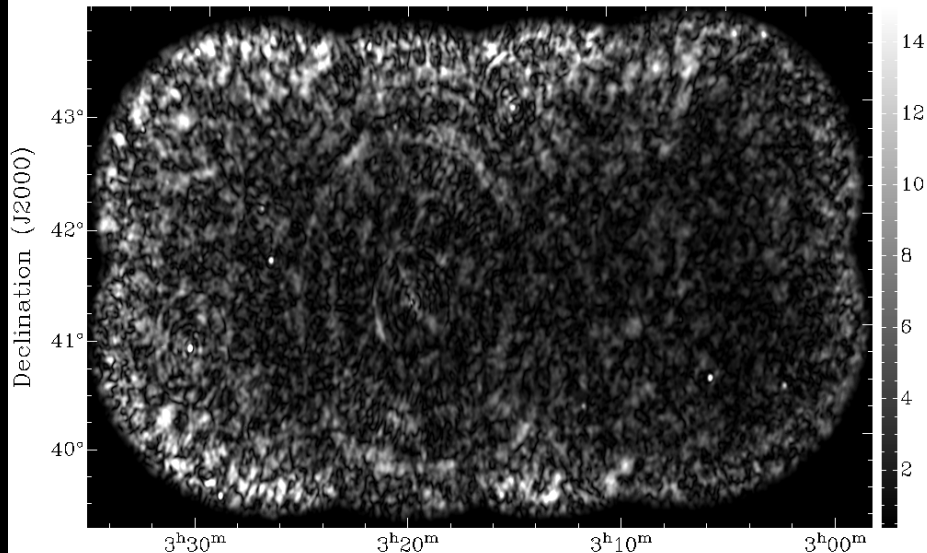
RM: -2.100000e+01



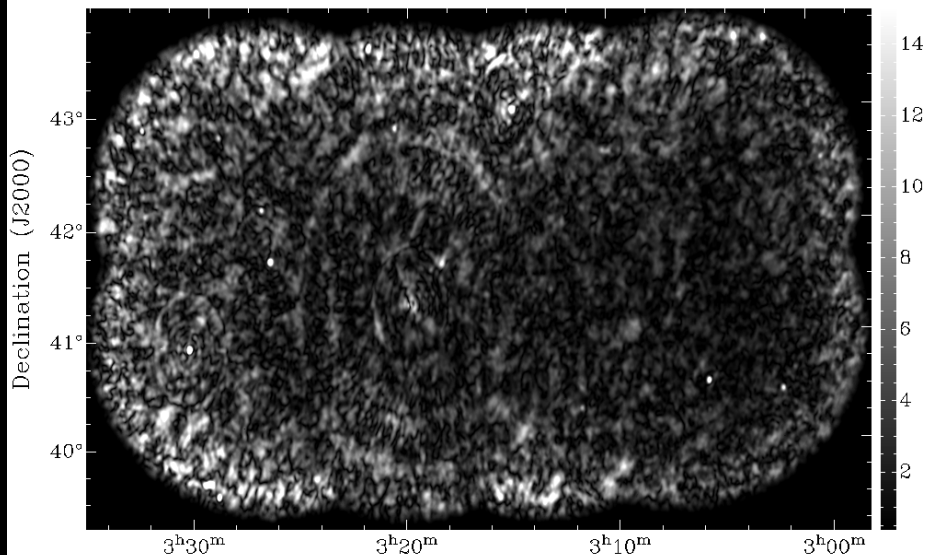
RM: -1.800000e+01



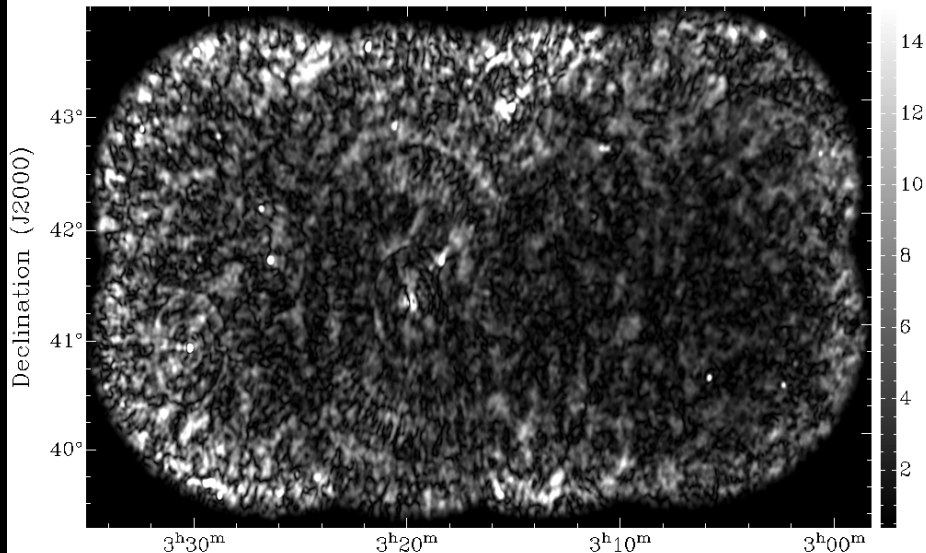
RM: -1.500000e+01



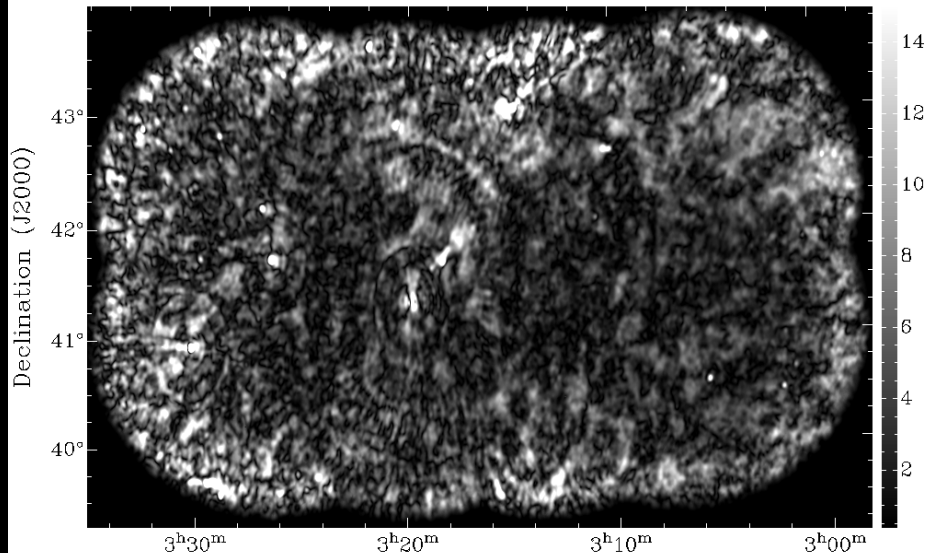
RM: -1.200000e+01



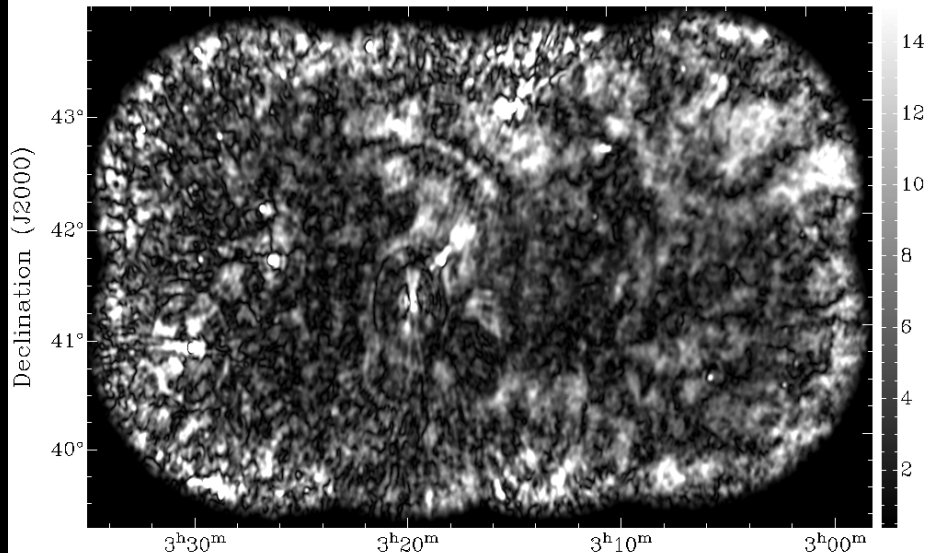
RM: -9.000000e+00



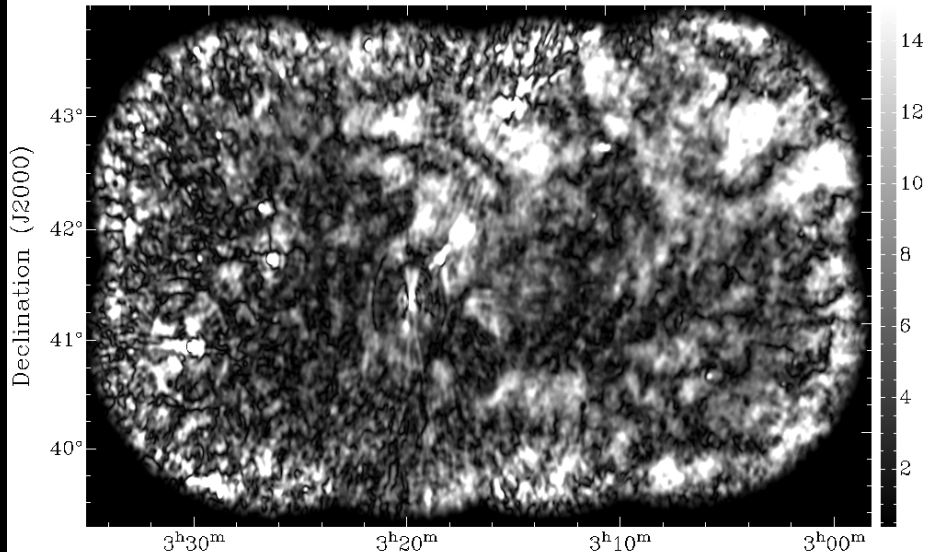
RM: -6.000000e+00



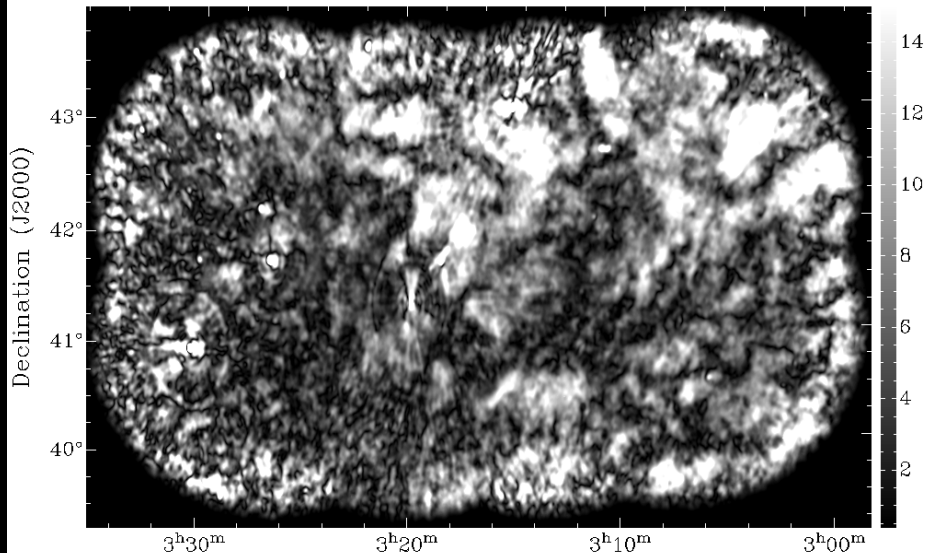
RM: -3.000000e+00



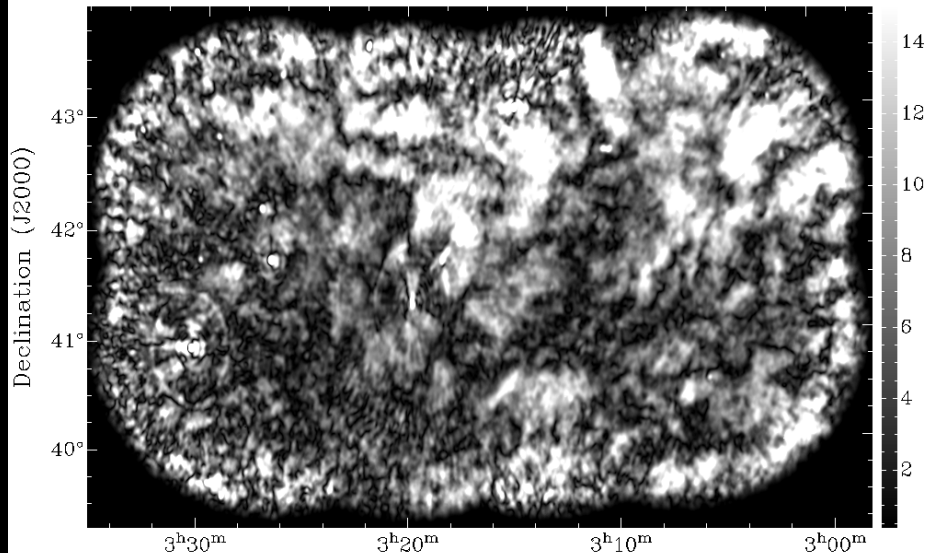
RM: 0.000000e+00



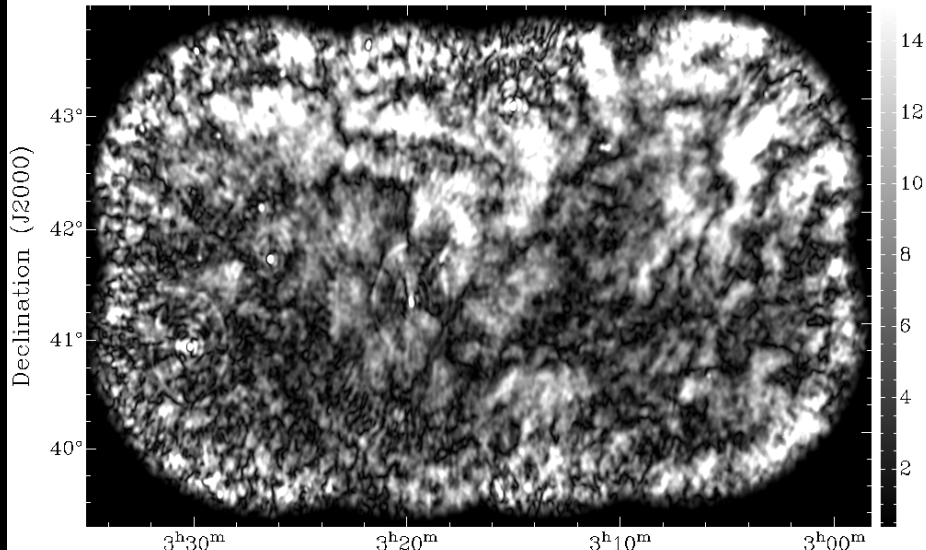
RM: 3.000000e+00



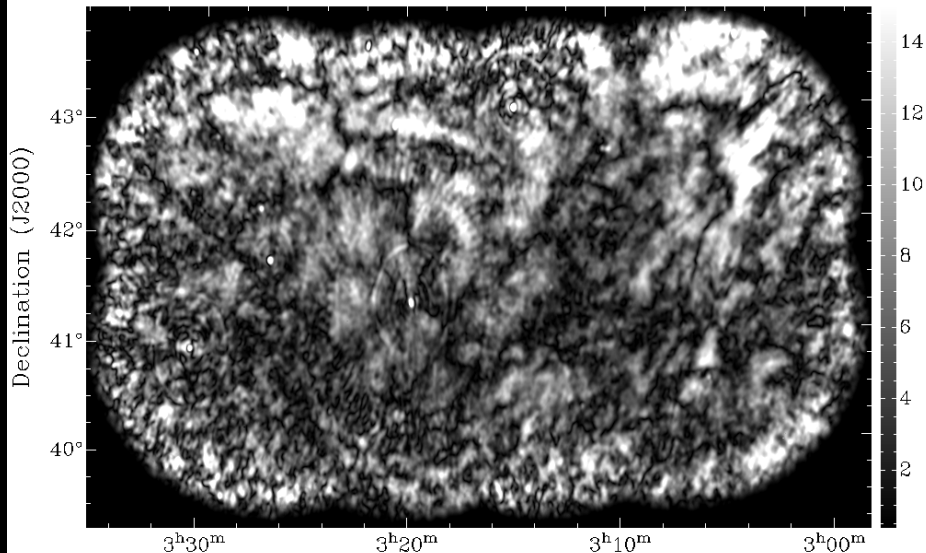
RM: 6.000000e+00



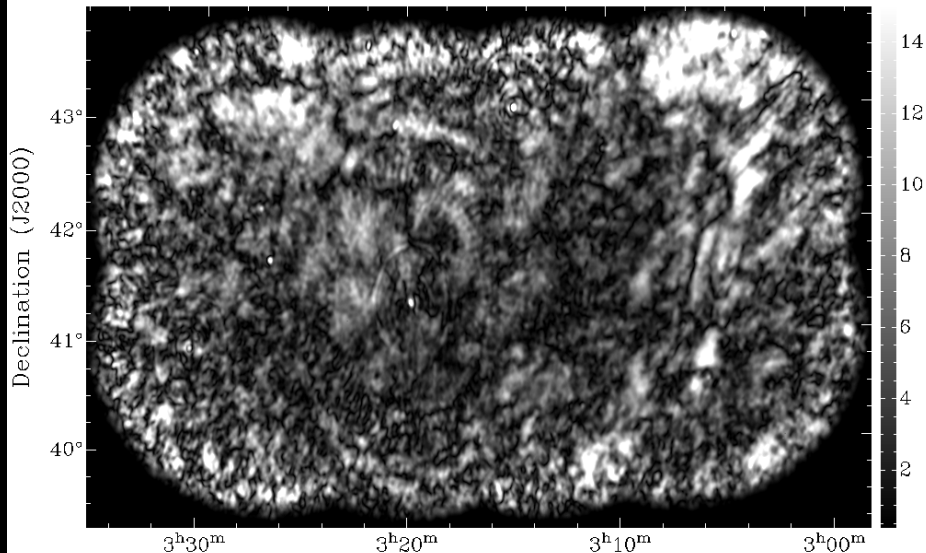
RM: 9.000000e+00



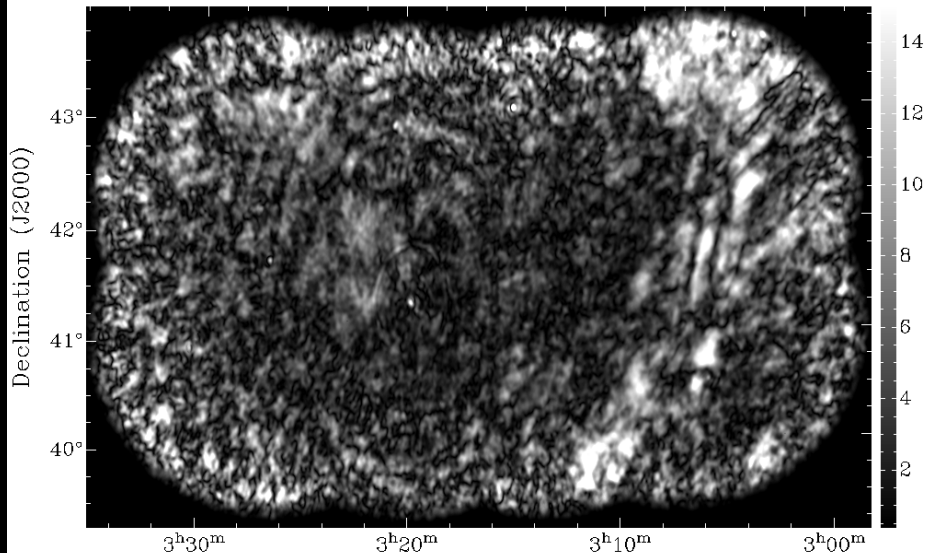
RM: 1.200000e+01



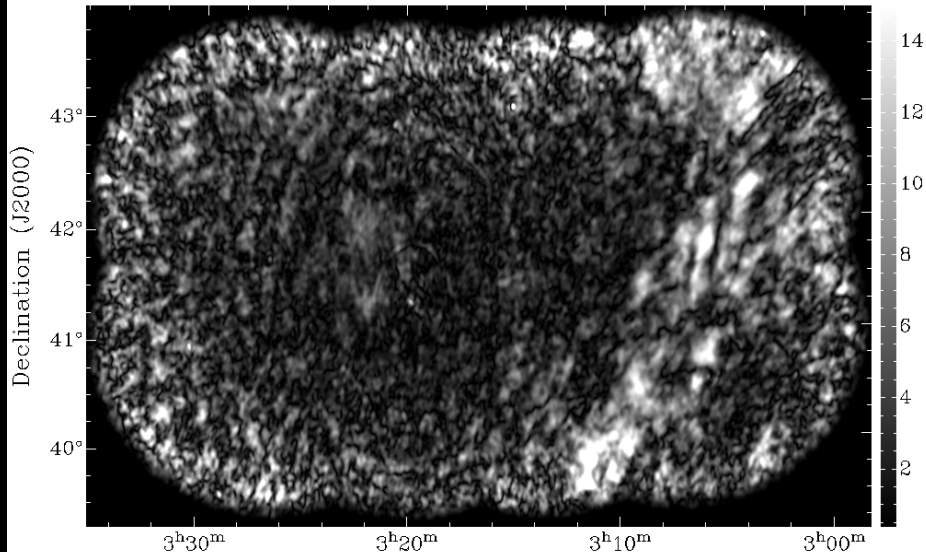
RM: 1.500000e+01



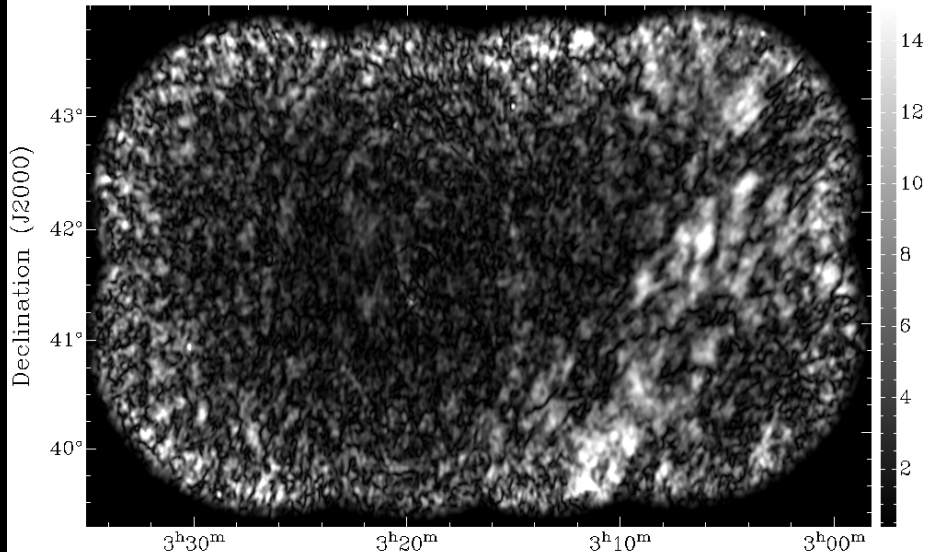
RM: 1.800000e+01



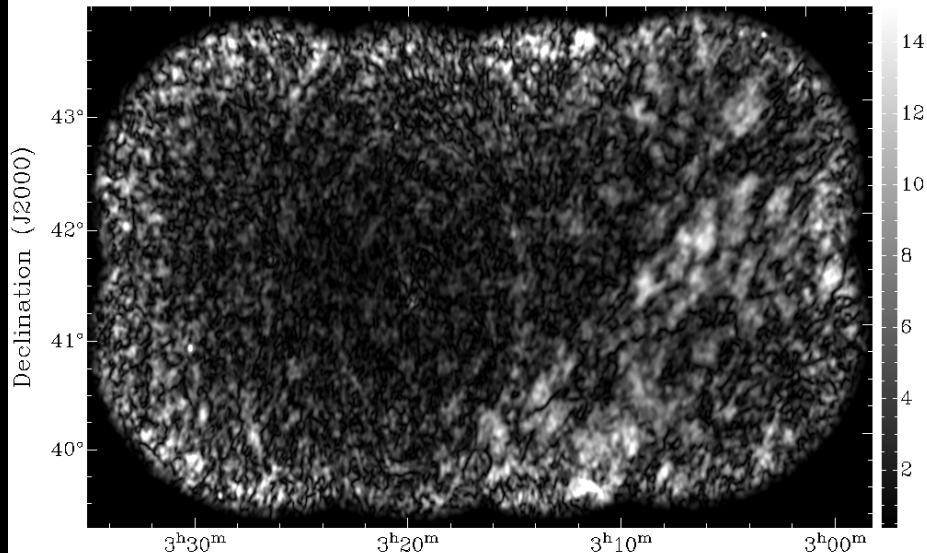
RM: 2.100000e+01



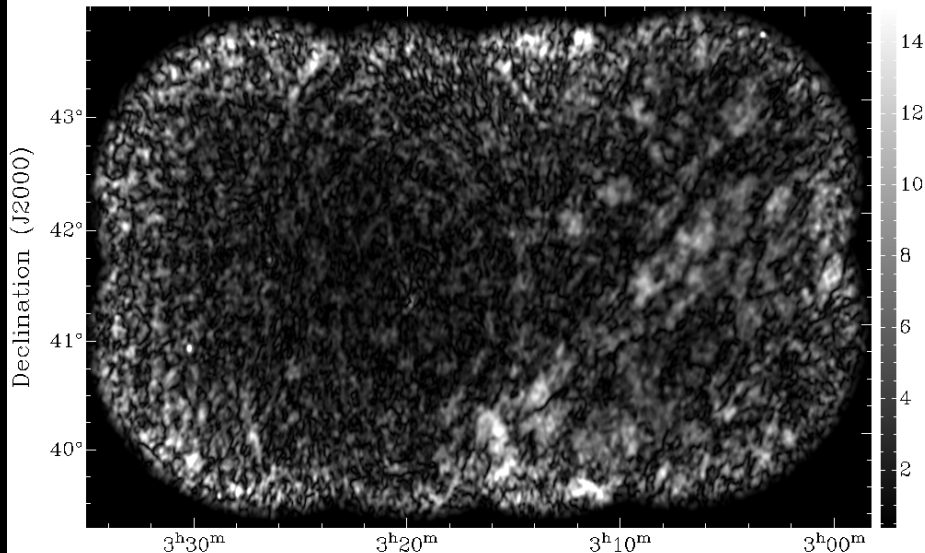
RM: 2.400000e+01



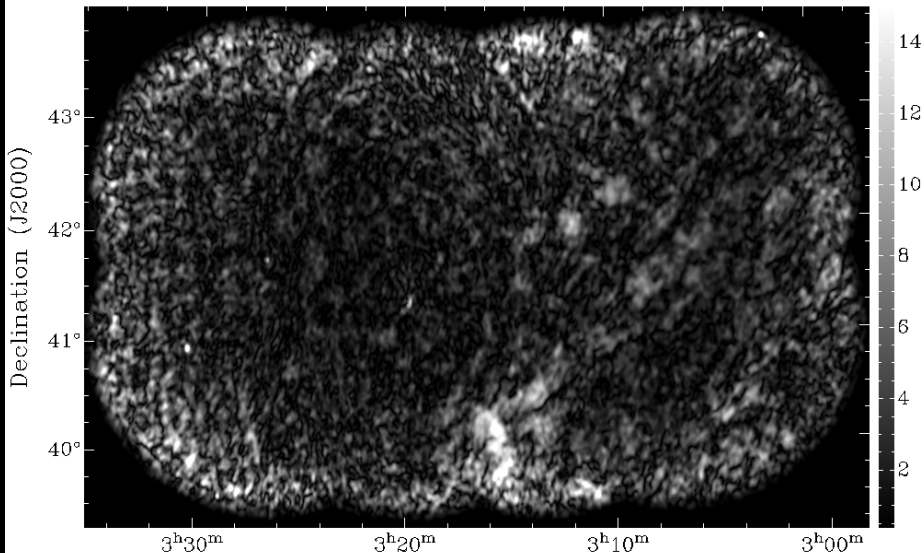
RM: 2.700000e+01



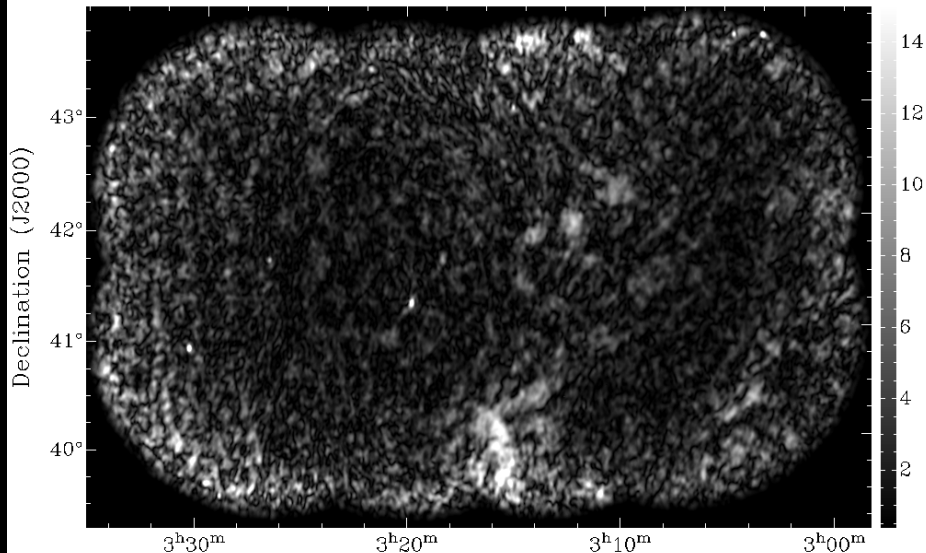
RM: 3.000000e+01



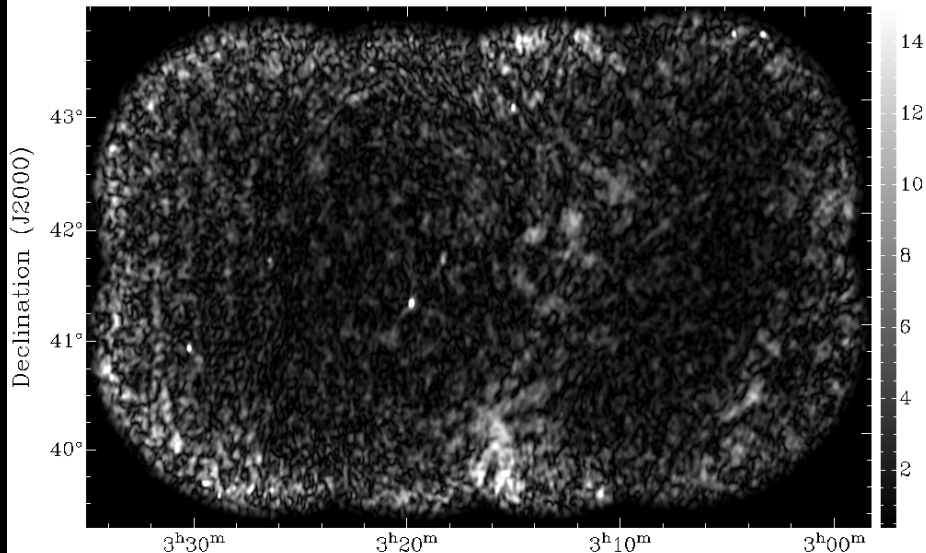
RM: 3.300000e+01



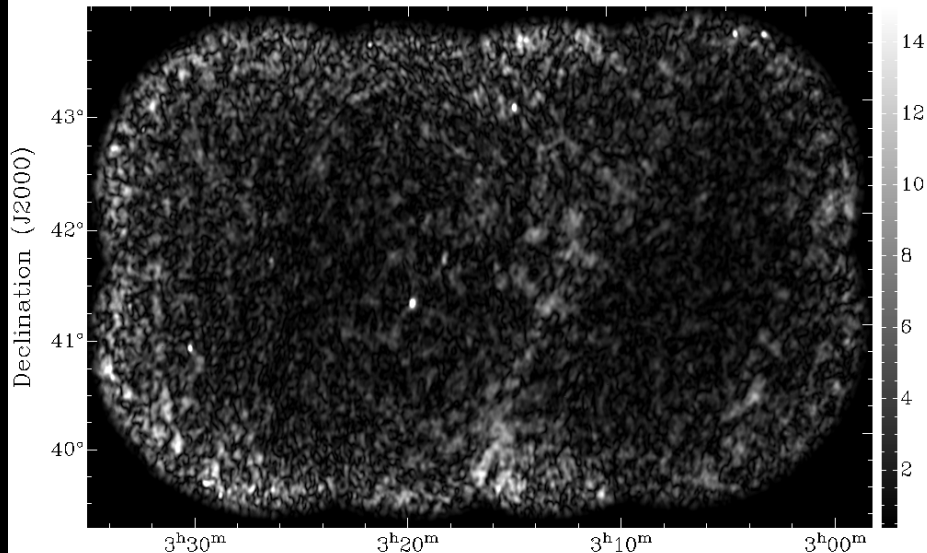
RM: 3.600000e+01



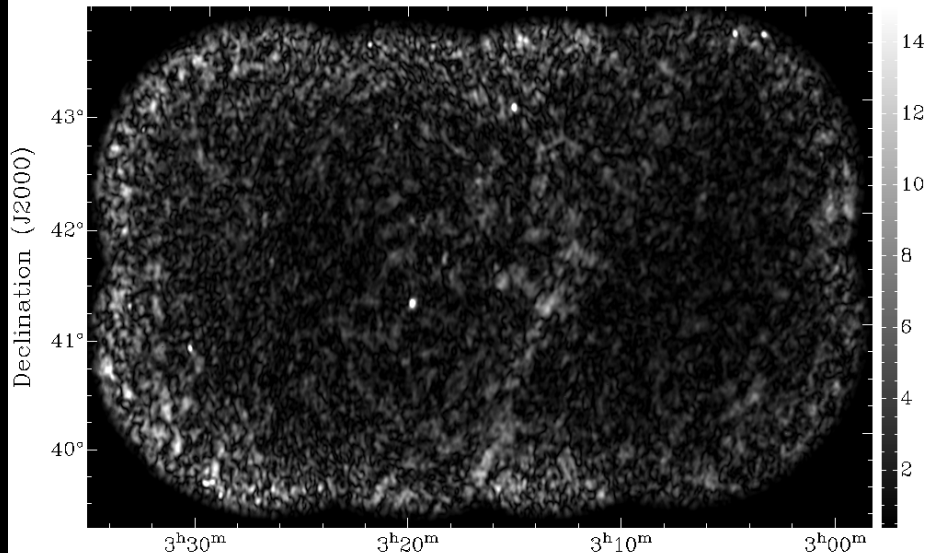
RM: 3.900000e+01



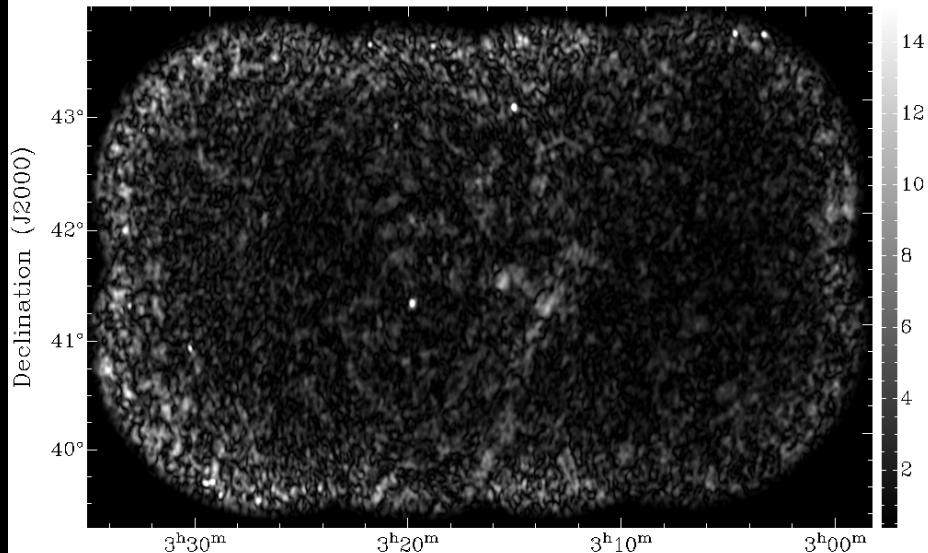
RM: 4.200000e+01



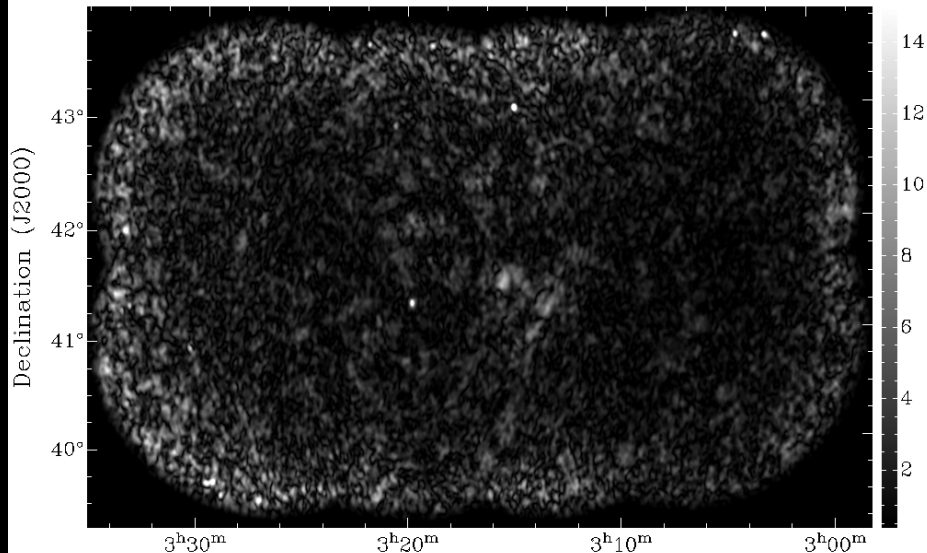
RM: 4.500000e+01



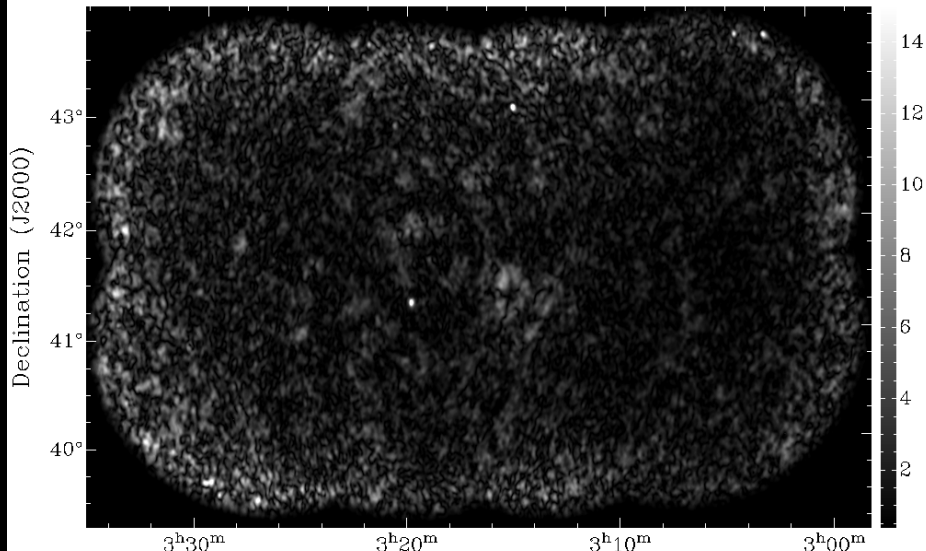
RM: 4.800000e+01



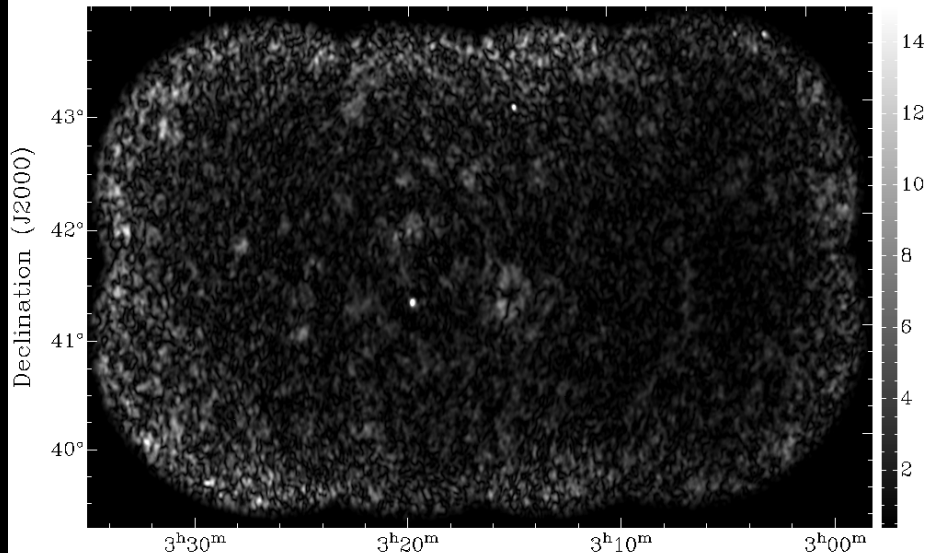
RM: 5.100000e+01



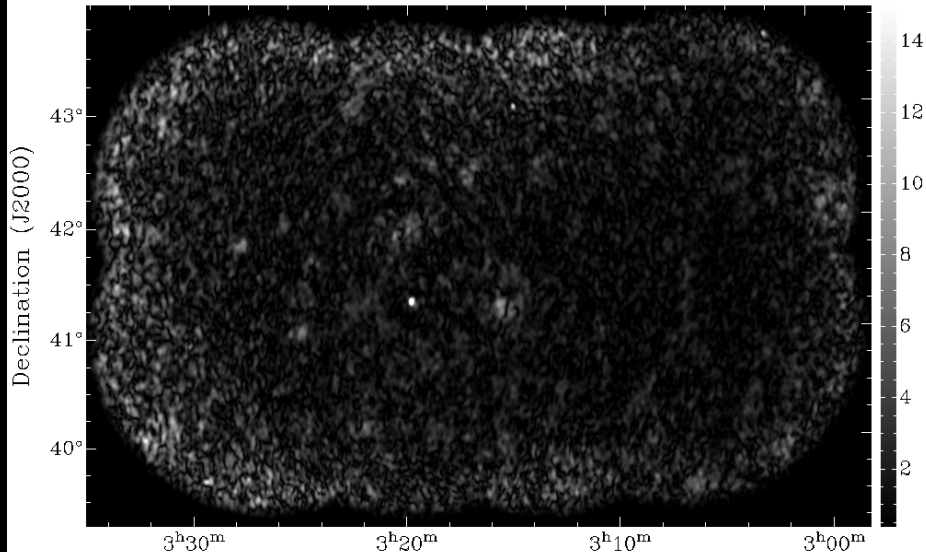
RM: 5.400000e+01



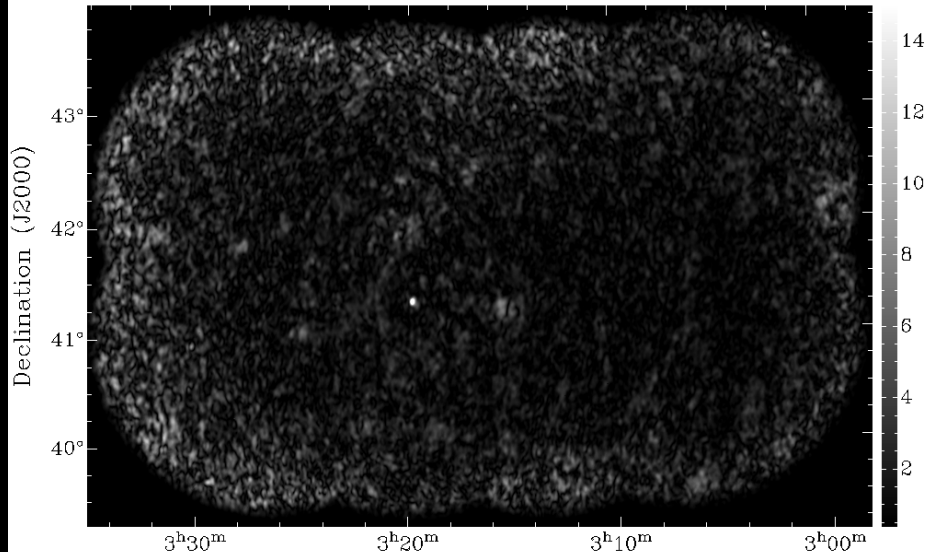
RM: 5.700000e+01



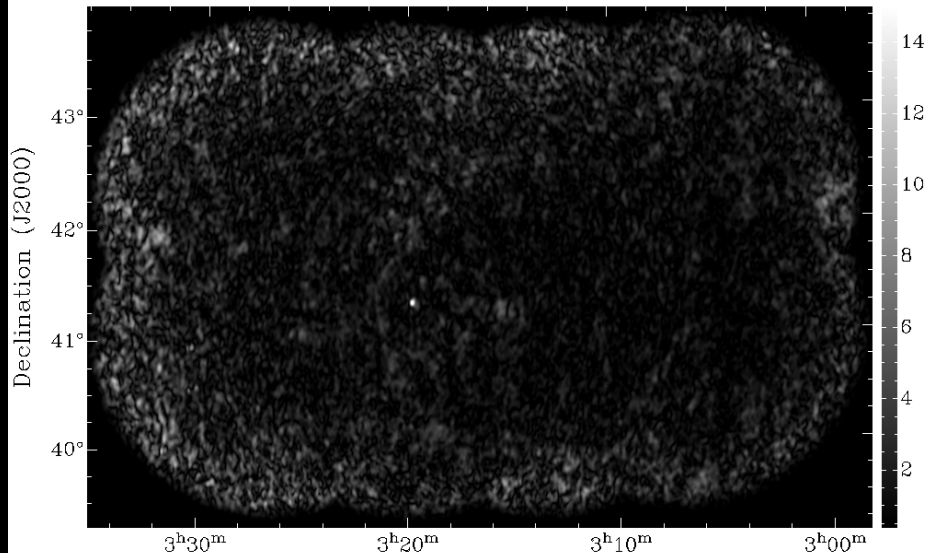
RM: 6.000000e+01



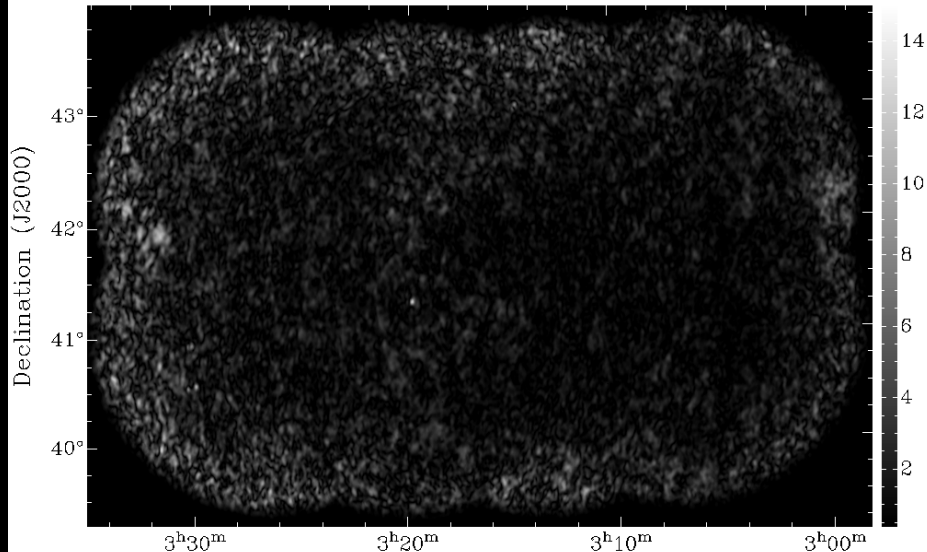
RM: 6.300000e+01



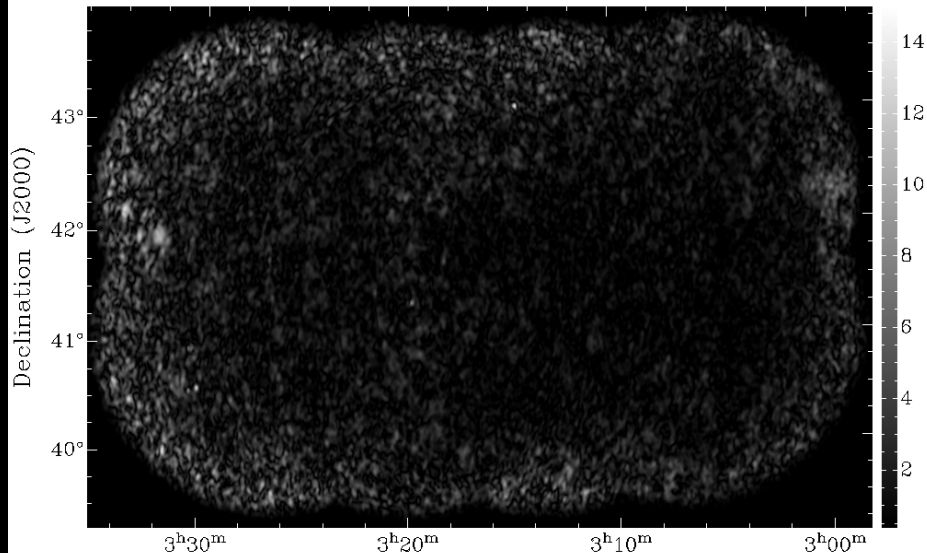
RM: 6.600000e+01



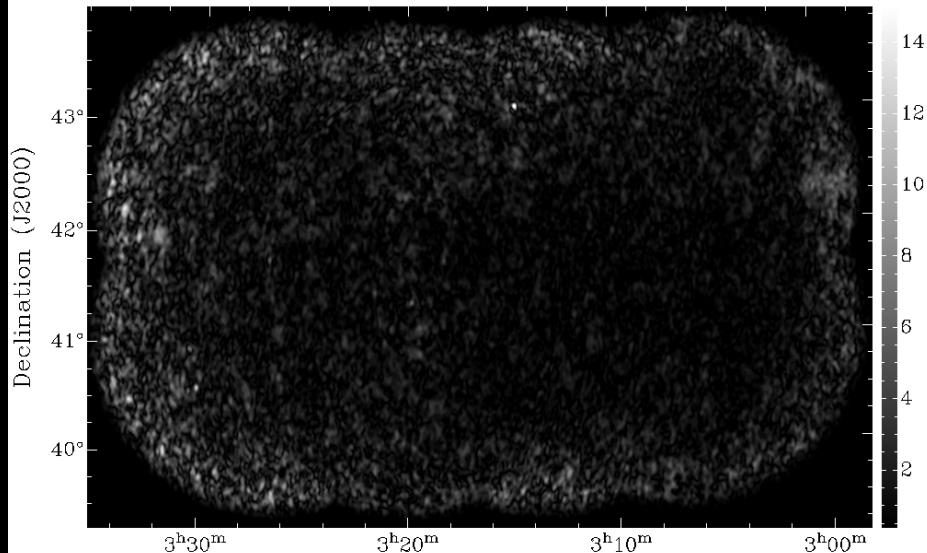
RM: 6.900000e+01



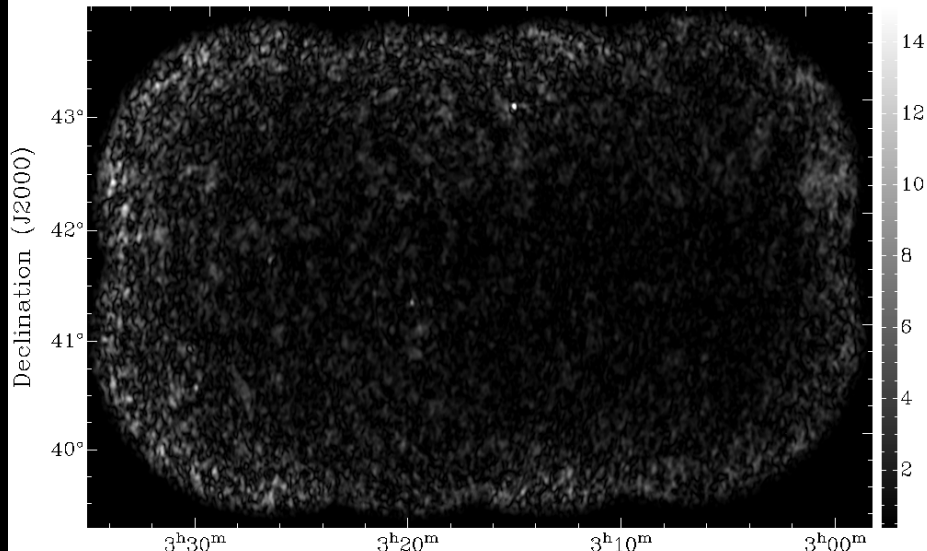
RM: 7.200000e+01



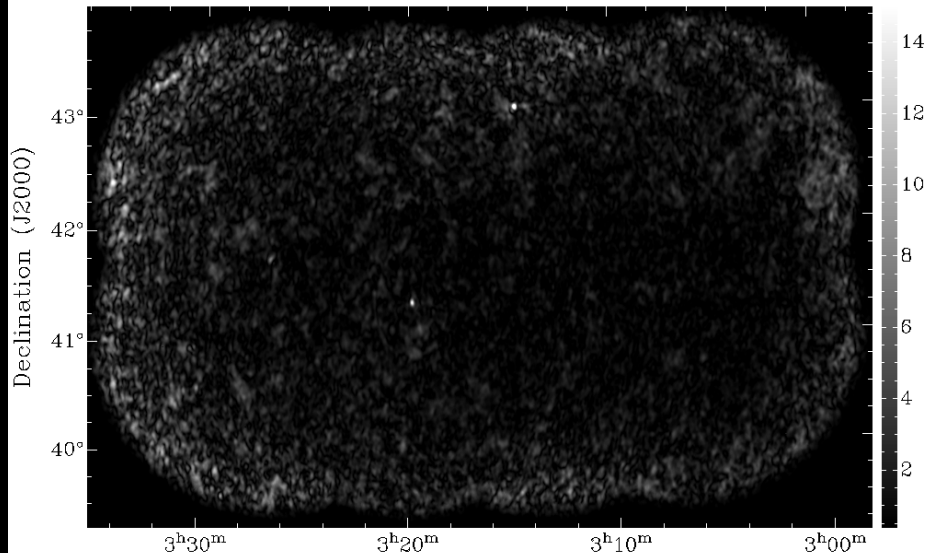
RM: 7.500000e+01



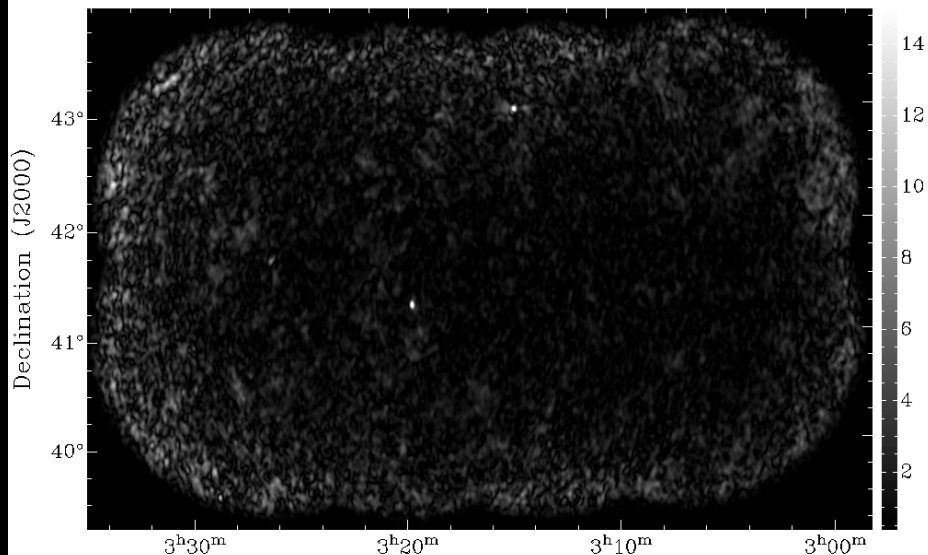
RM: 7.800000e+01



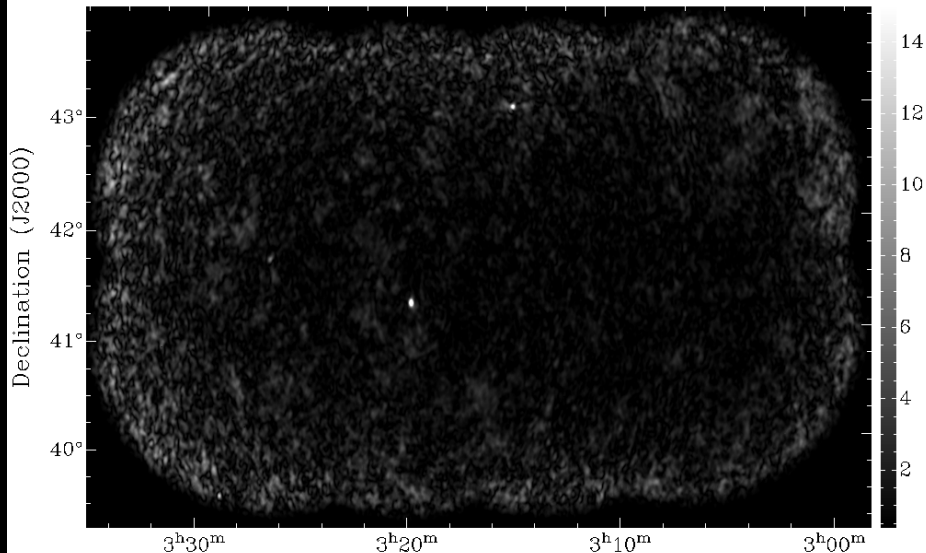
RM: 8.100000e+01



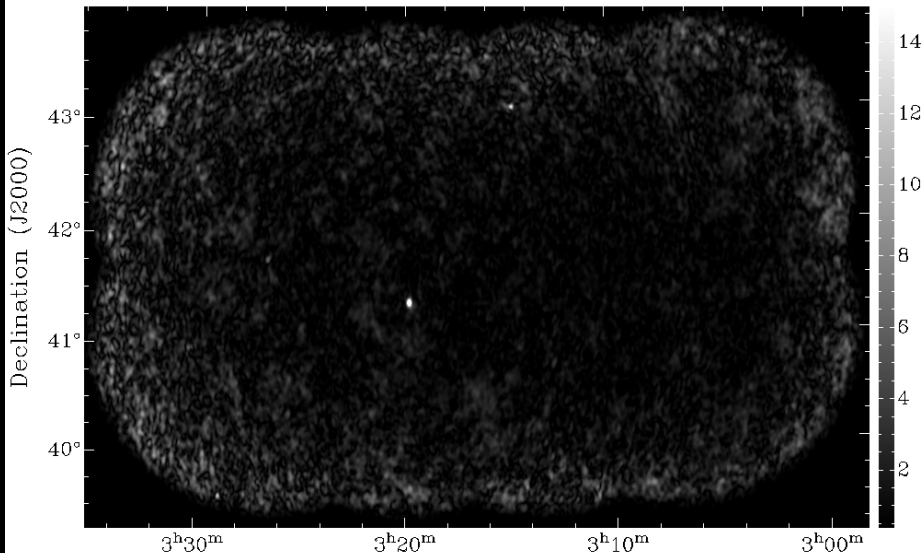
RM: 8.400000e+01



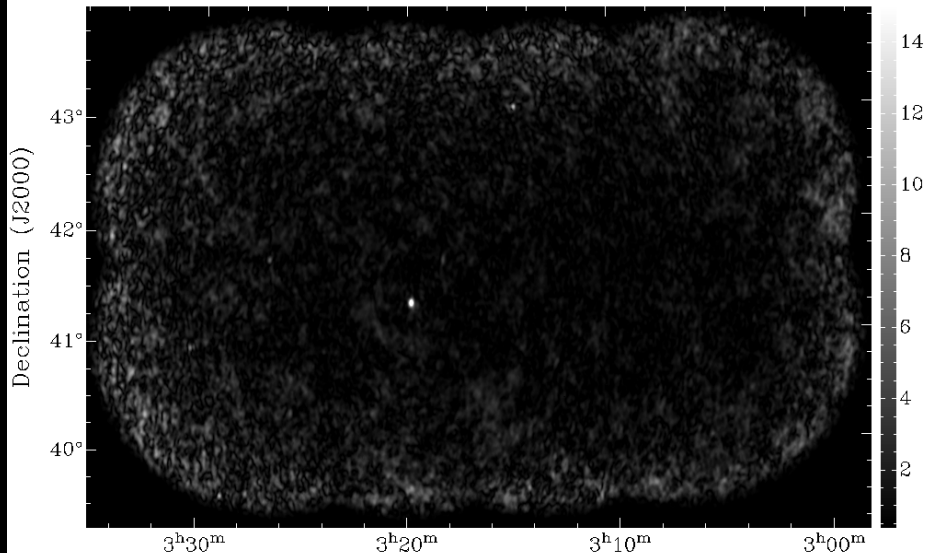
RM: 8.700000e+01



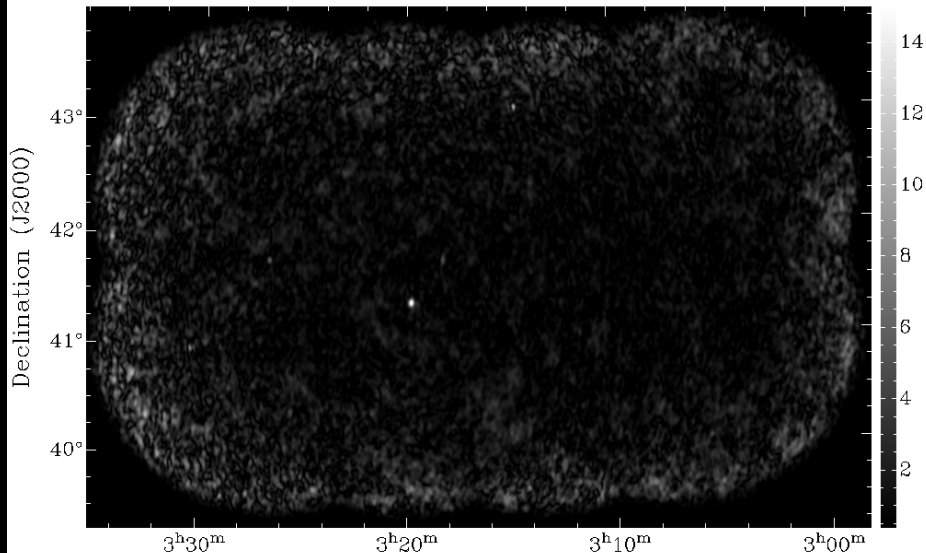
RM: 9.000000e+01



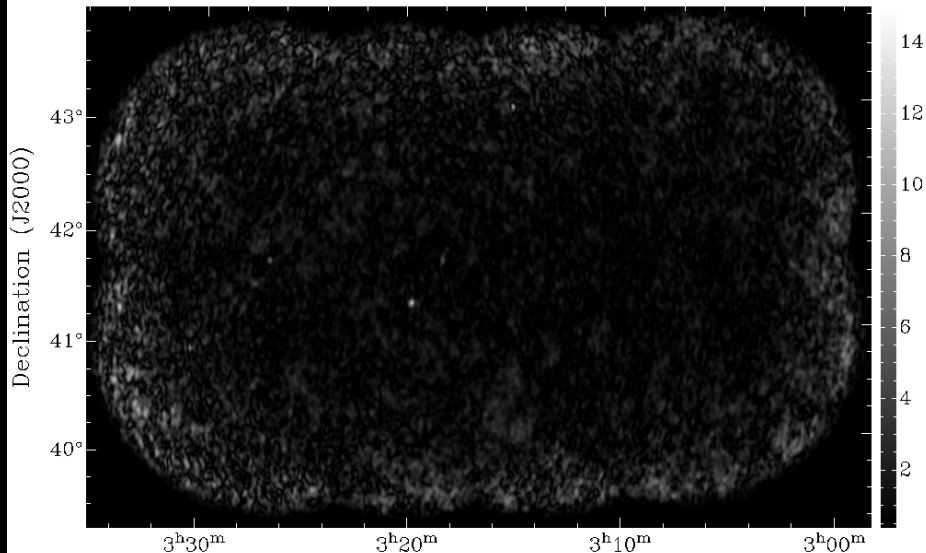
RM: 9.300000e+01



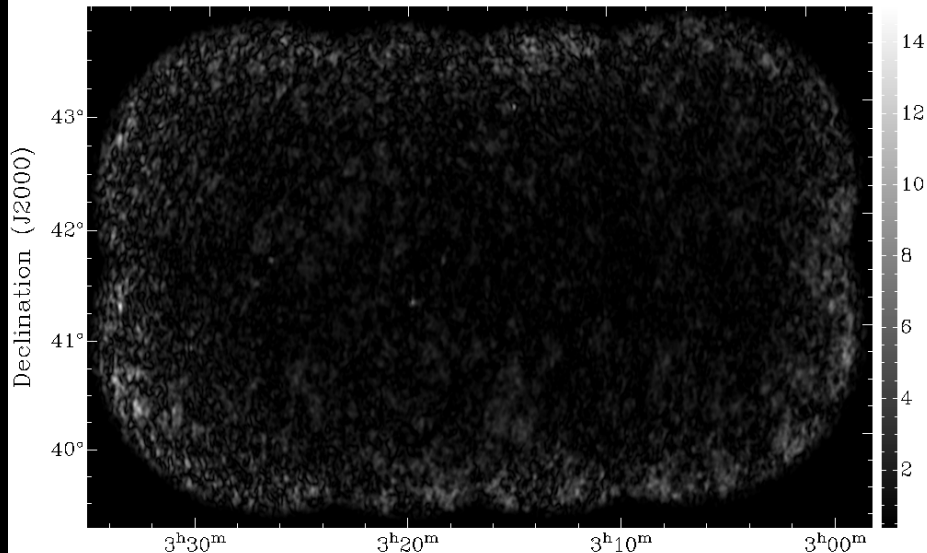
RM: 9.600000e+01



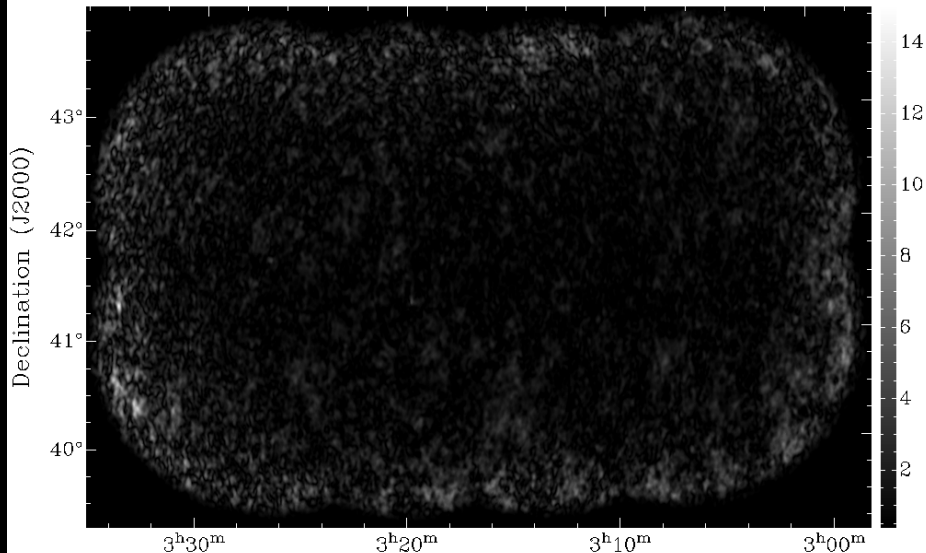
RM: 9.900000e+01



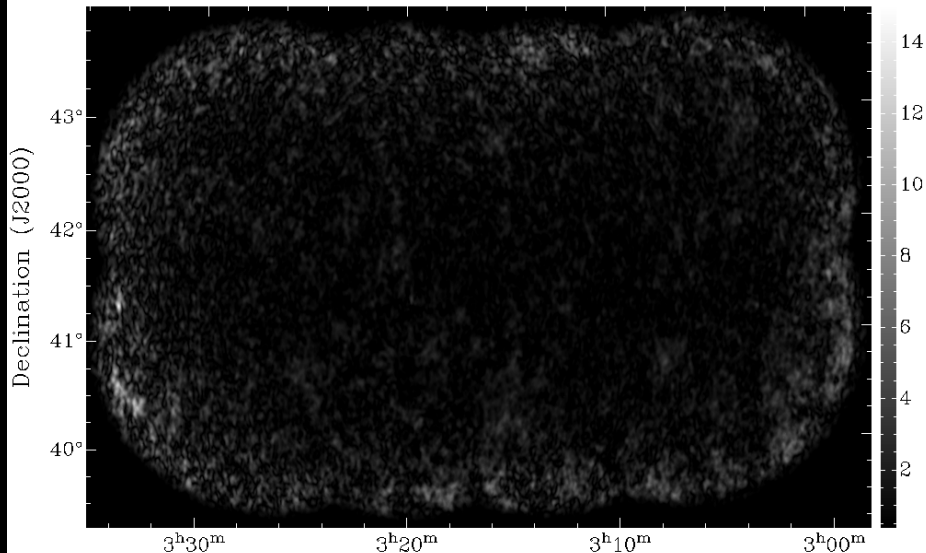
RM: 1.020000e+02



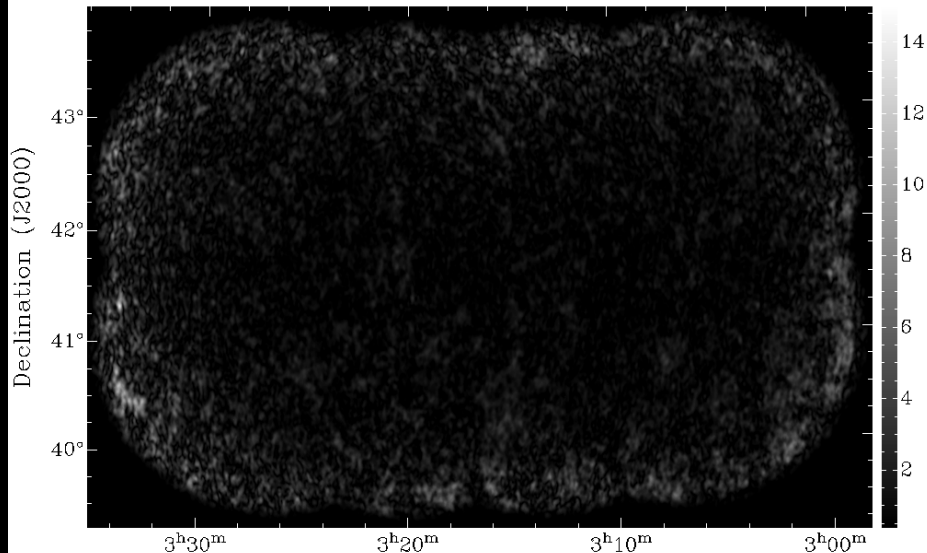
RM: 1.050000e+02



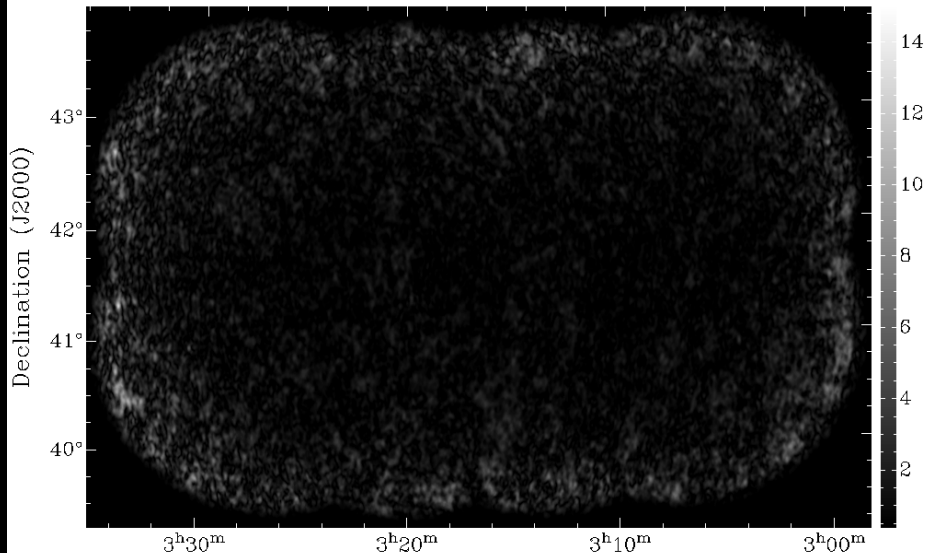
RM: 1.080000e+02



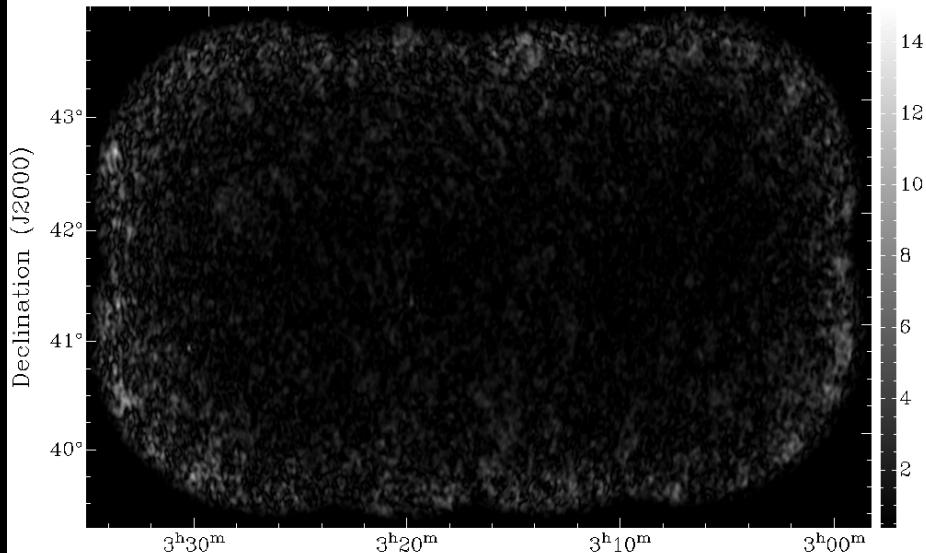
RM: 1.110000e+02



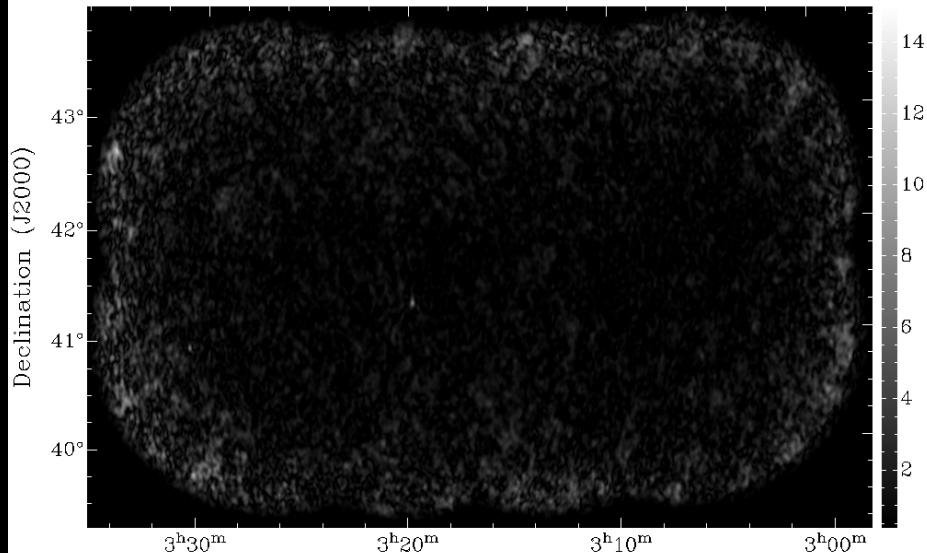
RM: 1.140000e+02



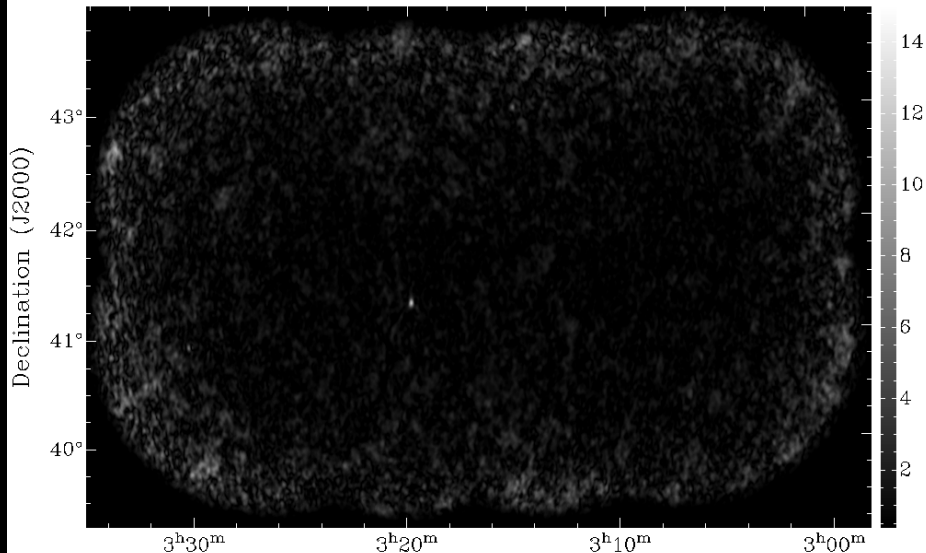
RM: 1.170000e+02



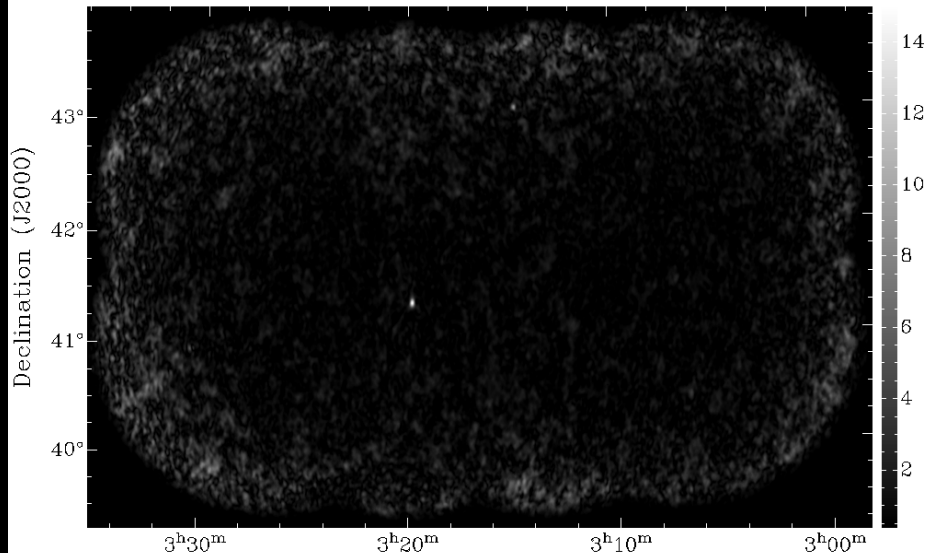
RM: 1.200000e+02



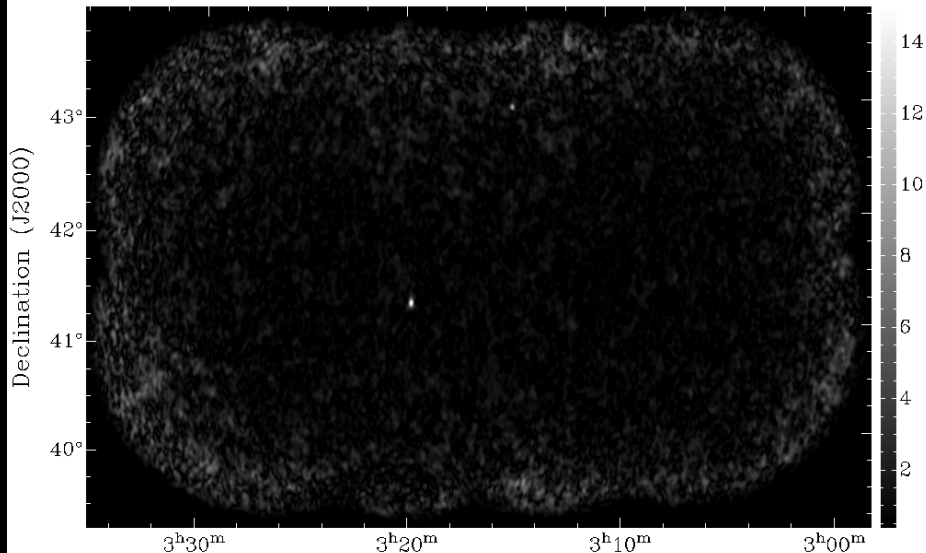
RM: 1.230000e+02



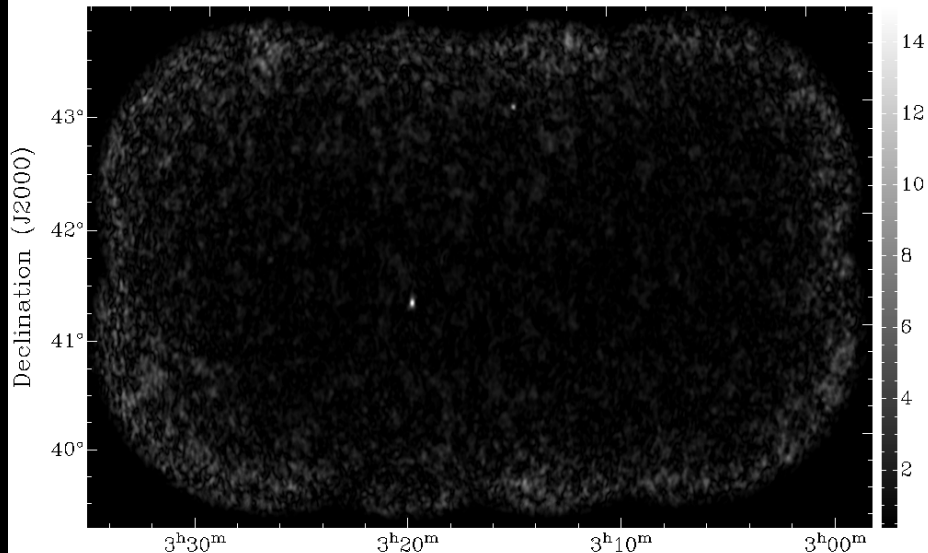
RM: 1.260000e+02



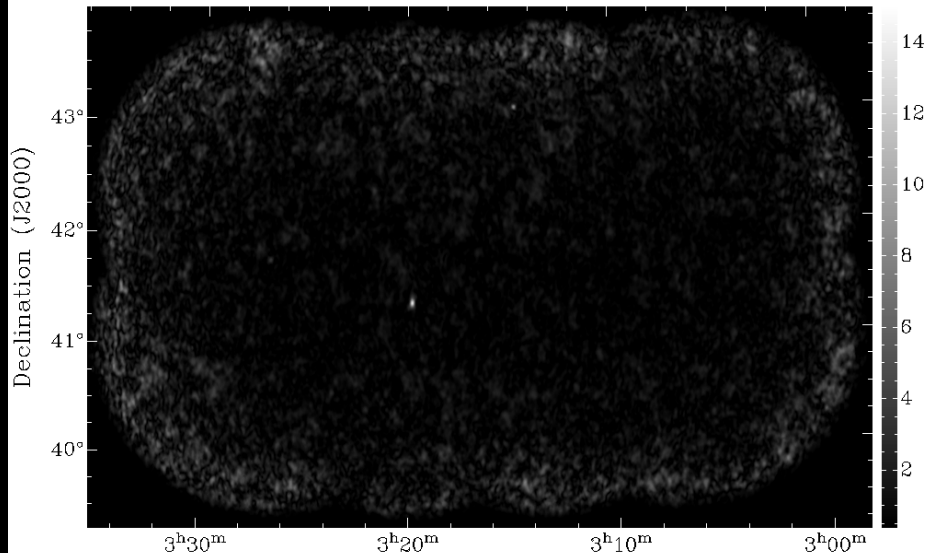
RM: 1.290000e+02



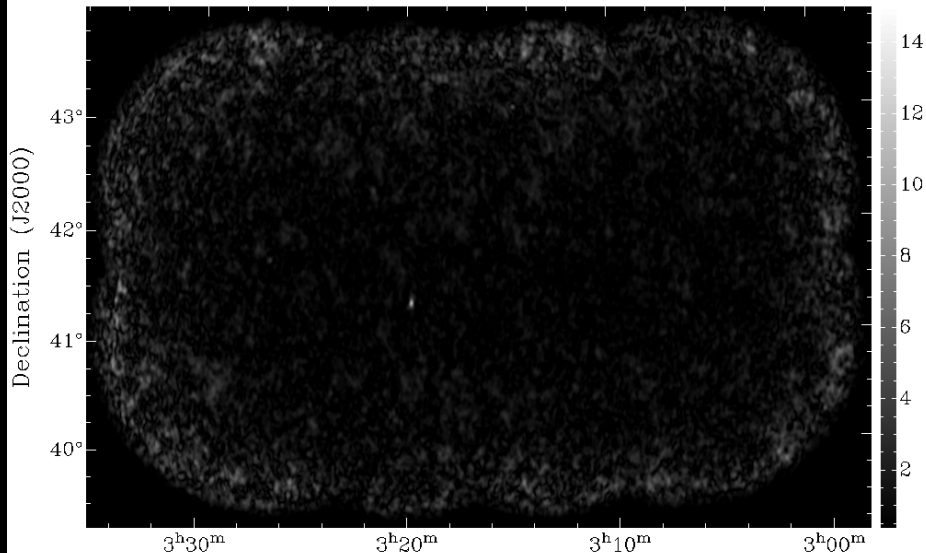
RM: 1.320000e+02



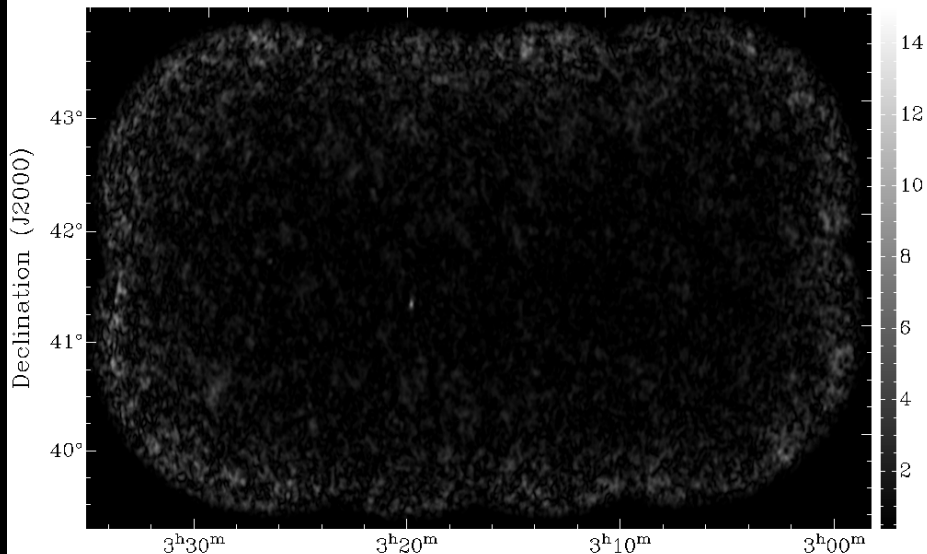
RM: 1.350000e+02



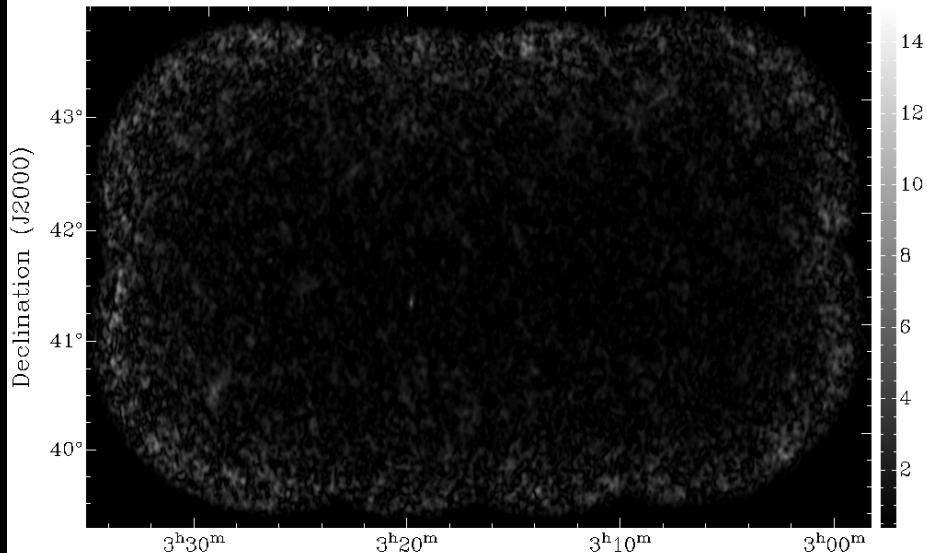
RM: 1.380000e+02



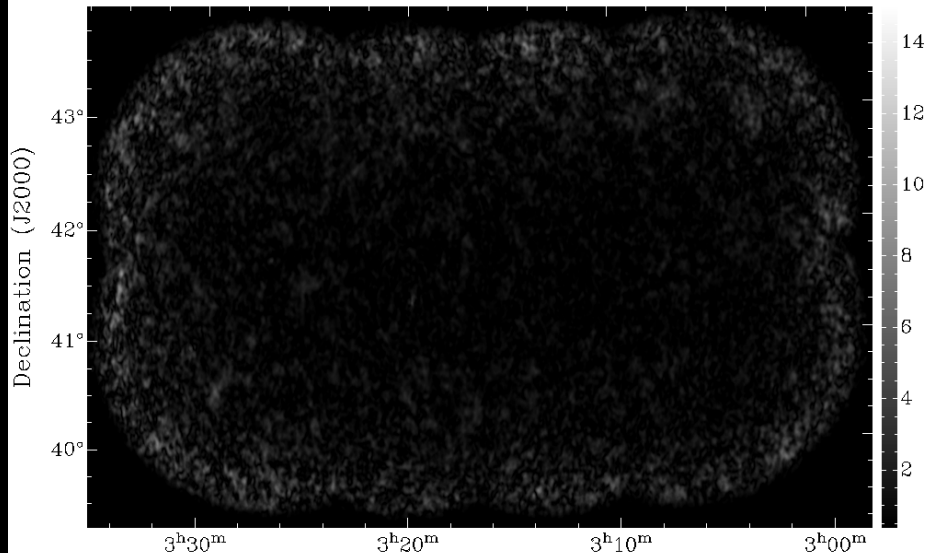
RM: 1.410000e+02



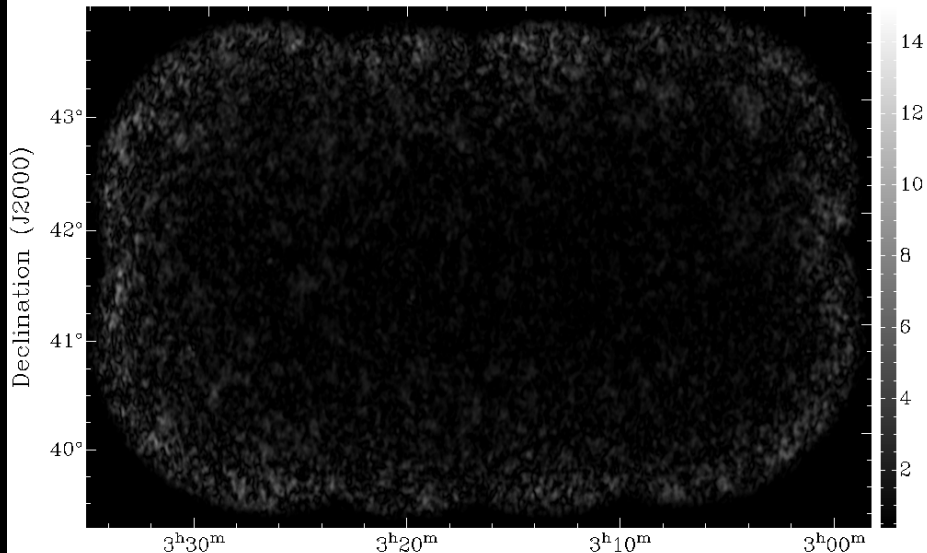
RM: 1.440000e+02



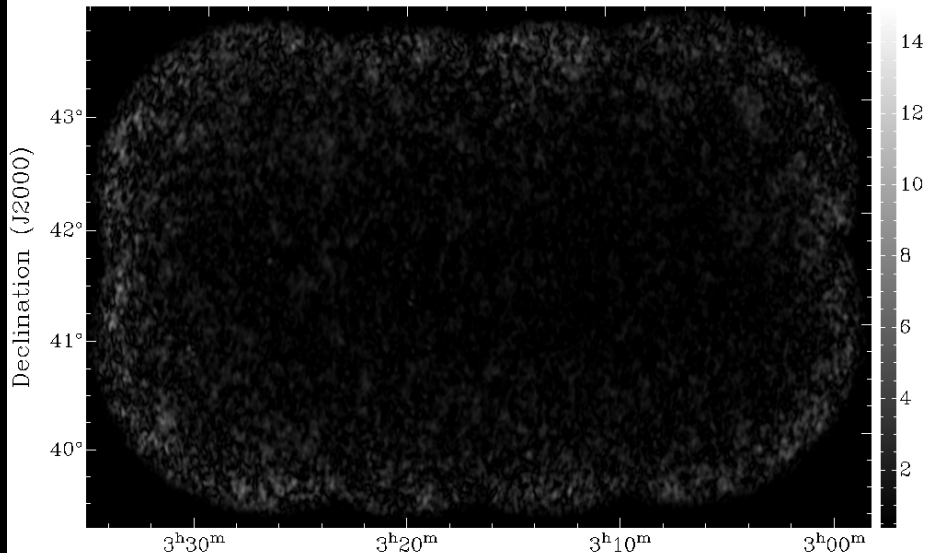
RM: 1.470000e+02



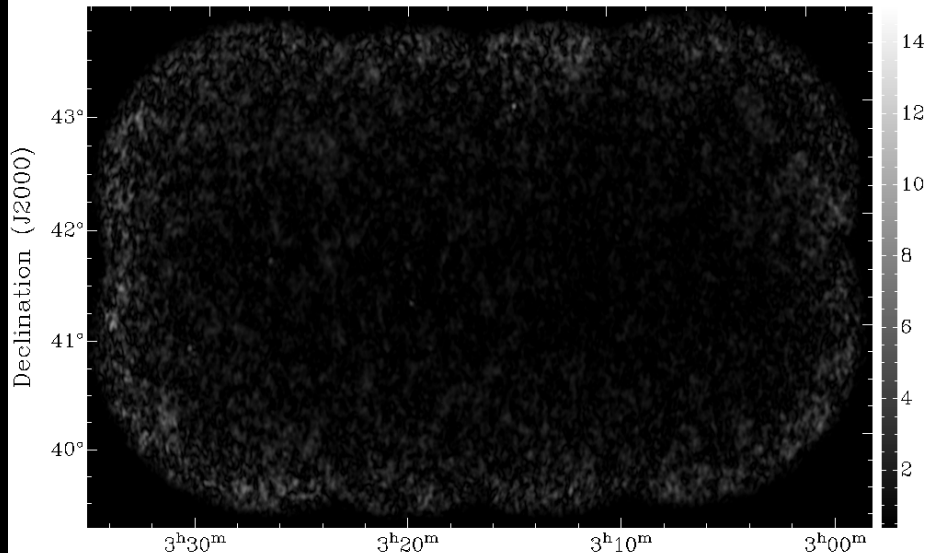
RM: 1.500000e+02



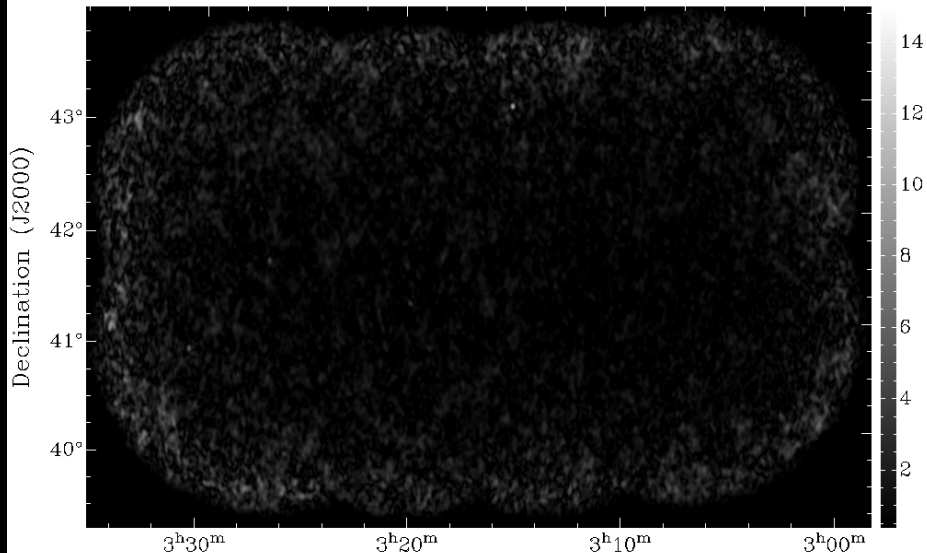
RM: 1.530000e+02



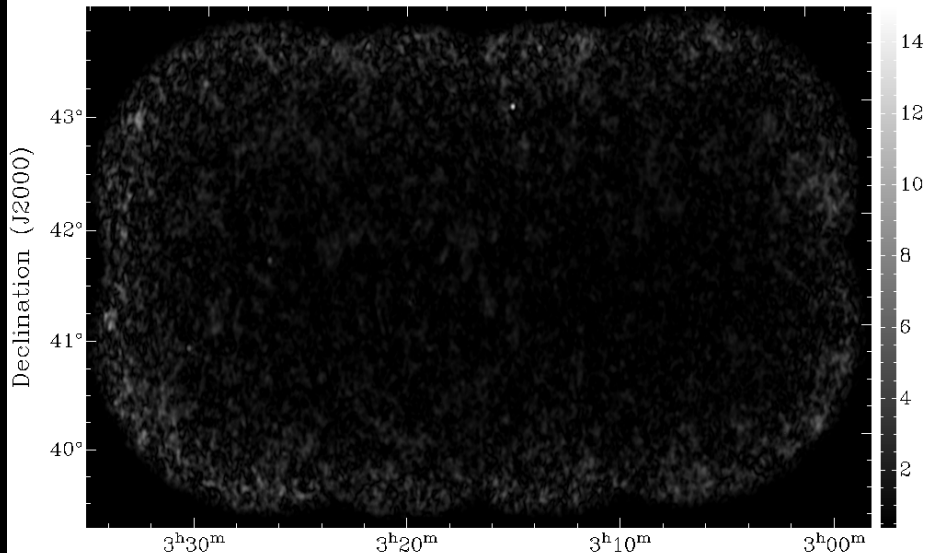
RM: 1.560000e+02



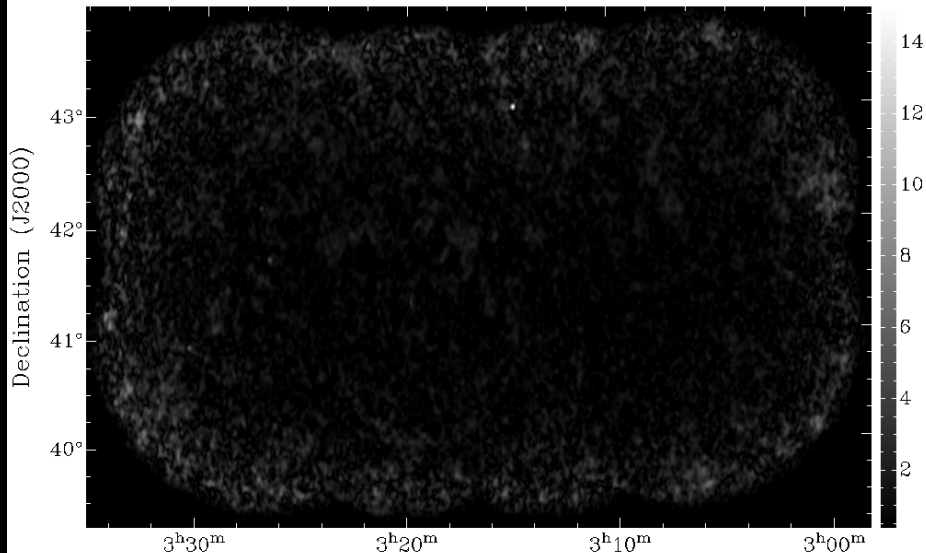
RM: 1.590000e+02



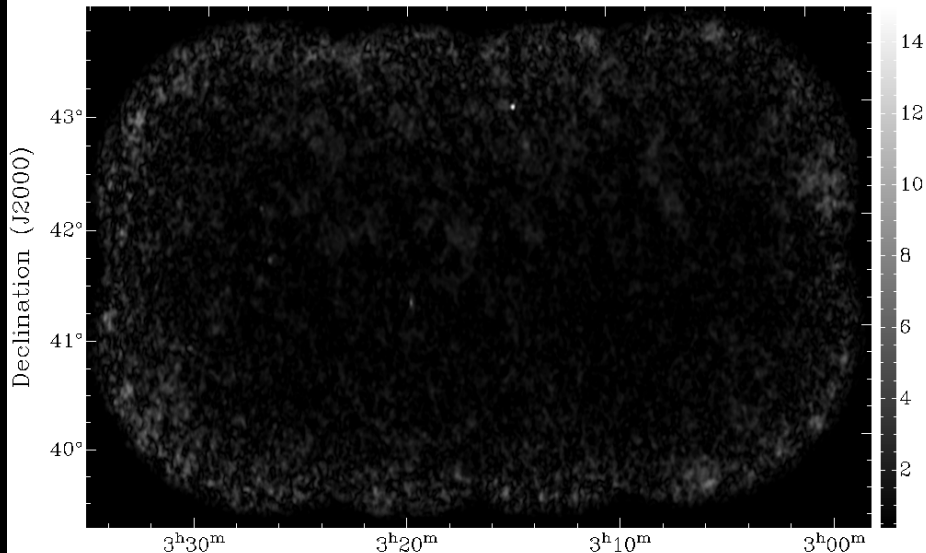
RM: 1.620000e+02



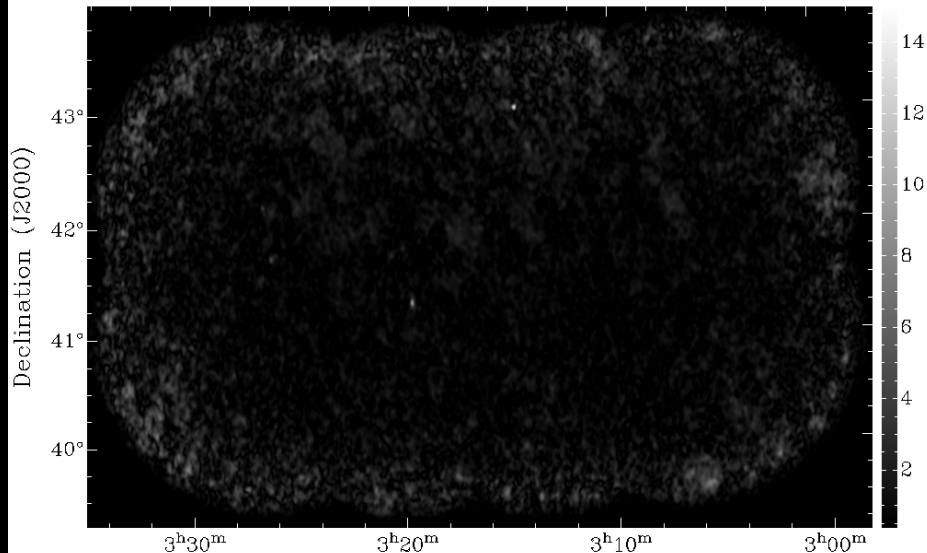
RM: 1.650000e+02



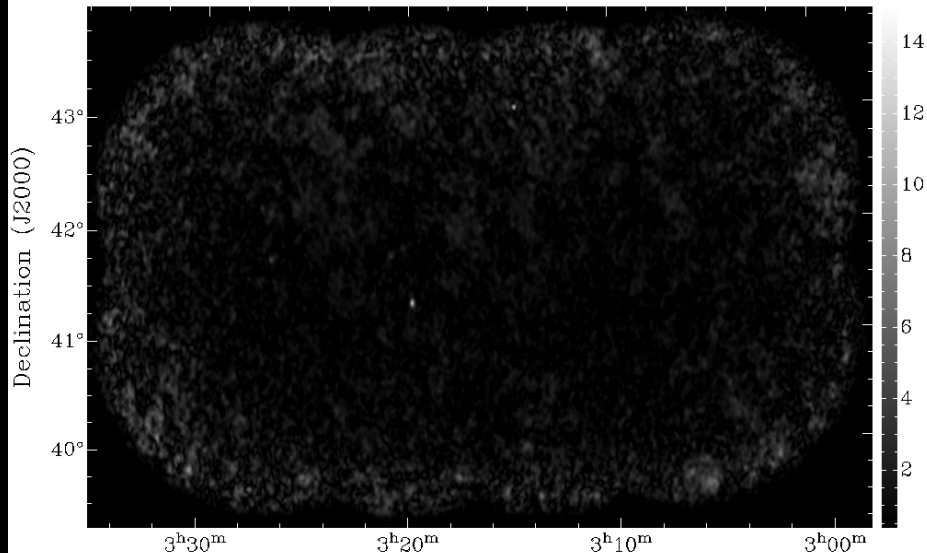
RM: 1.680000e+02



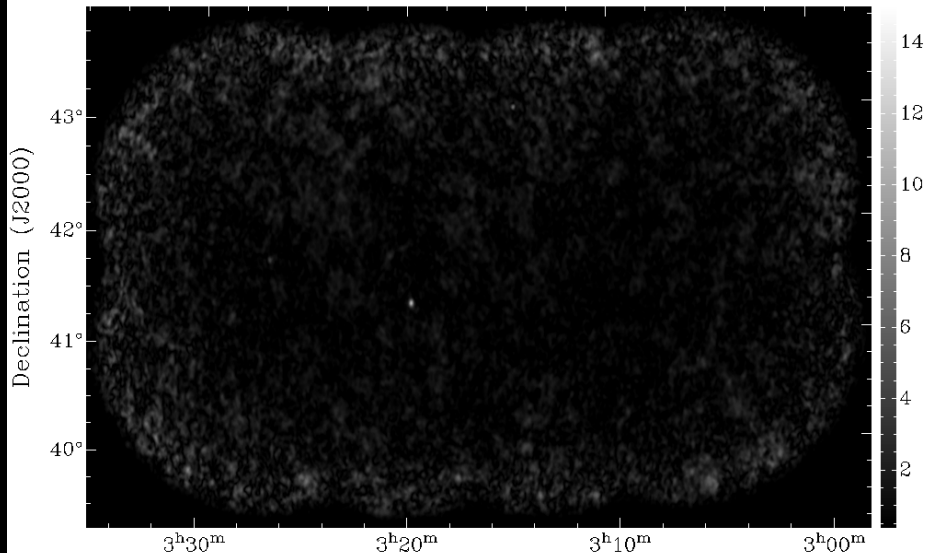
RM: 1.710000e+02



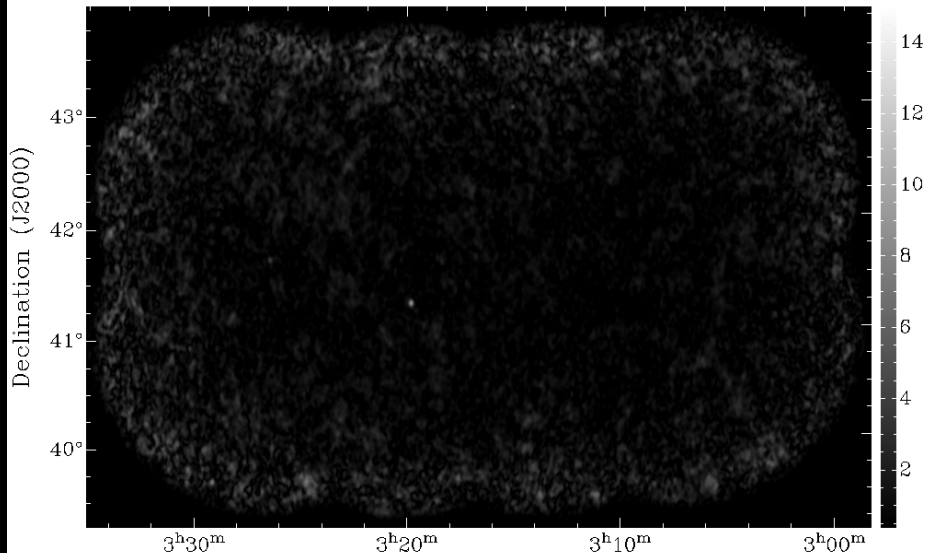
RM: 1.740000e+02



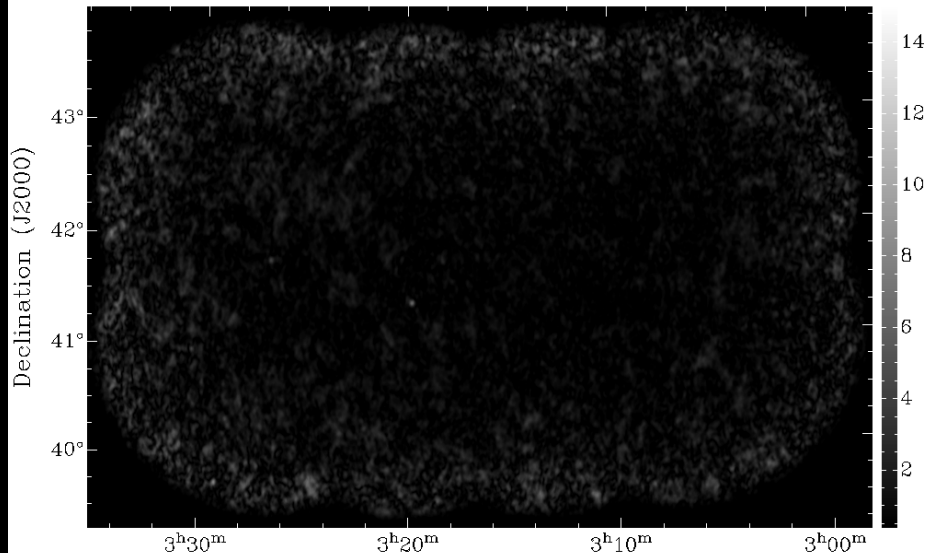
RM: 1.770000e+02



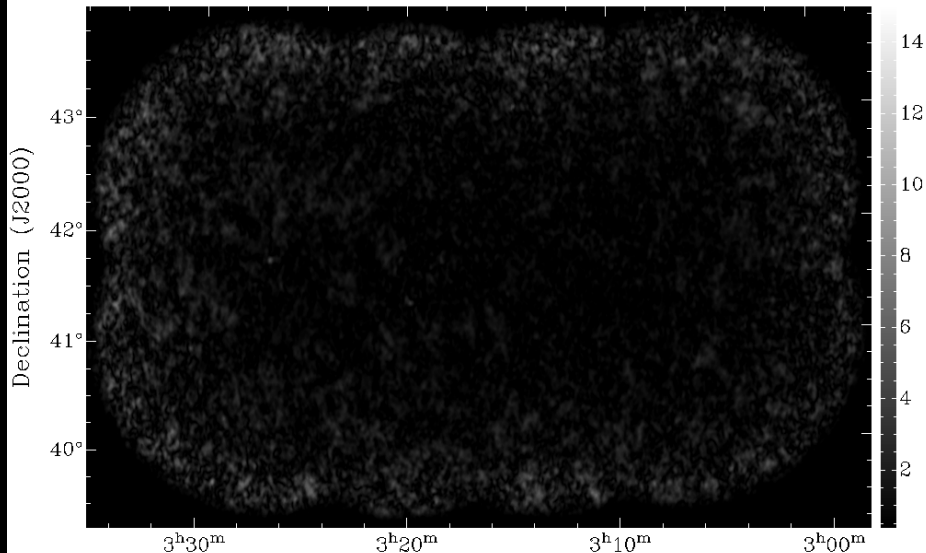
RM: 1.800000e+02



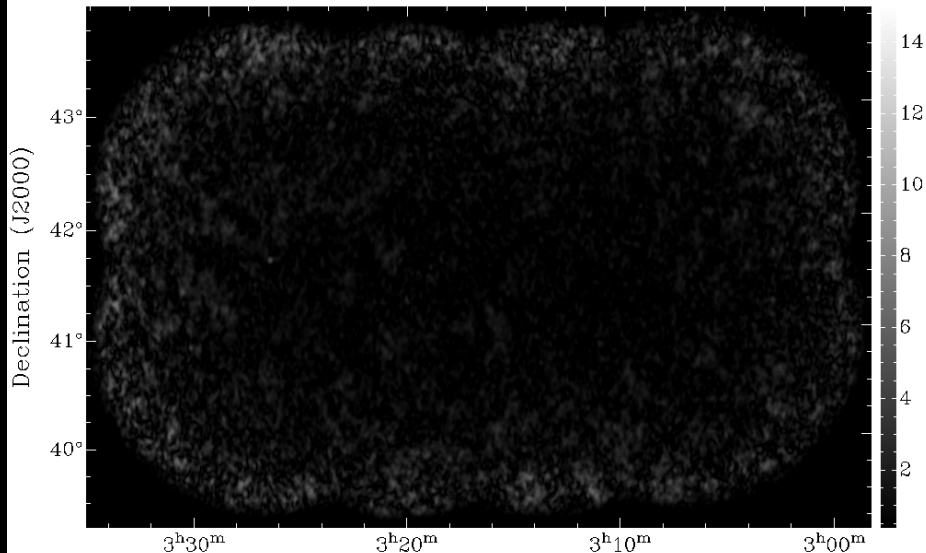
RM: 1.830000e+02



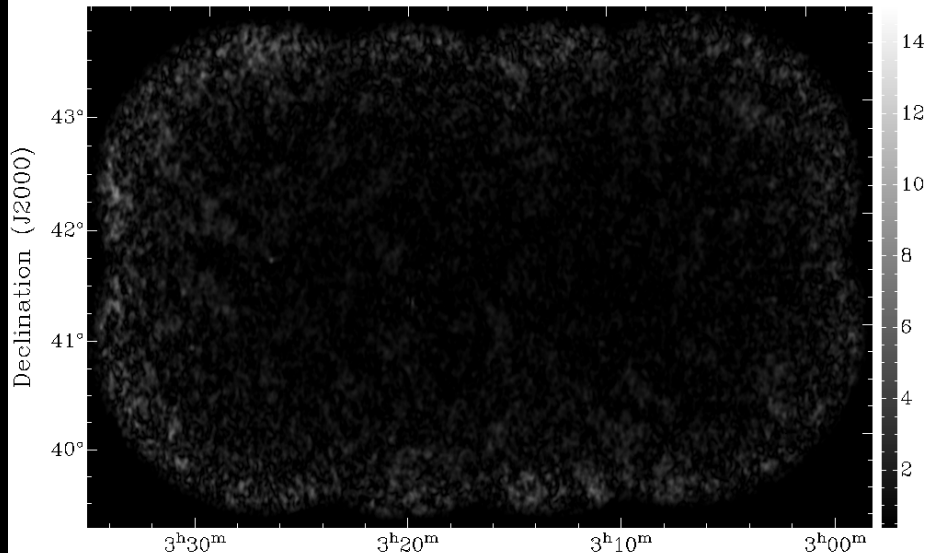
RM: 1.860000e+02



RM: 1.890000e+02



RM: 1.920000e+02



Existing, but unpublished/(un?)processed data

- WSRT at 150 MHz (Low Frequency Frontends / LFFEs 2005)
- WSRT at L-band 2004 6x 12h
- WSRT at L-band (MFFE test with Tom Oosterloo, see Morganti)
- LOFAR (nov 2013)

